**Verónica Catarina Ferreira Amado**

Licenciada em Bioquímica

# "One-pot" enzymatic conversion of $CO_2$ to methanol

Dissertação para obtenção do Grau de Mestre em Biotecnologia

Orientador: Susana Barreiros, Professora Associada com Agregação
Universidade Nova de Lisboa
Co-orientador: Alexandre Paiva, Investigador Doutorado
Universidade Nova de Lisboa

Júri:

Presidente: Prof. Doutor Carlos Alberto Gomes Salgueiro
Arguente: Doutora Ana Sofia Diogo Ferreira
Vogal: Prof. Doutora Susana Filipe Barreiros

**Setembro de 2013**

# “One-pot” enzymatic conversion of $CO_2$ to methanol

**Ao meu irmão Rafael**

# AGRADECIMENTOS

Gostaria de agradecer a todos aqueles que me apoiaram nesta jornada e que, de algum modo contribuíram para a realização desta tese.

Quero expressar a mais sincera gratidão aos meus orientadores. Em primeiro lugar à minha orientadora Prof. Doutora Susana Barreiros por todo o interesse e entusiasmo que demonstrou no meu trabalho, por todas as críticas científicas que tanto o enriqueceram, e por estar sempre disponível para discutir o mesmo. Gostaria de agradecer também ao meu co-orientador o Doutor Alexandre Paiva pela paciência, concelhos dados, discussão de ideias e alternativas, pelo espírito crítico sempre incisivo em pontos fulcrais e também pelos momentos de descontracção.

À Rita Craveiro que me acompanhou sempre em primeira mão, me apresentou o sol-gel, por toda a (enorme) paciência para me aconselhar e animar nos dias menos bons, por todos os conselhos dados sempre na perspectiva de enriquecer o trabalho desenvolvido e ajuda em todos os estágios do trabalho.

À Doutora Marta Corvo pela realização dos espectros de NMR a alta pressão tal como em na preciosa ajuda para a interpretação dos mesmos e ao Prof. Doutor Eurico Cabrita por me possibilitar a realização dos mesmos.

Gostaria de agradecer também a todos os meus colegas do Lab. 427 e os seus associados, foram não só colegas de trabalho como uma autêntica família, em que cresci como pessoa e profissional. À Sílvia por ter sempre uma palavra amiga e de ânimo, à Carmen por ser sempre tão alegre e alegrar todos à sua volta (e pelas maravilhosas tortilhas também), à Rita R. pelas palavras amigas, à Tânia por ser das melhores pessoas que eu conheço, à Sónia pela amizade ,ao Pedro e ao Ricardo pela alegria, à Amanda e Gabi por partilharem comigo o que é o vosso Brasil.

Aos meus companheiros nesta jornada que é tentar realizar uma dissertação Mariana, Cristina, José e Ekaterina, por todos os momentos de companheirismo, diversão, pânico e entreajuda.

Quero também deixar um beijinho aos novos combatentes, Michael, Luiza, Francisca, Verónica e Kevin, muito boa sorte para todos e que consigam chegar onde desejam.

Finalmente, agradeço à minha família, à minha mãe e pai, por tantas vezes me consolarem e darem força para seguir em frente, sem vocês nunca teria conseguido. À minha irmã por ser quem é sempre refilona, ao meu irmão por me receber sempre com um sorriso que me aquece o coração, e ao meu avô por me dar força para continuar. Ao Jacinto por tantas vezes me ouvir, ralhar comigo, e puxar por mim para dar o meu melhor.

A todos vós, um grande obrigada.

# ABSTRACT

Methanol is a substance of high industrial interest due to its various applications. It can be a raw material for chemicals, a solvent, or an alternative fuel. In the scientific community and in industry, different methods for methanol production are under development, with predominance of heterogeneous catalysis at high pressures and temperatures.

The main goal of this work is the transformation of $CO_2$ into valuable products, namely methanol, and to quantify it. A biocatalytic system composed of three oxido-reductases was used to catalyse the production of methanol from $CO_2$.

The catalysed reactions were performed in aqueous medium but also in an alternative solvent, ionic liquid (IL) [BMIM][$BF_4$], in order to study the influence of the medium on methanol production.

For methanol quantification/detection, different methods were used, namely ultraviolet/visible spectroscopy (UV/Vis), Headspace Gas Chromatography (HS-GC), Nuclear Magnetic Resonance (NMR) and High Pressure Nuclear Magnetic Resonance (HP-NMR).

Different parameters that influence the catalysis were evaluated, such as:

- The reaction medium, either aqueous buffer or IL;
- Form of the enzyme, either free or immobilized in a sol-gel matrix;
- The effect of the immobilization matrix on the reaction medium.

In aqueous medium, it was observed a number of side reactions (phosphate buffer reacting with the cofactor NADH and Tris buffer reacting with $CO_2$). The parameters of pH were also found to be crucial. The aqueous medium that gave the best conversion of NADH was TBS buffer medium.

When using an IL medium, a judicious choice was also needed, since the IL to be used must be able to give a good response for methanol when using HS-GC, and also it must be able to dissolve the cofactor NADH so that the biocatalysts are able to convert $CO_2$. [BMIM][$BF_4$] combines these requirements and therefore it was used in this work. Although methanol production was not directly verified, indirect measurements indicate its production, namely NADH consumption (enzymes' cofactor) and $CO_2$ (raw material) conversion.

**Keywords:** Carbon dioxide, ionic liquids, methanol, oxido-reductases, NADH

# RESUMO

O metanol é uma substância de elevado interesse industrial devido às suas várias aplicações. Pode ser utilizado como matéria-prima para a produção de químicos, como solvente, ou como combustível alternativo. Actualmente estão a ser desenvolvidos diferentes métodos de produção de metanol, predominando a catálise heterogénea recorrendo a elevadas temperaturas e pressões.

O principal objectivo deste trabalho consiste na conversão de $CO_2$ em compostos de valor, nomeadamente metanol, e respectiva quantificação. Um sistema biocatalítico composto por três oxido--redutases foi utilizado para catalisar a produção de metanol a partir de $CO_2$.

As reacções catalisadas foram realizadas em meio aquoso, e também num meio alternativo, líquido iónico (LI) [BMIM][$BF_4$], de forma a estudar a influência do meio na produção de metanol.

Para a quantificação/detecção de metanol, foram utilizados diferentes métodos, nomeadamente a espectroscopia no ultravioleta visível (UV/Vis), Cromatografia Gasosa de "Headspace" (HS-GC), Ressonância Magnética Nuclear (RMN) e Ressonância Magnética Nuclear a Alta Pressão (HP-NMR).

Foram avaliados diferentes aspectos que influenciam a catálise, nomeadamente:

- O meio reaccional, quer tampão aquoso, quer um líquido iónico;
- Forma da enzima, ou livre, ou imobilizada numa matriz sol-gel;
- O efeito da matriz de imobilização no meio reaccional.

Em meio aquoso, verificou-se a existência de reacções laterais (tampão fosfato a reagir com o cofactor NADH, e o tampão Tris a reagir com $CO_2$). Os parâmetros de pH revelaram também cruciais. O meio aquoso em que se verificaram as melhores conversões de NADH foi o tampão TBS.

Quando se utiliza um LI como solvente, é necessário fazer uma escolha criteriosa desse LI, pois o mesmo tem de dar uma boa resposta para o metanol em análise por HS-GC, e tem também de ser capaz de dissolver o cofactor NADH para que os biocatalizadores possam converter o $CO_2$. O LI [BMIM][$BF_4$] satisfaz estes requisitos e portanto foi o escolhido. Embora a produção de metanol não tenha sido quantificada directamente, foi-o indirectamente, através do consumo do NADH (cofactor das enzimas) e do $CO_2$ (matéria prima).

**Palavras chave:** Dióxido de carbono, líquidos iónicos, metanol, oxido-redutases, NADH

# TABLE OF CONTENTS

# LIST OF FIGURES

# LIST OF TABLES

# ABBREVIATIONS:

ADH – Alcohol dehydrogenase

AldDH – Aldehyde dehydrogenase

Aliquat® 336 – Tricaprylylmethylammonium chloride

[BMIM] [Ac] – 1-Butyl-3-methylimidazolium acetate

[BMIM] [$BF_4$] – 1-Butyl-3-methylimidazolium tetrafluoroborate

[BMIM] [Cl] – 1-Butyl-3-methylimidazolium chloride

[BMIM] [$NTF_2$] - 1-Butyl-3-methylimidazolium bis(trifluoromethylsulfonyl)imide

[BMIM] [DCA] –1-Butyl-3-methylimidazolium dicyanamide

[BMIM] [OTf] - 1-Butyl-3-methylimidazolium trifluoromethanesulfonate

[BMIM ] [$PF_6$] – 1-Butyl-3-methylimidazolium hexafluorophosphate

BSA – Bovine Serum Albumin

$CO_2$ – Carbon Dioxide

DME – Dimethyl ether

[EMIM][$EtSO_4$] – 1-Ethyl-3-methylimidazolium ethyl sulphate

[$Et_3NMe$] [$MeSO_4$] – Triethylmethylammonium methyl sulphate

FaldDH – Formaldehyde dehydrogenase

FAME - Fatty Acid Methyl Esters

FateDH – Formate dehydrogenase

FID - Flame Ionization Detector

GDH – Glutamate dehydrogenase

HLADH – Horse liver alcohol dehydrogenase

HPLC - High Pressure Liquid Chromatography

HP-NMR – High Pressure Nuclear Magnetic Resonance

HS-GC – Headspace gas chromatography

IL – Ionic Liquid

LB-ADH – Alcohol dehydrogenase from *Lactobacillus brevis*

MDH – Methanol dehydrogenase

[MIm] [$BF_4$] – 1-Methylimidazolium tetrafluoroborate

[MIm] [Cl] – 1-Methylimidazolium chloride

[MMIM][$MeSO_4$] – 1-Methyl-3-methylimidazolium methyl sulphate

MOPS – 3-(N-morpholino)propanesulfonic acid

m-PEG - Methoxy-poly(ethylene) glycol

MTBE – Methyl *tert*-butyl ether

$MV^{2+}$ – Methyl viologen

NaCl – Sodium chloride

$NAD^+$ – β-Nicotinamide adenine dinucleotide

NADH – β-Nicotinamide adenine dinucleotide, reduced disodium salt hydrate

NMR – Nuclear Magnetic Resonance

PDB – Protein Data Bank

PHB – Poly-*β*-Hydroxybutyrate

PIPES – 1,4-Piperazinediethanesulfonic acid

PQQ – Pyrroloquinolinequinone

RTIL – Room Temperature Ionic Liquid

SSL – Split/splitless

TBADH – Alcohol dehydrogenase from *Thermoanaerobacter brockii*

TBS – Tris-buffered Saline

Tris – 2-Amino-2-hydroxymethyl-propane-1,3-diol

TEOS – Tetraethoxysilane

TMOS – Tetramethylsilane

UV/Vis – Ultraviolet/visible spectroscopy

Sc-$CO_2$ – Supercritical carbon dioxide

SSL – Split/splitless

YADH – Alcohol dehydrogenase from yeast

% (v/v) – Percentage volume/volume

# 1. INTRODUCTION

# 1. INTRODUCTION

At the present time, the world has an increasing demand for energy, whether it is for transportation, electricity or heating, obtained mainly through fossil fuels such as oil, natural gas and coal, overcoming in 2009 80% of the energy needs worldwide [1].

The energy demand in the future will increase, not only by the increase of the world's population, that is expected to be between 8 to 10 billion in 2050 [2], but also by the increase of the average life expectancy, but also by the high life style standard driven by the economic development of the countries.

Nonetheless, fossil fuels that are currently being used for energy supply are limited resources and highly pollutant, increasing the $CO_2$ emissions every day by their combustion.

To minimize the environmental footprint caused by $CO_2$ emissions there are already some strategies that use $CO_2$ as a building block for the production of fuels or solvents such as methanol, which is less harmful for the environment. By using processes that take place at milder temperatures and use alternative solvents there will be less energy consumption, which translates into less $CO_2$ emissions. By using solvents that are recyclable, there is also a prevention of the waste instead of remediating it.

## 1.1. CARBON DIOXIDE ($CO_2$)

In the last few years, the carbon dioxide ($CO_2$) emissions are increasing in a daily basis, as is demonstrated in Figure 1.1, contributing to the greenhouse effect, so a great effort is being made in order to reduce its emissions.

$CO_2$ is managed in nature by photosynthesis, in which plants convert atmospheric $CO_2$ with water and sunlight in to organic compounds [1]. Carbon moves through atmosphere, oceans, sediments, soils, geological formations and living creatures, so it is present in nature in all this forms, as it represented in Figure 1.2.

Before the industrial era, the atmospheric $CO_2$ concentration was stable around 280 ppm, but with the combustion of carbon-based fossil fuels such as coal or oil this concentration increased until the current value of 393 ppm [2].

The human activity has a huge impact in the increase this carbon dioxide emissions, mainly by the combustion of fossil fuels, and in less extent by the land-use, especially through deforestation. Also, the production of the fossil fuels took place on a geologic time scale, however our consumption rate is much faster.

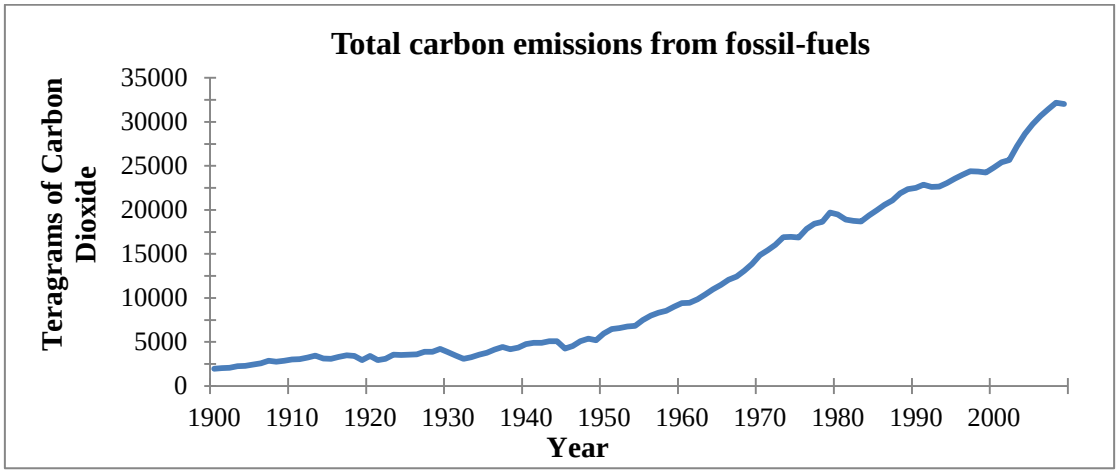


**Figure 1.1 –** Carbon emissions from fossil fuels between 1900 and 2009 [3].

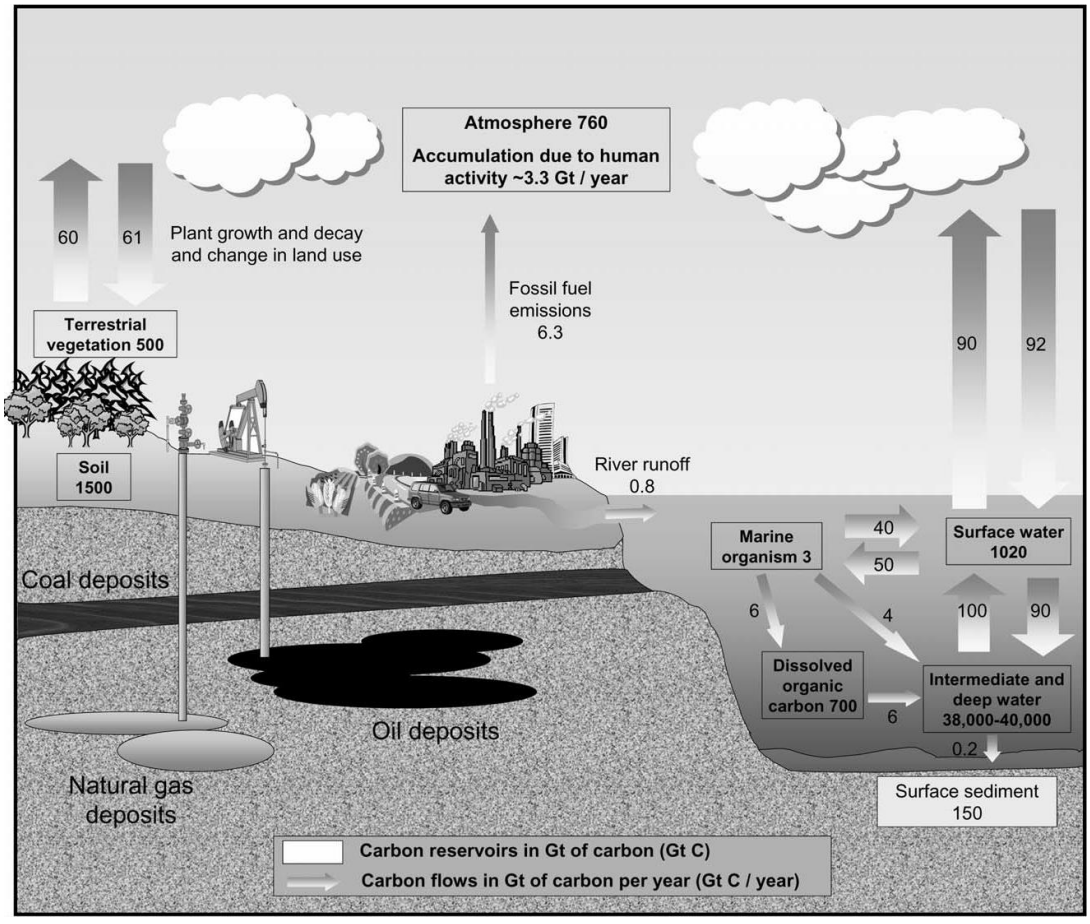


**Figure 1.2** – Carbon cycle [2].

Approximately half of the human based $CO_2$ emissions is absorbed by the oceans and vegetation, while the remainder goes to the atmosphere [2]. In an attempt to control the $CO_2$ emissions

to the atmosphere, they need to be regulated in the future. In consequence of that, some companies began "trading credits" in $CO_2$ emissions [1,4] – carbon quotes started by the Kyoto Protocol [1,2], corresponding to one tonne of carbon dioxide prevented from entering the atmosphere. In this system, $CO_2$ has a "negative value" and when used as a raw material, allows one to theoretically reduce the cost of the process or product. This has led to an enhancement in the research and development on processes or products that consume and transform $CO_2$ [4].

The increase of $CO_2$ emissions has serious environmental consequences. Especially it has an impact in the increase of the global temperatures as well in the marine environment, by the defrosting of the glaciers, acidification and rise of the water level and the possible change in the marine currents. Mitigation of $CO_2$ harmful effects is then a necessity, not only by diminishing the industrial emissions, but also in the smaller sources such as office and home heating, cooking, and most importantly the transportation sector [1].

One of the strategies to reduce $CO_2$ emissions is to use $CO_2$ as a feedstock material for the production of a liquid fuel [5], by reducing the amount of emitted $CO_2$ to the atmosphere [6], or to capture $CO_2$ by compressing and sequestrate it underground in geological formation, depleted oil, gas reservoirs or in the ocean [2].

Capture of $CO_2$ from gas streams can be performed through both chemical and physical processes, including absorption into a liquid solution, adsorption onto suitable solids, cryogenic separation, and permeation through membranes. Nevertheless, this has high-energy requirements for the regeneration step and limited loadings. Also the purification to eliminate pollutants ($H_2S$ and $SO_x$) is necessary [1].

$CO_2$ is the most abundant $C_1$ compound and an important energy source [6]. It is used as a solvent and as a raw material, and it is studied since 1950 [4]. It presents unique characteristics such as non-flammability, relatively non-toxicity, it is relatively inert, and it is also safer than most of current organic solvents [4,7]. Its properties of pressure, volume, dielectric constant and temperature are highly studied.

Most of the $CO_2$ employed today in processes is collected from the effluent of ammonia plants or derived from naturally occurring deposits, being its utilization considered as pollution preventing [4]. $CO_2$ also finds applications in the most varied industrial processes, such as caffeine and aroma extraction from coffee beans [4,8], dry cleaning, polymer impregnation [9], as solvent for chain polymerizations and foaming polymeric materials that are applied mainly for purposes of insulation [4].

As many other substances carbon dioxide can be present in different states of matter, namely gas, liquid and solid. The physical state of a substance depends on its chemical structure, pressure and temperature. In the solid state, matter occupies a fixed volume and has fixed shape with molecules very closely arranged. In the liquid form, matter occupies a fixed volume and has a variable shape, its particles are still close together but move freely. In the gaseous state a substance has neither definitive

volume or shape, adapting both to fit its container. These properties are related with the different intermolecular forces between the atoms in the different physical states, namely Van der Waals forces, permanent dipole interactions, and the strongest one - hydrogen bonds. These interactions also have influence in the substance physical properties, e.g. the ebullition temperature, that enhances with the strength of the intermolecular forces between matter.

Carbon dioxide is a gas at atmospheric pressure and temperature, and, by pressurization and heating, it reaches the critical point, which is for a pure substance, the highest temperature and pressure at which vapour and liquid phases coexist at equilibrium. When $CO_2$ has a temperature and pressure above 31ºC and 73.8 bar respectively (Figure 1.3), corresponding to its critical point, it becomes a supercritical fluid (sc-$CO_2$). A supercritical fluid has properties similar to a gas, such as low viscosity and high diffusivity rates, and has the density similar to a liquid [8,10]. Sc-$CO_2$ finds applications in various areas [8].

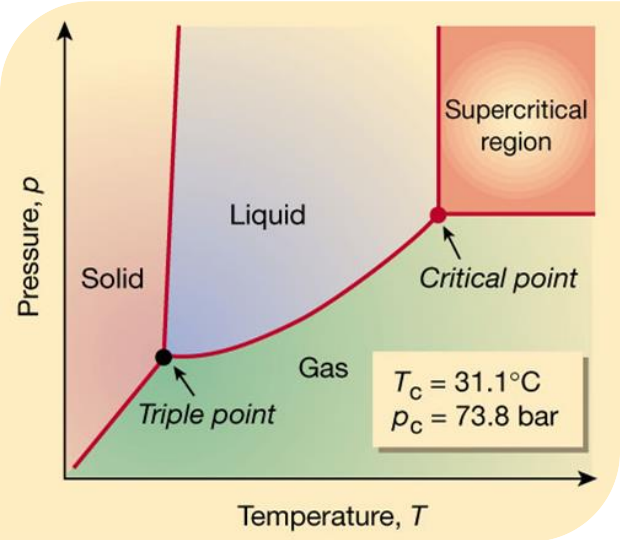


**Figure 1.3 –** Phase diagram for carbon dioxide [8].

The density and the viscosity at conditions near to the critical point change drastically by changing the pressure and temperature [7], so by depressurization it is possible to fractionate different products and even precipitate them [4], which is why supercritical fluids find so many applications as extraction solvents. $CO_2$ is inert towards oxidation, so it can be used as solvent in oxidation reactions [4]. It is also a highly stable molecule [6,11], being necessary energy to convert it into other synthetic hydrocarbons [11].

However the use of sc-$CO_2$ has some challenges when comparing with the same process performed at atmospheric pressure, namely the potential safety hazard and the capital cost associated with the need of specialized equipment. Also, exothermic reactions can be problematic since the

pressure is directly proportional to temperature. Sc-$CO_2$ has also a low dielectric constant, so it is non-polar and has poor solvent power for polar compounds [4].

## 1.2. METHANOL

Methanol is a hydrocarbon, and the simplest of alcohols. It has properties such as high volatility, it is colourless, flammable and polar [12]. In the chemical industry (annual production of more than 40 Mt in 2007 [6]) it can be used as solvent, as an intermediate raw material for chemicals [12,13], (Figure 1.4), in biodiesel production (Figure 1.12 a) ) and also as a hydrogen carrier [13]. It is also used as a gasoline oxygenated additive (octane number of 10) and as an alternative to fossil fuel [2], making it a product of added value.

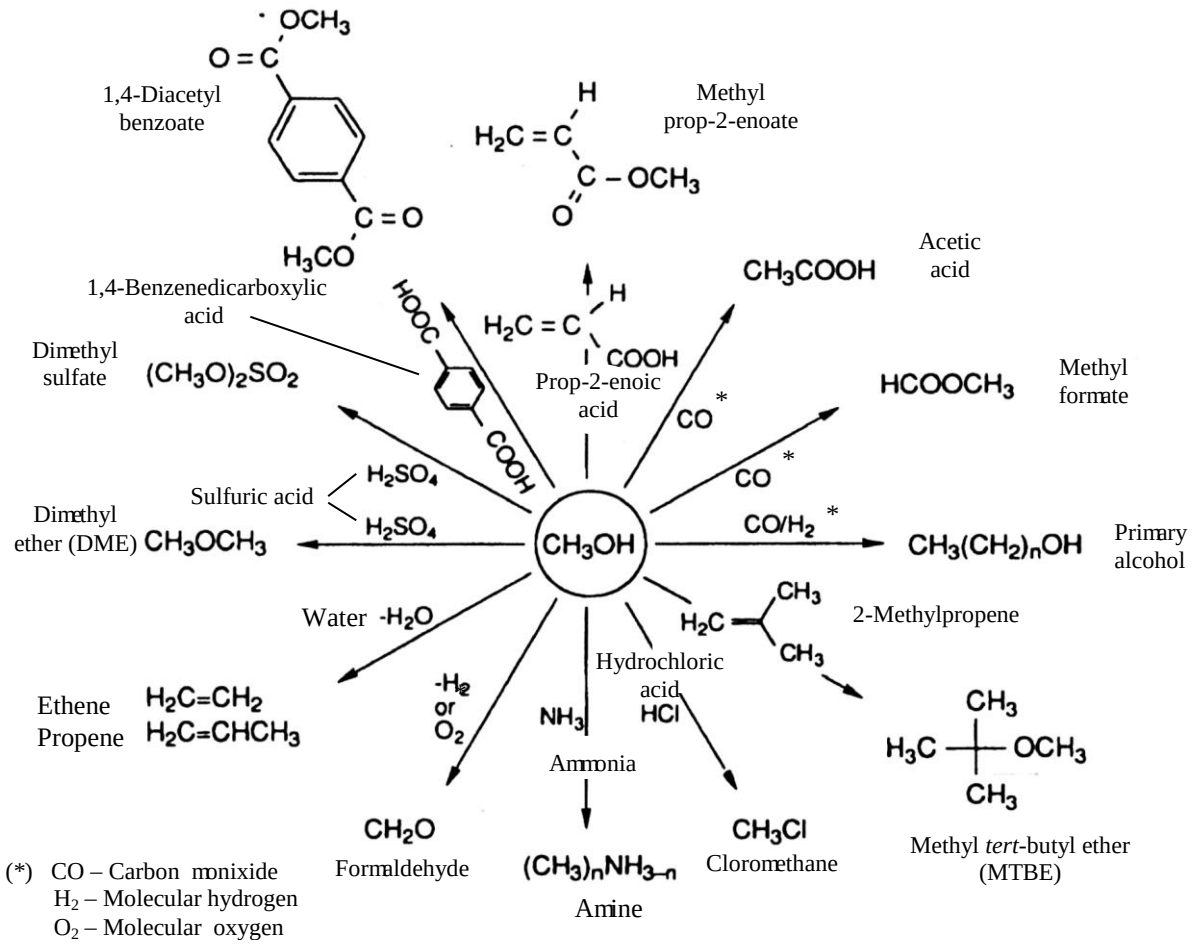


**Figure 1.4 –** Examples of methanol based chemicals [12].

Methanol was first obtained as a by-product of the destructive distillation of wood, so it is often called "wood alcohol" [1,2]. Nowadays it is mainly produced from synthesis gases, also called syngas ($CO/H_2$ with a small amount of $CO_2$) [6,12,14] using as source natural gas (75%), coal [13,14] or biomass. The conversion of synthesis gas to methanol has been commercially accomplished since World War II [1], using heterogeneous catalysis and by a two-step process in which the raw-material (natural gas, coal or biomass) is converted to synthesis gas by steam reforming [1,5], $CO_2$ reforming or partial oxidation, followed by either Fischer-Tropsch synthesis of hydrocarbons or methanol synthesis [5]. This process is highly efficient, but it is only economically viable if it is conducted on a large scale, due to the high cost of the syngas production [5]. Another route for methanol transformation is a one-step process in which methane or natural gas is oxidized with oxygen or other oxidizing species [5].

The raw material selection for the production of methanol is determined by its price. As an example, the United States of America is the second larger producer of natural gas, so they use it to produce methanol [2]; China has less natural gas [15] but is the main producer of coal, so they use coal as a raw material to methanol production [1,2].

Methanol can also be produced from fuel gases (like carbon dioxide, $CO_2$) prevenient from fossil fuel-fire power plants, cement factories or the atmosphere [13].

The production of methanol by $CO_2$ reduction uses traditionally heterogeneous catalysis, through photo catalysts and electrocatalyts [5], and has the disadvantages of using high temperatures and pressures [2,5], and external electric or luminous energy, but both selectivity and yields are usually low [5].

If methanol is produced using renewable energy, it is called renewable methanol and its production process is summarized in Figure 1.5. The world's first renewable methanol production plant is operated by Carbon Recycling International (CRI), that uses $CO_2$ flue gas and electricity from a geothermal power plant to make renewable methanol [1].

Some historic perspective on the catalytic process of methanol production and utilization is presented below [16]:

**1920 -** Methanol synthesis, high pressure process – Zn, Cr oxide catalysts [16];

**1970 -** Methanol synthesis, low pressure, (Imperial Chemical Industries Ltd - ICI) – Cu-Zn-Al oxide catalysts [16];

**1960** – Production of acetic acid from methanol (carbonylation) – Co catalyst [16];

**1970** – Production of acetic acid from methanol (carbonylation, low pressure process, Monsanto) – Rh catalyst [16];

**1980 -** Gasoline from methanol process (Mobil) – Zeolite catalyst [16].

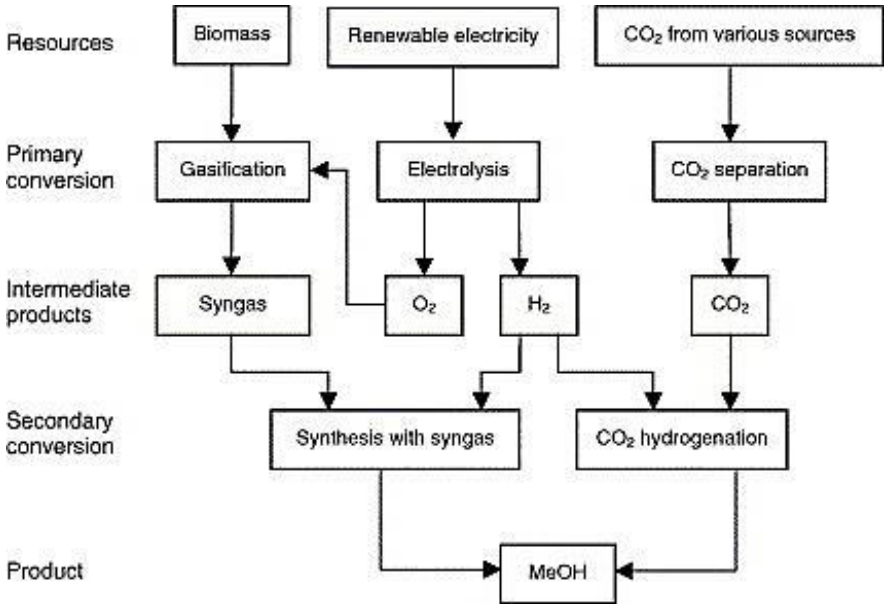


**Figure 1.5 –** Production of renewable methanol [13].

Figure 1.6 shows the variation of methanol price over the past years, which is affected by different aspects, such as methanol demand, price of the raw material (natural gas mainly), shipping and finally the production capacity and efficiency of the same [2]. The current price of methanol from the company Methanex (world's largest supplier of methanol) is about 532 US$/tonne in North America and 390 €/tonne in Europe [17].

Methanol prices closely follow crude oil prices (Figure 1.6), because it is a substitute for oil-driven fuels. However, methanol is mainly produced from natural gas since it has a lower cost, however is snot a renewable energy source.

In 2013, the global methanol demand is expected to be around 65 million tonnes [18]. The main consumer and producer of methanol is China, more than 41% as it is possible to observe in Figure 1.7. In China methanol production occurs mainly *via* syngas, with the abundant feedstock – coal [1,6] and blended it with gasoline as an alternative fuel to the scarce oil or natural gas [15].

By analysing the net exportations (difference between exportations and importations) in Figure 1.8, it is also possible to have a clue on the shipping of methanol through the different regions being Northeast Asia the biggest importer, and South America and Middle East the biggest exporters.

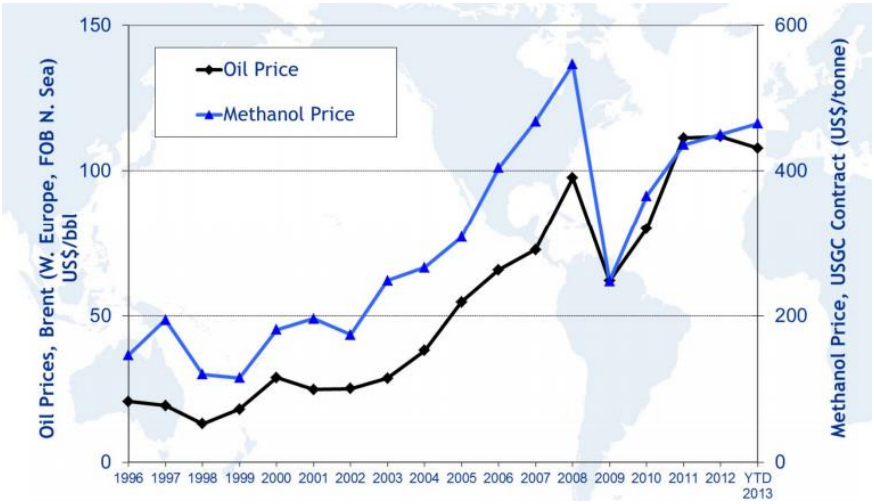


**Figure 1.6** – Historic methanol and oil contract prices (data are averages for the period shown) [19], data from IHS Chemical.

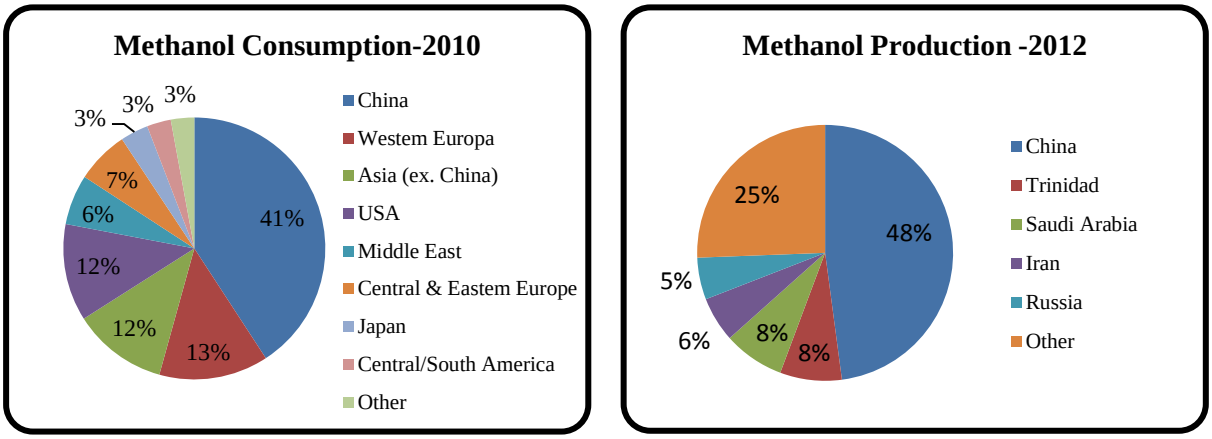


**Figure 1.7** – Global methanol consumption (2010) [20] and production (2012) [21] by region.

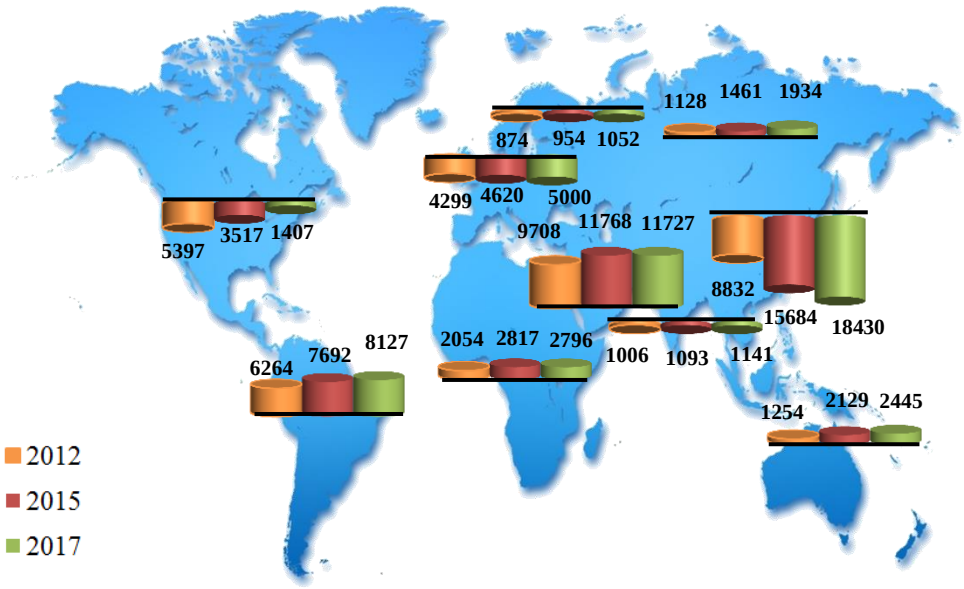


**Figure 1.8** – Methanol Net Exports (difference between total values of exports and imports) in thousands of tonnes by region. Positive values indicate that is a mainly exporter region and negative values indicate a mainly importer region. Adapted from [22].

One of methanol applications is in the automobile industry, being used in traditional vehicles without any modifications, normally in a mixture of 85% methanol with 15% gasoline named M85 [13]. When it is essentially pure methanol, it is called M100. This is a cleaner energy compared to other fuels [14], and it is adequate fuel for fuel cells, by its oxidation to $CO_2$ and hydrogen [2] and it is the simplest, safest and easiest way to store and transport liquid oxygenated hydrocarbon [2,13], since it is easier to handle when compared to hydrogen gas [13]. Regarding to its toxicity for humans, methanol by itself is not highly toxic but when consumed via oral, cutaneous or inhalation, it can cause methanol poisoning. Since in the human organism the formation of formaldehyde and formic acid from methanol catalysed by a alcohol (ADH) and formaldehyde (FaldDH) dehydrogenase occurs (Figure 1.9), resulting in metabolic acidosis, blindness, cardiovascular instability, and eventually death [23,24]. The intoxication can occur from the ingestion of contaminated alcohol beverages, with added methanol to adulter them, since methanol is much cheaper than ethanol [23]. Methanol can also be unintentionally formed during the fermentation of beverages with high pectin content.

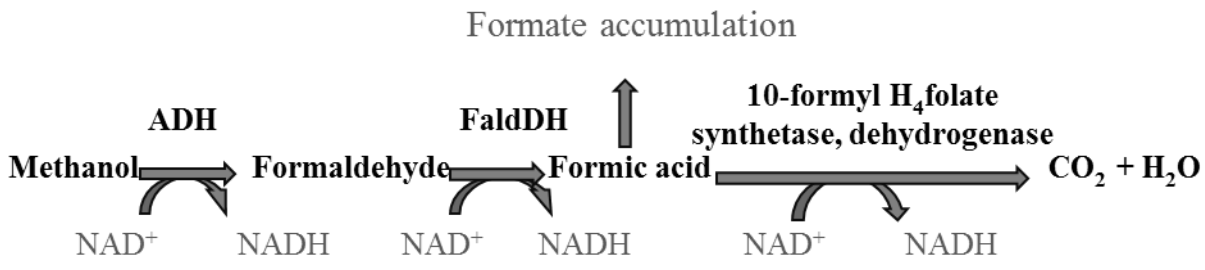


**Figure 1.9** – Methanol metabolism in humans, based on [23,24].

In the human organism, the formate produced by the methanol metabolization (Figure 1.9) is slowly eliminated, mainly by its oxidation to $CO_2$ [24]. So to prevent formate accumulation one therapeutic strategy is to inhibit the enzyme (ADH) with substances like fomepizole, or by adding another substrate that competes with methanol for enzyme binding site, such as ethanol [23], which produces a less toxic metabolite, acetaldehyde [25].

There has been much effort put into the development of methanol detection sensors, that are produced with ADH, to detect methanol in commercial beverages, such as a sensor for alcohols and aldehydes with ADH encapsulated in silica [26], as well as a sensor for formaldehyde analysis developed with a different dehydrogenase, recombinant formaldehyde dehydrogenase, FaldDH [27].

## 1.3. $CO_2$ TO METHANOL

As it was said before $CO_2$ is the most oxidized form of carbon [5], so it is in the lower energy level, and to chemically convert it without using a catalyst, additional energy is needed.

Carbon dioxide can be converted to other compounds using several approaches, namely:

- heterogeneous and homogeneous catalysis [6,16];
- electrochemical[6,11] ;
- photochemical [6,11];
- thermochemical [11];
- enzymatic catalysis [6].

Because $CO_2$ is rather inert, its chemical transformations are thermodynamically highly unfavourable [5]. For example, the non-catalysed conversion of $CO_2$ to methanol, has a Gibbs free energy value ($\Delta G$) of 3.30 kJ/mol (Eq. 2), being nonspontaneous. A large input of energy is required to overcome the energy barrier from the raw material lowest energy state, for its transformation into useful chemicals.

Traditionally to overcome this thermodynamic barriers, high-energy reactants are used such as epoxides (small-membered ring compounds), hydrogen, unsaturated compounds [5,6], organometallic catalysts (temperatures from 150 to 300 °C and pressures from 30 to 140 bar are needed [28]) [5]. Some other source of energy can also by supplied as light, electricity [5,6] or heat [6]. Also, the equilibrium can be shifted if the product is removed [5,6].

The thermodynamics of the main reactions of the methanol production via carbon monoxide and carbon dioxide hydrogenation (Eq. 1 and 2) with water - gas shift reaction (Eq. 3), in industry are showed below, Gibbs free energy (ΔG) and enthalpy (ΔH) at 25ºC and 1.013 bar.

Hydrogenation reactions are exothermic, having negative enthalpy (ΔH) values. The, CO hydrogenation is a spontaneous and exothermic reaction, with a Gibbs free energy value (ΔG) of – 25.34 kJ/mol, and a enthalpy value of - 90.8 kJ/mol. In industry, to avoid the accumulation of a large amount of reaction heat, the water - gas shift reaction (Eq. 3) occurs as a side reaction in conventional processes, consuming water from the carbon dioxide hydrogenation (Eq. 2) (driving force into the non-spontaneous carbon dioxide hydrogenation).

| | | | |
|---|---|---|---|
| $CO + 2\ H_2 \rightarrow CH_3OH$ | ΔH = - 90.8 kJ/mol [5,6,12] | ΔG = - 25.34 kJ/mol [14] | (1) |
| $CO_2 + 3\ H_2 \rightarrow CH_3OH + H_2O$ | ΔH = - 49.6 kJ/mol [5,6,12] | ΔG = 3.30 kJ/mol [14] | (2) |
| $CO + H_2O \rightarrow CO_2 + H_2$ | ΔH = - 41.2 kJ/mol [6] | ΔG = - 28.6 kJ/mol [14] | (3) |

In this work, a different strategy was used, taking advantage of enzymatic catalysis (Figure 1.10) in order to overcome these thermodynamic energy barriers, without the use of high temperatures.

The first enzymatic approach to this process was developed by Kuwabata *et. al.* [29] where the reduction of carbon dioxide to methanol is performed with formate dehydrogenase (FateDH) and methanol dehydrogenase (MDH) with electron mediators. Obert and Dave [30] studied a multi-enzymatic system with formate, formaldehyde and alcohol dehydrogenases (FateDH, FaldDH, ADH) in an aqueous medium, using β-Nicotinamide adenine dinucleotide in its reduced form (NADH) as electron donor [30]. More recently, other authors used this system with different matrix, as will be explained in the following sections (section 1.4 - Enzymatic conversion of CO2 to methanol) [31–34].

The enzymatic reduction of $CO_2$ to methanol can also be accomplished by photochemical NADH regeneration, by a processes such as production of methanol from formaldehyde catalysed by ADH [35], using hydrogen carbonate ($HCO_3^-$) as reagent to methanol production, catalysed by the enzymes FateDH, aldehyde dehydrogenase (AldDH) and ADH [36], and with photochemichal NADH regeneration.

Microorganisms can also achieve the conversion of $CO_2$ into other organic compounds. They use FateDH as the lead enzyme for the conversion of $CO_2$, and the reaction is the reverse of biological metabolic pathway reactions [28]. For example, microorganism *Methylosinus trichosporium* IMV 3011 reduces methane to $CO_2$ [37], and $CO_2$ to extracellular methanol, using the Poly-β-Hydroxybutyrate (PHB) as an endogenous reducing agent [38].

## 1.4. ENZYMATIC CONVERSION OF $CO_2$ TO METHANOL

In the present work, a biocatalytic system that uses carbon dioxide ($CO_2$) as reactant for the production of methanol, was studied. The reduction of $CO_2$ is catalysed by three oxido-reductases, which are dependent on the cofactor β-Nicotinamide adenine dinucleotide in its reduced form (NADH); formate (FateDH), formaldehyde (FaldDH) and alcohol (ADH) dehydrogenases. The enzymes are co-immobilized in a sol-gel matrix, and catalyse the sequential reduction of $CO_2$ to formate, formaldehyde, and methanol, presented in Figure 1.10.

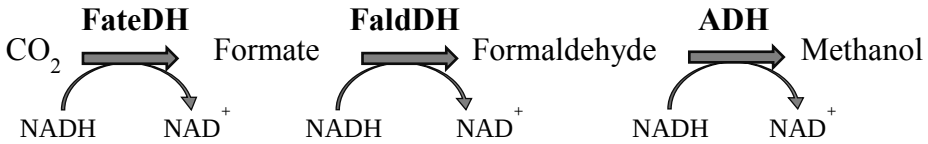


**Figure 1.10 –** Bioconversion of $CO_2$ to methanol, catalysed by FateDH, FaldDH and ADH.

This has been a widely studied strategy to convert $CO_2$ in a product of interest, such as is methanol.

In 1994, Kuwabata, *et. al.* [29], studied the electrochemical conversion of carbon dioxide to methanol using methyl viologen ($MV^{2+}$) or pyrroloquinolinequinone (PQQ) as an electron mediator and two enzymes FateDH and methanol dehydrogenase (MDH) as catalysts, the first enzyme reduces $CO_2$ to formate and the second enzyme reduces formate in formaldehyde and finally to methanol.

In 1999 Obert and Dave [30] performed the reduction of $CO_2$ to methanol, with the multi-enzymatic system, FateDH, FaldDH and ADH in aqueous medium, using NADH as electron donnor with the enzymes in solution and immobilized in an sol-gel matrix, the higher yields being respectively 21.0 % with 100 µmol NADH and 91.2% with 50 µmol NADH.

The same multi enzymatic system was used by El-Zahab, *et. al.* [31], with the addition of the *in situ* enzymatic cofactor regeneration (NADH), by adding a fourth enzyme, glutamate dehydrogenase (GDH), and glutamate, to the system used by Obert and Dave [30] and immobilizing the enzymes in polystyrene particles, (Figure 1.11) with an accumulated methanol yield of 127%, after 11 cycles of reusing.

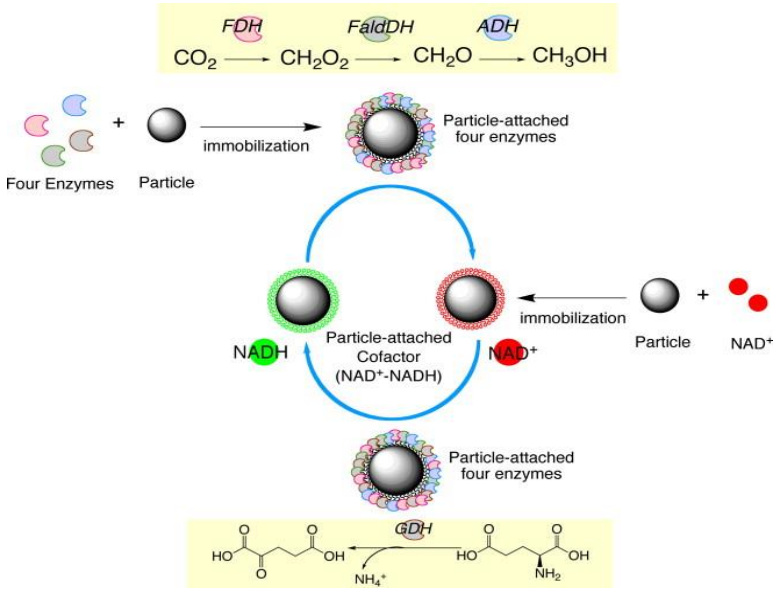


**Figure 1.11 –** $CO_2$ reduction to methanol by co-immobilized enzymes with *in situ* regeneration of NADH [39], performed by El-Zahab, *et. al.* [31].

Sun, *et. al.* (2009) [32] also used different matrices to immobilize the multi-enzymatic system with the three enzymes, by the entrapment in titania particles having a methanol production yield up to 60%. To enhance enzyme stability and reactivity Xu, *et. al.* [33], immobilized the three enzymes in a composite of sol-gel silica with alginate, and in 2012 Dibenedetto, *et. al.* [34], used this method coupled with the independent photocatalytic NADH regeneration, achieving a yields of approximately 95 % in the first utilization.

Previous work with the biocatalytic system under study, was developed within our laboratory, using ionic liquid [EMIM][$EtSO_4$] as the reaction medium. The biodiesel transesterification reaction was coupled with the $CO_2$ reduction to methanol, and its quantification was made indirectly by the production of fatty acid methyl esters (FAME), commonly known as biodiesel. An estimative of production of 0.7 mg/mL of methanol was achieved, with the enzymatic regeneration of the cofactor, NADH, also performed by adding a fourth enzyme glutamate dehydrogenase (GDH) and glutamate (Figure 1.12).

In the present work, the strategy is to reduce $CO_2$ into a liquid fuel, using the multi-enzymatic system described above. Also, ionic liquid is used as the reaction solvent, which is advantageous since the quantity of carbon dioxide dissolved in this reaction medium is enhanced and the separation is easier [40].

A more detailed description of the enzymes and of the whole biocatalytic system used in this work is presented in the following sections.

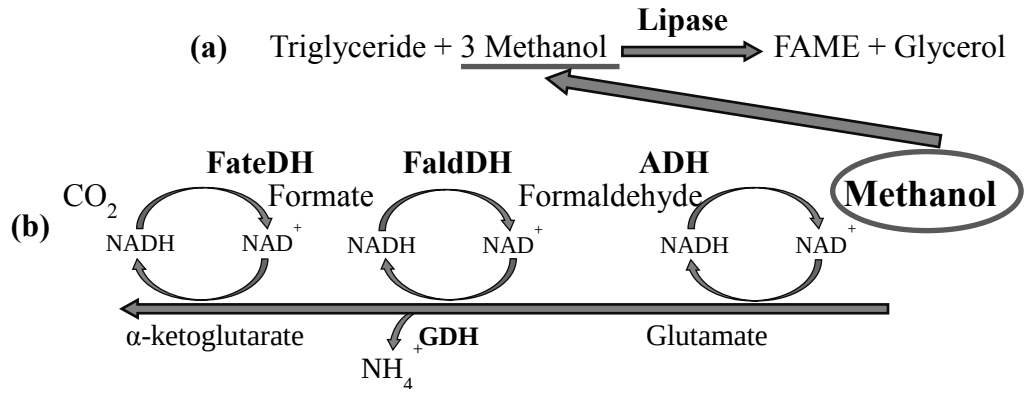


**Figure 1.12 – (a)** Conversion of methanol in biodiesel, catalysed by a lipase. **(b)** The enzymatic transformation of $CO_2$ in methanol, coupled with the *in situ* regeneration of cofactor NADH.

## 1.5. IONIC LIQUID (IL)

In this work, an alternative solvent was used, as a reaction medium for the byocatalytic system under study. A brief introduction of Ionic liquids (ILs) is presented here.

Ionic liquids are organic salts composed of cations and anions, which are liquid below a threshold temperature, normally 100ºC [40–42] and when they are liquid at room temperature are named room temperature ionic liquid (RTIL) [9,43]. This is due to a non-efficient ion packing, of their structures [9].

ILs are able to dissolve both organic and inorganic species [41,44] and are 'tailored solvents', because with the different combinations of anions and cations [44] it is easy to change their properties than for organic solvents. [9,41,43]. They can be consider possible "green" solvents since they are not volatile and it may be feasible to recycle and repeatedly reuse [9,41],in comparison with organic solvents [43], although their synthetic process is not normally an environmentally friendly one.

ILs have a very attractive of properties. One of them is their water miscibility, which varies from immiscible to fully miscible [10,40] being mainly determined by the anion [10]. Other parameter from IL is the polarity, is also dependent on its ionic species, polarity decreases with the increase of anion size [10]. Their vapour pressure is considered as negligible [9,41,44], so they are non-volatile [42] [41,43]. They are also chemically stable and non-flammable [44]. This is useful to remove volatile products, such as methanol, for example. They can even be used in vacuum processes [43], sublimation, distillation or supercritical extraction [40].

Another important property of the ionic liquid is their high viscosity, as a result of the strong electrostatic and other interaction forces between the solvent molecules [41,43]. For example, [BMIM][$BF_4$] has a viscosity similar to ethylene (19.6 cP at 25 ºC), much higher than water (0.9 cP at

25 ºC). The viscosity is mainly dependent of the alkyl chain length of the cation, being directly proportional to it [43].

ILs different properties enables its applications on diverse areas, exemplified in Figure 1.13..

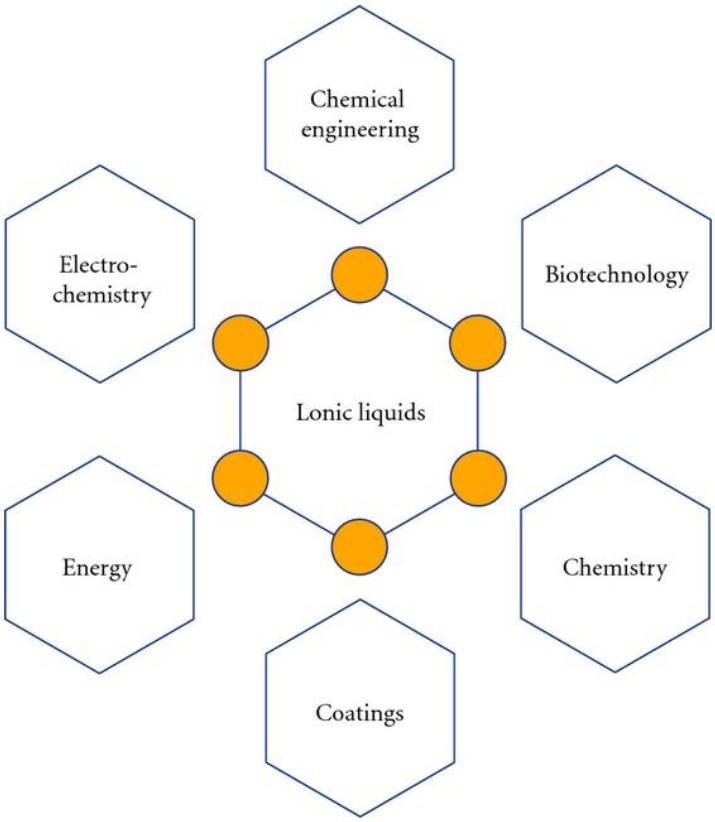


**Figure 1.13 –** Ionic Liquids applications [41].

Regarding $CO_2$ solubility, ILs can dissolve carbon dioxide but the opposite phenomenon is not observed [40,45]. If $CO_2$ is at is supercritical fluid form (sc-$CO_2$), it has a high solubility in ionic liquid, with mole fraction of more than 0.6 [46]. [EMIM][$EtSO_4$] is an example of an IL than can dissolve a molar fraction of $CO_2$ ($X_{CO2}$) of 0.421 ,at a temperature of 40ºC and pressure of 92.68 bar [45]. IL [BMIM] [$BF_4$] at temperature of 40ºC and at pressure of 100 bar presents $X_{CO2}$ of ca. 0.72, and for the same temperature but at a pressure of 10 bar, $X_{CO2}$ of only 0.1 [47].

Nowadays, ILs are known to raise some concerns in terms of their toxicity [9]. To overcome that, some strategies are under development, like synthesis of ILs using biomolecules (amino acids, betaines, choline, etc.) [44].

## 1.6. BIOCATALYSIS

In the biocatalytic system under study, where the reduction of $CO_2$ to methanol takes place (Figure 1.10) the biological catalysts used are three oxido-reductases – FateDH, FAldDH and ADH with the enzyme classification – EC 1 by the classification system of the Enzyme Commission.

In catalysis, a molecule accelerates a chemical reaction by lowering the activation energy required to the reaction- the catalyst. It forms a chemical bond with the reacting molecules, allowing them to react to a product, and detaches from the catalyst without being chemically altered in the process. The catalyst may be an atomic specie, molecules or larger structures such as zeolites or enzymes. In biocatalysis specifically, natural catalysts are used, such as an isolated enzyme or a microorganism in a fermentative process to perform chemical transformations.

The main enzymes used in biocatalysis are divided in six groups, represented in Table 1.1.The enzymes used for the bioconversion of $CO_2$ to methanol are members of the group of oxido--reductases, commonly known as dehydrogenases or oxidases. Dehydrogenases use substances called coenzymes, to catalyse the electron transfer from one molecule (reductant) to another (oxidant).

**Table 1.1 -** Classification of enzymes by the type of chemical reaction catalysed [16].

| Type of chemical reaction catalysed | Enzyme type | Enzyme classification |
|---|---|---|
| Oxidation – reduction | Oxido-reductases | EC 1 |
| Transfer of functional groups | Transferases | EC 2 |
| Hydrolysis | Hydrolases | EC 3 |
| Addition and elimination | Lyases | EC 4 |
| Isomerization | Isomerases | EC 5 |
| Carbon bond formation | Ligases | EC 6 |

One alternative to biocatalytic systems that use enzymes as catalysts (Figure 1.10), are systems where the catalysts are microorganisms, and this presents several advantages and disadvantages. One of the advantages of using microorganisms is to replace multi-step processes by the conversion of a starting material into the end product through a metabolic pathway. Also there is no need of recovery or purification of intermediate products like NADH [16,48] or enzymes [48] and processes such as cofactor regeneration can be carried out by the living cell [16].

The disadvantages of using microorganisms are the possible inhibition of the reaction by the substrate and/or product, and its toxicity to the cells [48] and also resources can be consumed for biomass production in fermentation [16].

Regarding enzymes, their potential is still not totally explored, with a estimative of only less than 1% of the microorganisms in the environment were cultured and had their enzymes identified. Although many enzymes are commercially available to this date, some are less expensive than others, depending if they are already from recombinant sources and on the degree of difficulty of their isolation [49], since they are normally highly specific [49,50]. The majority of the enzymes that are used do not require cofactors (hydrolases, transferases, lyases and isomerases) [16], however their activity can be limited by inhibition [50].

Compared with microorganisms, enzymes also have the advantage of not dispensing resources for biomass production, and do not require careful conductions to keep them alive [16]. Enzymes work in a wider range of temperature, pH, solvent (up to working in almost aqueous free environments) and pressure [10,16], and enable the conversions to take place under much more concentrated conditions [16].

Nonetheless, when dissolved in the reaction medium it is difficult to retain enzyme activity [49]. A solution for this problem can be enzyme immobilization, in which an interaction between the enzyme and the carrier occurs [49], through covalently or non-covalently bonding. The immobilization of enzymes onto solid materials can be traced back to the 1950s [51], and in the past years the major focus was the development of robust enzymes that are not only active but also stable and selective in hostile conditions [51]. The immobilization enables continuous processing and reutilization of the biocatalyst [16,49] and confers some protection to the enzyme core when exposed to organic solvents [49,51].

### 1.6.1. ENZYMES – OXIDO-REDUCTASES

In this work, three NADH dependent oxido-reductases were used in a "one-pot" system with formate, formaldehyde and alcohol dehydrogenase, for the catalytic reduction of $CO_2$ to methanol. Figure 1.14 describes the oxidation–reduction reactions between the different substrates and the cofactor, NADH.

Enzymes are normally proteins and they have high catalytic power and specificity. With dimensions much larger than the dimensions of the substrates, only some catalytic residues bind to the substrate (and the cofactor, if any) by multiple weak attractions, and carry out the reaction. These active structures are defined as the enzymes' active site.

In terms of structure, the active sites are normally a three-dimensional cleft or crevices formed by groups that come from different parts of the amino acid sequence.

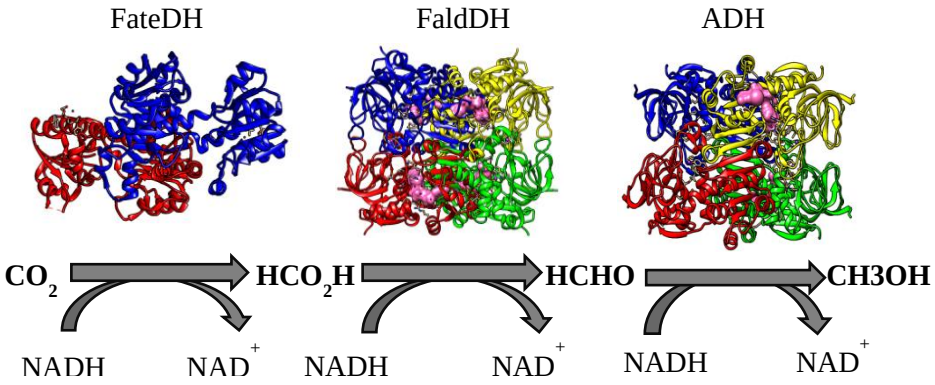


**Figure 1.14 –** Conversion of $CO_2$ to methanol catalysed by oxido-reductases – formate (FateDH), formaldehyde (FaldDH) and alcohol (ADH) dehydrogenases.

The flexibility of the enzymes enables a close contact between the enzyme and the substrate is necessary to their interaction, leading to the active sites being markedly modified by the binding of substrate. The arrangement of the atoms in an active site also determinates the specificity of binding.

Oxido-reductases are structurally divided in two domains, mainly the "NAD binding domain" and "catalytic domain". The "NAD binding domain'' displays a Rossmann fold structure with a spatially conserved area [52,53], two units (βαβαβ) arranged in a supersecondary structure [54] responsible for recognition and binding of the NADH or $NAD^+$ molecules in an active conformation. The "catalytic domain" contains the amino acid residues essential for catalysis, correctly oriented in the active site and is specific for the particular enzyme [53].

The reduction of the cofactor NADH by the oxido-reductases proceeds as follows, with the respective reaction in the Figure 1.15, more specifically:

- cofactor and substrate bind to an enzyme;
- the substrate is reduced, while the cofactor is oxidized;
- the cofactor and product dissociate from the enzyme [39,55].

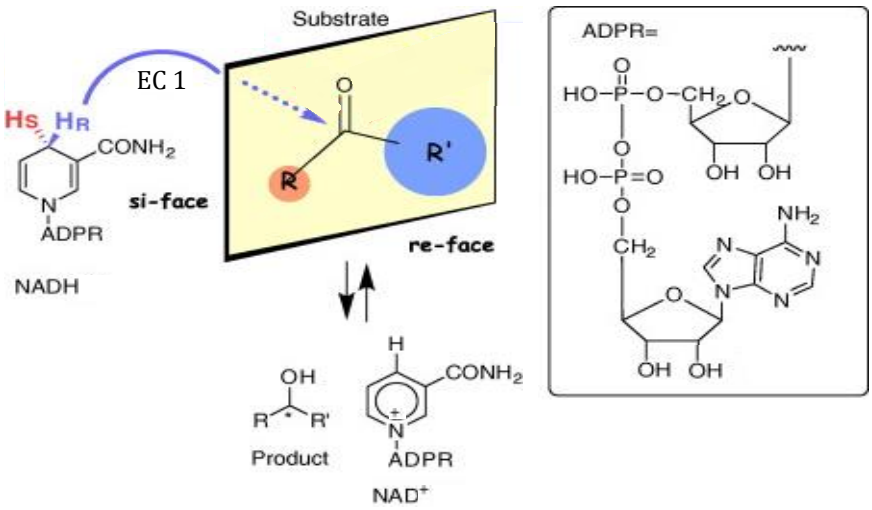


**Figure 1.15 –** Oxidation – reduction reaction between the coenzyme - NADH, and a subtract, catalysed by oxido-reductases (EC 1). Adapted from Matsuda, *et. al.* [39].

In industry, oxido-reductases can catalyse reactions that conventional chemical catalysts fail to [56]. For example they have the ability to work in mild conditions and tolerate impurities such as sulphur compounds (from the combustion gases) that are toxic to some chemical catalysts. However, to regulate and optimize oxido-reductase activity, some important parameters need to be controlled like temperature, pH and ionic strength (I) of the media. A theoretical study from Baskaya, *et. al.* [28] indicates that the most sensitive parameter in the specific case of methanol production is pH. For pH values lower than 6, there is a favourable reaction for methanol production, and the opposite occurs for pH values higher than 6 [28]. Nevertheless, it must be noted that NADH is unstable at low pH [57–59]. From the work of Baskaya *et. al.* [28], it is also known that the production of methanol should be favoured by conducting the redox reactions at low pH and low ionic strength, combined with high temperatures. The values for ΔG were obtained with ionic strength (I), pH and temperature ranging from 50 to 225 mM, 4 to 37ºC and pH 2 to 7, respectively. The lowest ΔG value is -127.11 kJ/mol for I of 50mM, pH 2 and a temperature of 37ºC [28].

In this specific work, with the enzymes used FateDH, FaldDH and ADH and the catalysed reactions, it is not possible to use these pH and ionic strength parameters, because the low pH and high temperature can have denaturation effects, and the pH can be more difficultly controlled at low ionic strength [28]. A solution for this, may be enzyme engineering, with the utilization of whole cells and combined systems [28,60].

One of the major challenges that the biocatalytic system under study presents, are the low reaction yields and rates, making it not suitable to an industrial scale system for $CO_2$ conversion [28]. There are many reasons for the low yields of this system. For example, if the reaction is conducted in an aqueous medium, enzymatic deactivation can occur by the formation of carbonic acid from the contact of the reactant, $CO_2$, with water. Activity of the enzymes can also be challenged by the

reaction of the enzymes amine groups with $CO_2$, and the formation of carbamates [10] and other species such as $CO_3^{2-}$, $HCO_3^-$, and $H_2CO_3$, that also have an impact in the pH [28], so a buffered medium must be used.

Oxido-reductases are also known to be active in non-aqueous solvents, but their immobilization is necessary in some cases, to stabilize the enzyme [39].

This study also presents the drawback of using NADH as electron donor, 3 moles of NADH per mole of methanol produced. As the cofactor is relatively expensive, its regeneration is mandatory. To render an economically feasible enzyme-catalysed reduction [55], several methods were developed to recycling NADH and can be classified into several categories for instance:

- chemical regeneration [34,61–64], with catalyst such as sodium dithionite [34] and ruthenium (II) and rhodium (III) complexes [61];
- enzymatic regeneration [31,39,56,61–70] mainly by the following oxido-reductases:
    - GDH with glutamate as subtract [31];
    - ADH with ethanol as subtract [62];
    - NADH oxidase [63];
    - lactate dehydrogenase with lactic acid as subtract [65];
    - FateDH with formic acid [66];
    - glucose dehydrogenase [67] and glucose-6-P dehydrogenase[68].
- microbial regeneration [37,56,62–64,71], with microorganisms as *Geotrichum candidum* [71] and *Methylosinus trichosporium* IMV 3011 [37];
- photochemical regeneration [34,39,56,61–64,69] with photocatalyst such as $siO_2$-supported quantum dots [56], transition metal systems [34] and carbon nitrate [69];
- electrochemical [31,34,39,56,61–65,69,70,72–74] using as an example glassy carbon [64] or gold electrodes [72], vanadium-silica xerogels [70] rhodium mediators [73] and carbon nanofibers cathode [74].

### 1.6.2. FORMATE DEHYDROGENASE (FATEDH)

Formate dehydrogenase (FateDH) is the lead enzyme in the biocatalytic system under study (Figure 1.14) catalysing the reversible reduction of $CO_2$ to formate, and in nature it catalyses the reverse reaction, oxidizing formate to $CO_2$, using $NAD^+$ as cofactor, Figure 1.16.

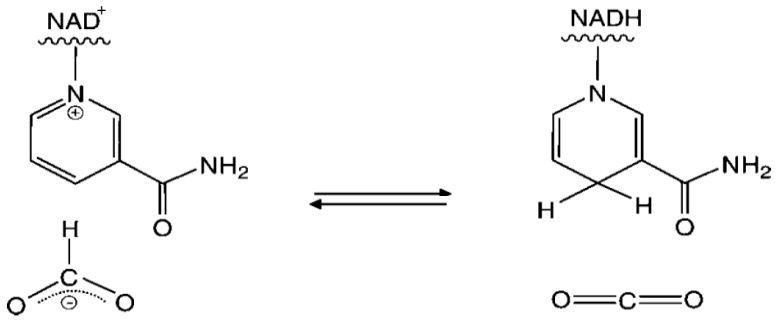


**Figure 1.16 –** Oxidation of formate to $CO_2$ catalysed by FateDH, using $NAD^+$ as cofactor [75].

Formate dehydrogenase is classified as EC 1.2.1.2 [52,76–78] by the classification system of the Enzyme Commission. It is possibly the most suitable model for investigating the general mechanism of catalysis involving hydride transfer [52,76]. It is also a catalyst to coenzyme regeneration [55,66,76], and in laboratory and pilot scale it is used for the production of bulk drug substances and agricultural products [52], and in fine organic and asymmetrical synthesis for production of highly value products [52,76]. It is also in high demand from the pharmaceutical and agrochemical industries [52].

FateDH plays a key role in some organisms. In methylotrophs microorganisms, it catalyses the terminal step of catabolism of $C_1$ compounds [76], having an important role in the energy supply [52,76] and as supplier of reducing equivalents. Methylotropic bacterium oxidizes methanol to $CO_2$ both through cyclic mechanisms or by chain dehydrogenases, although methylotropic yeasts oxidizes methanol to $CO_2$ via formaldehyde [76]. In prokaryotes and eukaryotes it is involved in methanol metabolism and in plants as a stress response [52,66].

FateDH is normally a homodimeric enzyme [52,76,79] (Figure 1.17 (a)) and does not contain metal ions or prosthetic groups [52,76]. It is active over a wide pH range (pH 5.5–11.0) [52,66], and can therefore be combined with almost any other dehydrogenase [52]. In the microorganism *Pseudomonas sp.*, FateDH is constituted by 393 amino acid residues [53,76] with a molecular mass of 86 kDa [53]. FateDH from *E. Coli* it is a 79 kDa polypeptide, is a component of the anaerobic formate hydrogen lyase complex [80].

The dimeric FateDH used in this work (Figure 1.17 (a)) is from the microorganism *Candida boidinii* and has 364 amino acids residues [52], corresponding to a molecular mass of 36 kDa per subunit [76,79], with a molecular mass of 74 kDa [79] for the two subunits. Its thermal inactivation temperature is 55ºC [52,76], with an isoelectric point (pI) of 5.4 [76], a pH optimum between 7.5 and 8.5 [79], a $K_m^{NAD^+}$ of 90 µM and $K_m^{formate}$ of 13 mM at 30ºC and at pH 7.5 [76]. Each subunit possess an independent active centre, and are non-metal containing enzymes[76,78].

The FateDH monomer from *Candida boidinii* contains of 15 α-helices and 13 β-strands [52] that are arranged into two domains [52,76], called the ‘‘NAD binding domain’’ and ‘‘catalytic domain’’. They are linked by two long helices, and are separated by a deep cleft where the active site is located [52].

The “NAD binding domain” with the residues N119 to S313 (Figure 1.17 (b)) displays a Rossmann fold structure (see 1.6.1 Oxido-reductases). The “catalytic domain” is formed by the remaining residues and has a flavodoxin-like topology [52]. The active site residues are located on the base of the cleft between the two domains, presented in Figure 1.17, with the conserved residues N119, V123, T256, D282, H311, S313, and G314 [52]. The residues R258 and N119 bind formate in the active site, and formate can be fixed between H311 and the nicotinamide ring [52]. The nicotinamide ring contacts with residues D282 and S313, and R174 binds the phosphate linker in $NAD^+$. The adenine ring can also interact with H232 and Y196 [52].

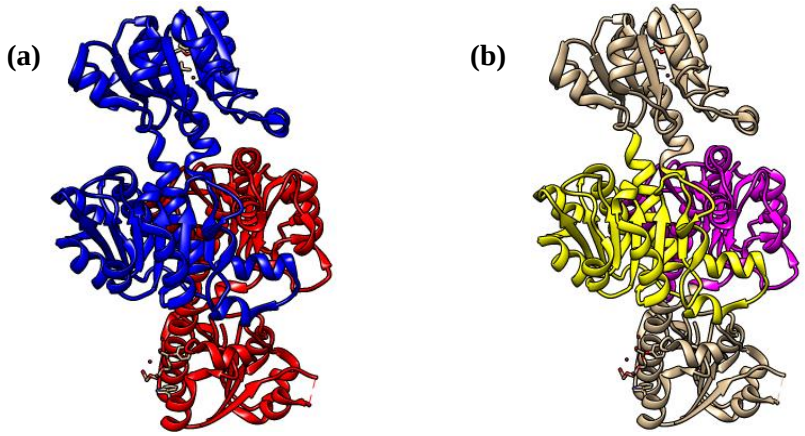


**Figure 1.17 –** Representation of FateDH from *Candida boidinii*; (**a)** with the different subunits in blue and red; (**b)** with the “NAD biding domains” in the colours yellow and magenta and the “catalytic domains” in beige. Structures from Protein data Bank (PDB) ID: 2J6I [52]. Sructures were produced using the program UCSF Chimera version 1.7.

### 1.6.3. FORMALDEHYDE DEHYDROGENASE (FALDDH)

Formaldehyde dehydrogenase (FaldDH) is the intermediate enzyme in the biocatalytic system described in Figure 1.14, catalysing the reduction of formate to formaldehyde, and in some organisms the reverse reaction to metabolize the toxic compound - formaldehyde [24,27,81], that can damage proteins, lipids and DNA [24,82].

FaldDH is classified as EC 1.2.1.46 [81,83] by the classification system of the Enzyme Commission. And it is a member of the zinc-containing medium-chain dehydrogenase/reductases family, in which ADH is also included [81,83,84].

The majority of the FaldDH requires $NAD^+$ and glutathione to perform the chemical reactions [81,85]. As examples FaldDH from the liver of organisms such as humans, rats [85], bovines [86] and *Candida boidinii* [79] are glutathione dependents.

The dimeric FaldDH from *Candida boidinii* has a molecular mass of 80 kDa [79] and from bovine liver haves a molecular mass of 82 kDa [86]. The FaldDH used in this work is from the microorganism *Pseudomonas sp.* and does not require the addition of the glutathione cofactor [81,83,87]. Another unique characteristic of this enzyme is that it is a nicotinoprotein, having an intrinsic tightly bound β-nicotinamide adenine dinucleotide or β-nicotinamide adenine dinucleotide phosphate in their reduced or oxidised forms (NAD(P)(H)) [81,83]. It catalyses the oxidation and reduction of aldehydes, without the release of cofactor from the enzyme to the media [83]. FaldDH from *Pseudomonas putida* is a homotetramer of identical subunits, in each subunit the two domains present are separated by a cleft, containing the "NAD binding domain" and the "catalytic domain" being the last one responsible for subtract binding and specificity [81,83].

The FaldDH tetramer from *Pseudomonas putida*, can be considered to be a dimer of dimers, because each dimer is composed of two subunits (Figure 1.18 (a)). Each subunit haves 398 amino acid residues [81,83] arranged in 17 α-helices and 16 β-strands [83], a molecular mass of 42 kDa [81,83] and two zinc ions [81,83,87], one catalytic and the other structural. The tetramer has a total molecular mass of 170 kDa [81,83], is thermal stable until 40ºC, an pI of 5.3, is active from pH 5 to 10, an optimum pH of 8.9 [85], a $K_m^{NAD^+}$ of 56 µM and $K_m^{formaldehyde}$ of 67 µM at 25ºC and at pH 7.8 [88].

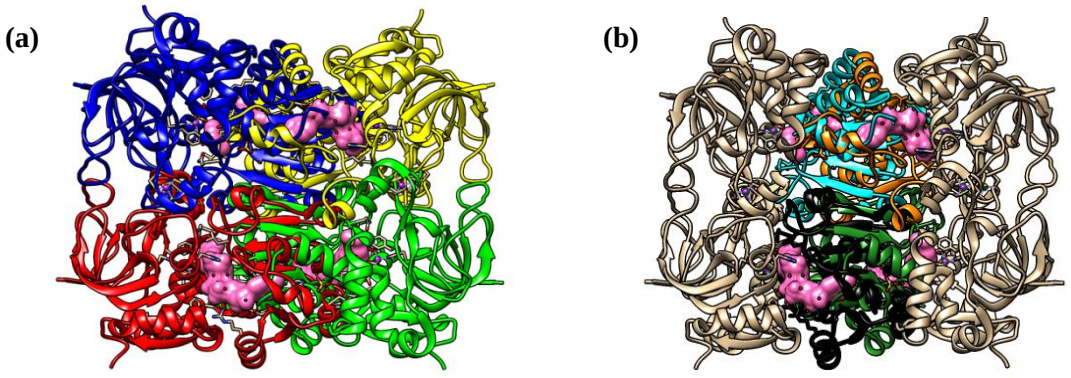


**Figure 1.18 –** Representation of FaldDH from *Pseudomonas putida*, with NAD represented in pink, zinc atoms in purple; **(a)** with the different subunits in yellow, green, blue and red; **(b)** with the "NAD biding domains" in the colours cyan, orange, green and black and the "catalytic domains" in beige. Structures from PDB ID: 1KOL [83]. Structures were produced using the program UCSF Chimera version 1.7.

As well in FateDH, the "NAD binding domain" from FaldDH contains a Rossmann fold structure, composed by a smaller domain of 167 residues, from the residues L171 to Q337 [81,83], Figure 1.18 (b). The "catalytic domain" is the larger domain with 231 residues, it is contained between residues S1 to I170 and between residues T338 to A398 [81,83].

Two zinc ions per subunit are bound to the ligands within the "catalytic domain". The catalytic zinc is bound to a water molecule and three protein ligands from the catalytic domain the C46, H67 and D169, Figure 1.19. The structural zinc is bound to four protein ligands from the catalytic domain. The ligands are sulphur atoms from four cysteines. The cysteines are C97, C100, C103 and C111 [81,83], Figure 1.19.

The NAD(H) molecule is connected to the protein surface through six hydrogen bonds, Figure 1.19. Three hydrogen bonds exist between the carboxyamide group of the nicotinamide ring and the protein residues T338, G336, P299. Another three hydrogen bonds exist between the hydroxyl group of nicotinamide ribose and the protein side-chain S48, and two hydrogen bonds with H51. There are more hydrogen bounds between the NADH and the protein surface namely with the residues G47, V197, R222, D217, R267 and H269 [81,83].

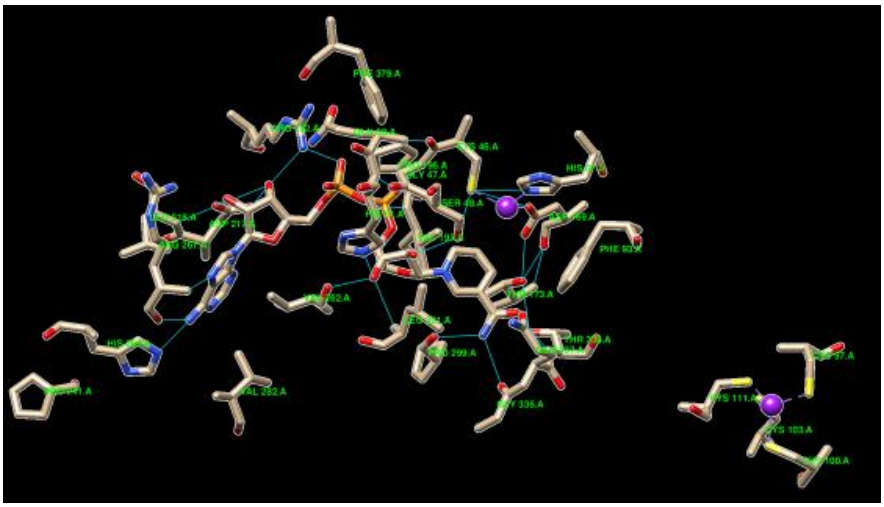

**Figure 1.19 –** Representation of NAD(H) binding to the active site, and the zinc (purple) binding site. Structures from PDB ID: 1KOL [83]. Structure produced using the program UCSF Chimera version 1.7.

### 1.6.4. ALCOHOL DEHYDROGENASE (ADH)

Alcohol dehydrogenase (ADH) is the final enzyme in the biocatalytic system under study (Figure 1.14) catalysing the reversible reduction of formaldehyde to methanol. It is our primary

defence against alcohol poisoning, catalysing the oxidation of a primary alcohol into an aldehyde or a secondary alcohol to a ketone [89–91], (Figure 1.20), using $NAD^+$ as cofactor. A scheme of the methanol detoxification in humans is in Figure 1.9.

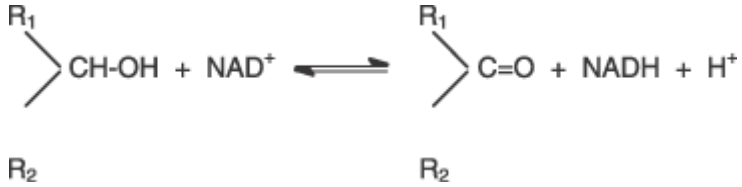


**Figure 1.20 –** Oxidation of an alcohol in to an aldehyde or a ketone catalysed by ADH, using $NAD^+$ as cofactor [91]. $R_1$ and $R_2$ are stand for alkyl groups.

Alcohol dehydrogenase is classified as EC 1.1.1.1 [91] by the classification system of the Enzyme Commission. As FaldDH is a member of the zinc-containing medium-chain dehydrogenase/reductases family [81,83,84,91].

ADH is a isoenzyme [91], from 4 diverging groups of organisms: vertebrates, plants, eukaryotic microorganisms and prokaryotic bacteria [91].

The homotetrametic ADH (4 identical subunits) [92], has a pI between 5.4 and 5.8, an optimum pH between 8.6 and 9.0 and a molecular mass of 141 to 151 kDa. Ethanol is the best subtract to the enzyme, indeed the methanol activity of the enzyme at pH 8.8 is only 0.07% of its ethanol activity [91].

The ADH used in this work is from the yeast Saccharomyces cerevisiae, represented in Figure 1.21, also named YADH has three isoenzymes: YADH-1 YADH2 and YADH3. They are analogues to horse liver alcohol dehydrogenase. It was one of the first enzymes to be purified and isolated. The subunits separated by a cleaf in the “NAD binding domain” and the “catalytic domain”, this one is the biggest it 3/5 of all amino acids[91].

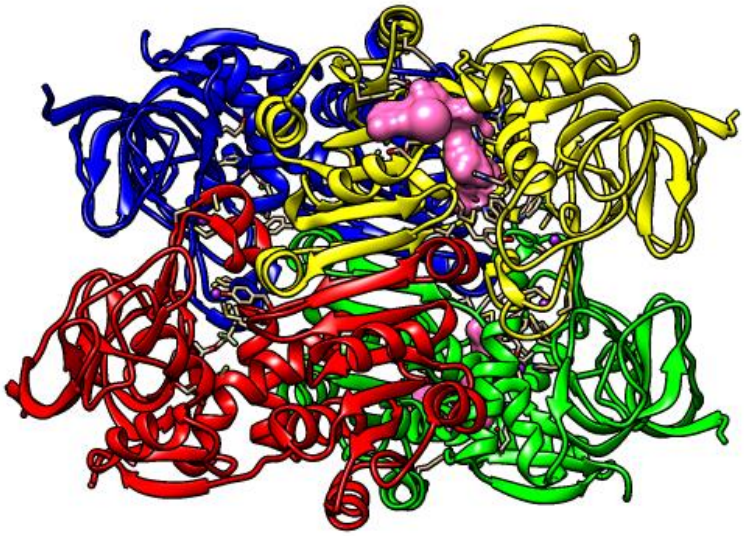

**Figure 1.21 –** Representation of ADH from *Saccharomyces cerevisiae*, , with a NAD analogue represented in pink, zinc atoms in purple; with the different subunits in in yellow, green, blue and red; Structures from Protein data Bank (PDB) ID: 2HCY [93]. Structures were produced using the program UCSF Chimera version 1.7.

Each subunit is constituted with 347 amino acid residues, with a molecular mass of 36 kDa and 2 Zn atoms, one with a structural play and the other catalytic [91]. The total molecular weight of proximally 150kDa [92]. In relation to its properties it has an optimum temperature and pH of 35ºC and 7.5 [94] and a $K_m^{NAD+}$ of 4.6 mM at 25ºC and a pH 8.2. [88].

The catalytic zinc is bound in the "catalytic domain" to C46, H67 and C174, and the structural zinc is bound to cysteines C 97, C100, C103 and C101 [91]. Also in Figure 1.22 is represented a model of the active site from ADH.

ADH can be utilized as a sensor for alcohols, aldehydes [26] and NADH in aqueous samples.

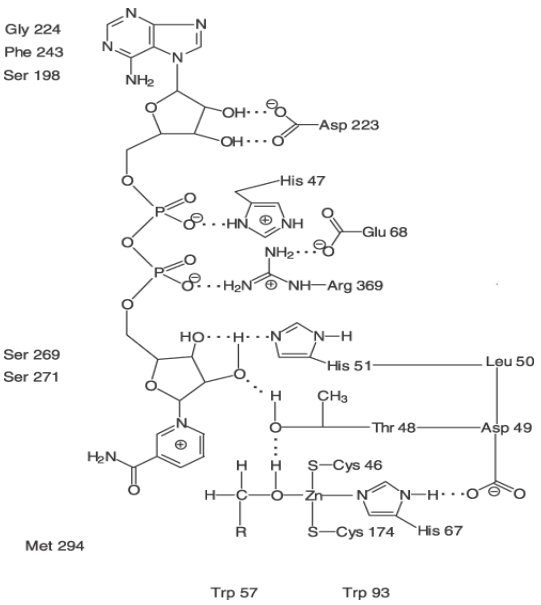


**Figure 1.22 –** Model of the active site of ADH [91].

## 1.7. BIOCATALYSIS IN ILS

The most common ionic liquids for biocatalysis are the imidazolium based ionic liquids [43], but when water is present they can dissociate into independent cations and anions, affecting protein stability as described in the Hofmeister series [10].

1-alkyl-3-methylimidazolium ionic liquids, (abbreviated $[C_nmim]^+$, where n number of carbon atoms in a linear alkyl chain, or [Xmim] (where X is M, E, P,B, etc. for a1,2,3,4,ect. carbon atoms in a linear alkyl chain), are unreactive with water and are the most widely used for biocatalysts. They are polar solvents and they are miscible with other polar solvents, enabling an increase of the solubility of polar compounds, like methanol, leading to faster reactions and changes in selectivity [41,43].

Zhang *et. al.* studied the negative effect of IL[BMIM][$PF_6$] on the activity of YADH (Yeast Alcohol Dehydrogenase) (Figure 1.23) [95]. The authors studied the effect of:

- resulting F- from hydrolysis in a basic medium;
- ions $Cl^-$ and $Br^-$;
- impurities in the ionic liquid;
- imidazole cation [95];

Concluding that the inhibition is mainly caused by competition of the imidazole group of [Bmim][$PF_6$] with the coenzyme $NAD^+$ for the binding sites on YADH[95].

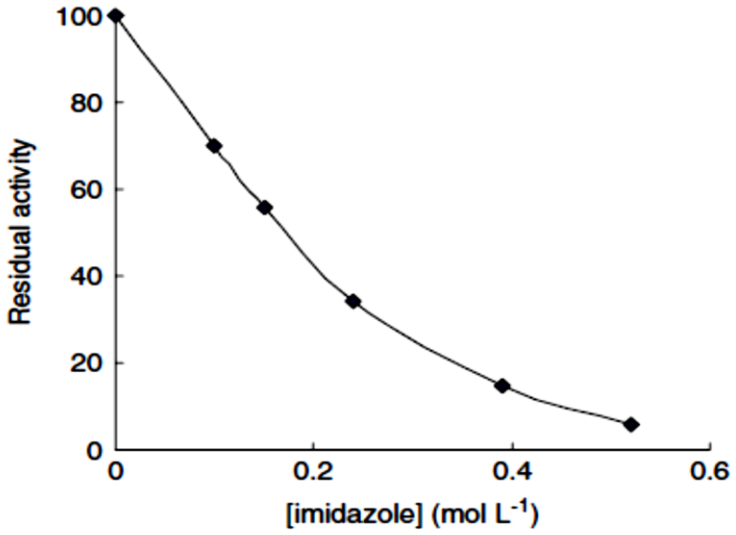


**Figure 1.23 –** Residual activity of YADH at different imidazole concentrations [95].

Oxido-reductases retain its activity in non-aqueous solvent, namely when suspended in ionic liquids [43], but immobilization is necessary for some cases to stabilize the enzyme [39]. Table 1.2 presents some examples of oxido-reductases reactions in different ILs.

**Table 1.2 -** Examples of enzymatic reaction with oxido-reductases in ionic liquid medium

| Ionic liquid | Enzyme | %(v/v) | Enzyme activity (%) * | Reference |
|---|---|---|---|---|
| [MMIM][$MeSO_4$] | FateDH | 75 in buffer | 98 | [42] |
| [$Et_3NMe$] [$MeSO_4$] | FateDH | 75 in buffer | 55 | [42] |
| [BMIM] [OTf] | FateDH | 25 in buffer | 38 | [42] |
| [BMIM][OTf] | YADH | 25 in buffer | < 5 | [42] |
| [MIm] [Cl] | TBADH | 0.3mM | 30 | [96] |
| [MIm][$BF_4$] | TBADH | 0.3mM | 40 | [96] |
| [BMIM][$BF_4$] | TBADH | 700mM | 0.1 | [96] |
| [BMIM][Cl] | TBADH | 700mM | 0.06 | [96] |
| [BMIM][$BF_4$] and [BMIM][OTf] | HLADH | 0.4mg/ml | 0 | [97] |
| [BMIM][$NTF_2$] | LB-ADH | Biphasic system | --- | [98] |

* Comparison to the activity in pure buffer solution)

## 1.8. CHARACTERIZATION METHODS

In this work, the multy-enzymatic system was immobilized in a sol-gel matrix, and the reactions were performed in a polar IL, [BMIM][$BF_4$]. Results are presented into the following chapter.

To evaluate indirectly the amount of methanol produced by the multy-enzymatic system, two main sets of experiments were performed, one using aqueous medium and another using ionic liquid as reaction medium.

In aqueous medium, an experiment using UV/Vis spectroscopy was used and the measurements of methanol production were made indirectly, by following NADH absorbance at 340 nm at different reaction times, i.e. meaning NADH conversion into $NAD^+$.

When using IL as reaction medium, a direct quantification of methanol was conducted through HeadSpace Gas Chromatography (HS-GC) and Nuclear Magnetic Resonance (NMR).

A brief description of this technique is present in this section.

### 1.8.1. HEADSPACE GAS CHROMATOGRAPHY (HS-GC)

Chromatography is a widely known separation technique, having a stationary phase (a column) and a mobile one that separates compounds according to their different affinity with the stationary phase. In particular, in gas chromatography, there is a solid or liquid stationary phase (capillary column) and a gaseous mobile phase (inert gas such as $H_2$, He, Ar, $N_2$, etc.), and the compounds can be separated according to their affinity (polarity) for the stationary phase and its boiling point. In this technique, an aliquot from a liquid sample is collected and vaporized in the injector before entering into the column.

In Headspace gas chromatography (HS-GC), namely static headspace, the sample is heated in order to vaporize the analytes in a previous incubation step, occurring a partition between the liquid phase and the gas phase. After the partition, an aliquot of the vapour phase is directly injected in the column, diminishing the solvent interference. The quantification can be made with an internal standard or with a calibration curve. A diagram of the HS-GC apparatus is presented in Figure 1.24.

HS-GC, is a largely used analytical technique for the determination of volatile substances in solids and liquids [99] and in this experiment was used to measure directly the amount of methanol in the IL reaction medium.

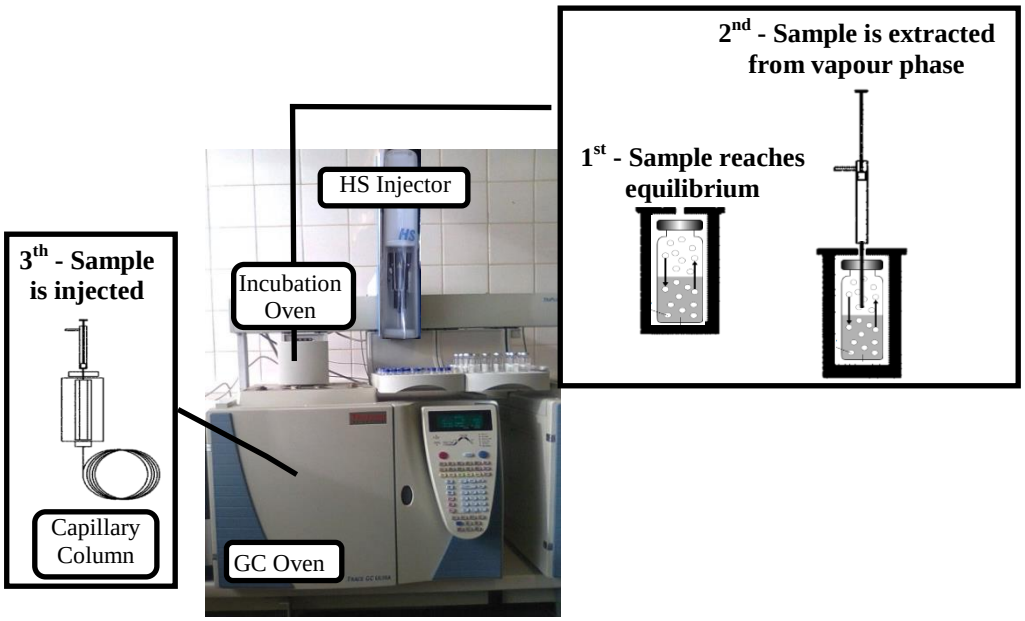


**Figure 1.24 –** HS-GC system components with the experimental procedure.

### 1.8.2. NUCLEAR MAGNETIC RESONANCE (NMR)

Nuclear Magnetic Resonance (NMR) spectroscopy is a very powerful analysis and quantification technique. It is based on the study of the transitions from different energy levels by atomic nucleus, induced by an intense external magnetic field ($B_0$). The nuclei can align or oppose against the magnetic field, resulting in the splitting of the initially degenerate energy levels (Figure 1.25). Only nuclei that possess spin, with a spin quantum number (I) value different than zero and have an even number of protons and neutrons, respond to NMR [100,101].

The spin has 2I + 1 different possible orientations relative to an axis, with I values of $^1/_2$, 1, $^3/_2$, and so on. For I=0 there is no spin value [100,101].

The most common nuclei studied is the hydrogen proton $^1$H, in which deuterated solvents (with $^2$H instead of $^1$H) are used to avoid a solvent-signal interference peek. But spectra of several different nuclei can be obtained, such as $^{13}$C, $^{15}$N, $^{19}$F and $^{31}$P [100,101].

The NMR signal is proportional to the population (N) difference between the two energy states (α and β). The ratio of N is in accordance with the Boltzmann distribution, (Eq. 4) where ΔE is the difference of energy between the spin states, k it is the Boltzmann constant and T is the temperature [100].

$$\frac{N_\beta}{N_\propto} = e^{-\Delta E/kT} = 1 - \frac{\Delta E}{kT} \quad (4)$$

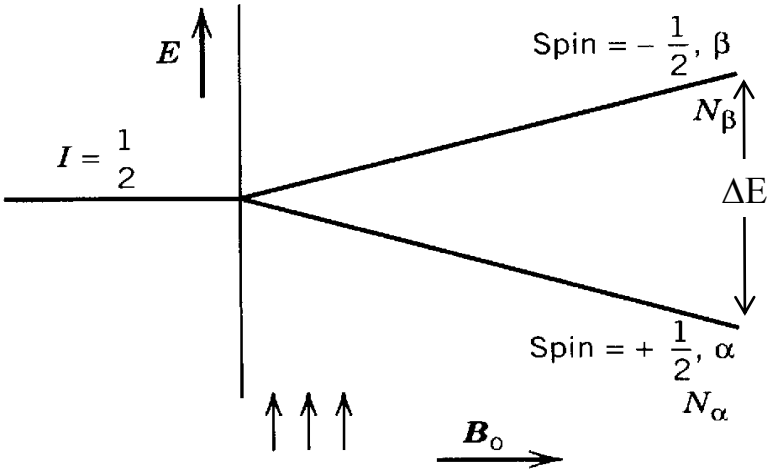


**Figure 1.25 –** Splitting of two energy levels from nuclei with Spin (I) = ½, by action of a magnetic field ($B_0$), with direction indicated (↑↑↑) N is population of spins in the higher ($N_\alpha$) and the lower ($N_\beta$) energy states [101].

The chemical shift (expressed in ppm) of a nucleus is the resonance frequency (the chemical environment influences it) relative to a standard; tetramethylsilane (TMS) is often used. This technique enables the determination of unknown compounds structures', quantitative and qualitative analysis.

The technique there was used in this specific work was high-pressure nuclear magnetic resonance (HP-NMR), in which pressurization is enabled through a quick pressure valve attached to the NMR tube, and the tube is composed of a much more heavy wall, that can stand higher pressures. This technique offers the possibility of acquiring information of the molecular interaction between the species under pressure *in situ* [102]. As an example of *in vivo* enzymatic reaction followed by HP--NMR was the reversible conversion of pyruvate to lactate by lactate dehydrogenase [103].

# 2. MATERIALS AND METHODS

# 2. MATERIALS AND METHODS

In the developed experimental work, the multi enzymatic system is immobilized in a sol-gel matrix. The Lowry method was used to determine the efficiency of immobilization. When performing the reactions in aqueous medium, the efficiency of the reaction was determined by quantifying NADH conversion through UV/Vis spectroscopy and by High-Pressure NMR (HP-NMR). When ionic liquid was the reaction solvent, methanol quantification was achieved through headspace gas chromatography (HS-GC) and Nuclear Magnetic Resonance (NMR).

## 2.1. SOL-GEL IMMOBILIZATION

The enzymes formate (FateDH) from *Candida boidinii* (0.77; 0.85; 1.24 and 1.3 U/mg, solid), formaldehyde (FaldDH) from *Pseudomonas sp* (3.1 U/mg, solid) and alcohol (ADH) from *Saccharomyces cerevisiae* (349 and 415 U/mg, solid) dehydrogenases, were acquired by Sigma--Aldrich, and encapsulated in a sol-gel matrix.

The buffers sodium phosphate 0.1 M at pH 7, and tris-buffered Saline (TBS - 0.05 M Tris--HCl, 0.150 M NaCl) at pH 7.6, were prepared with sodium phosphate monobasic monohydrate ($NaH_2PO_4.H_2O$) (98.8-102.0%, Sigma-Aldrich), sodium phosphate dibasic heptahydrate ($Na_2HPO_4.7H_2O$) (98-100.5%, Merck), Trizma® ($C_4H_{11}NO_3$) (99.5%, Riedel-de Haën), hydrochloric acid (HCl) (36.5-38%, Scharlau) and sodium chloride (NaCl) (99.5%, Panreac) and the pH is measured with a pH – meter Basic 20 + from Crison.

An enzyme solution was prepared in 500 µL of buffer TBS pH 7.6, by dissolving equal amounts (1.5 mg) of each dehydrogenase corresponding to 1.16 U from FateDH, 4.66U form FaldDH and 523U from ADH. The matrix solution was prepared by mixing 500 µL of tetramethylsilane (TMOS, 98%, Aldrich) as precursor, 111 µL of Mili-Q water and 7 µL of HCl 0.04M. The mixture was sonicated in an ultrasonic bath for 20 minutes. The matrix solution was then added to the enzyme solution and vortexed until gelation occurred, and then cooled in ice for 10 minutes. The sol-gel was allowed to age at 4ºC for 24 h [30], was air-dried at 35ºC for another 24 h [104]. After this process, 1 mL of buffer TBS pH 7.6, was added to the sol-gel, and it was centrifuged at 5400 rpm for 10 minutes and the supernatant was collected (in order to later determine the immobilization degree). The sol-gel is then transferred to a 30 mL fresh buffer TBS pH 7.6 solution, and placed at 4ºC for 24 h, this process was repeated two more times, for the complete removal of the methanol produced by the hydrolysis of TMOS [30].

## 2.2. LOWRY METHOD

To determinate the efficiency of immobilization, a modified Lowry method [105] was used, enabling the determination of protein concentration.

The Lowry method combines the Biuret reaction with the oxidation of aromatic residues, in the first one under alkaline conditions the proteins are pre-treated with cooper ($Cu^{2+}$) solution (Lowry Reagent) where the peptide bonds of proteins produce a complex [105]. With the addition of the Folin–Ciocalteau reagent, the cooper-protein complex reduces phosphomolybdate–phosphotungstate in the heteropolymolybdenum resulting in a colour enhancement (blue) [105,106] with an absorbance peak at 750 nm.

Oxidation of aromatic the amino acids (tyrosine, tryptophan, phenylalanine) is catalysed by copper [106]. The stronger the colour of the final product, the higher is the protein content [105]. Nevertheless, the colour intensity varies for different proteins, namely with the presence of tyrosine, tryptophan, cysteine, histidine, and asparagine, which enhances it [106].

In this method, bovine serum albumin (BSA) is used as a standard for a calibration curve. BSA is widely used because of its widely available in high purity at a low cost [106].

The following solutions were used:

Solution A – 30 g/L of $Na_2CO_3$ with 4g/L of NaOH;
Solution 2 – Potassium sodium tartrate at 2% (w/v);
Solution 3 – Aqueous solution of copper sulphate pentahydrate (CuSO4.5H2O) at 2% (w/v);
Lowry Reagent: Addition of 0,25 ml from solution 2 to 0,25 mL of solution 3 totalling 25 ml with solution A. The addition of solution 2 should be done first to prevent precipitation;
Folin-Ciocalteau Reagent (Merck) (dilution of 1:2);
BSA Standard Solution, 0.4 mg/mL.

For the Lowry method, 200 µL of sample are mixed with 1 mL of Lowry reagent and the solution was vigorously shaken on a vortex mixer; after 10 minutes 200 µL of folin-ciocalteau reagent are added and the solution is vigorously mixed in a vortex again. After 30 minutes the absorbance in the UV-Vis region of the solutions is measured at 750 nm against a blank prepared with 200 µL of buffer, with a DU® 800 Spectrophotometer from Beckman Coulter, Brea, USA.

## 2.3. QUANTIFYING $CO_2$ REDUCTION TO METHANOL - AQUEOUS MEDIUM

The previously prepared sol-gel matrix is crushed and transferred to a 4 mL vial, where it is added to 1 mL of NADH (≥ 97, Sigma) solution, (with concentrations of 5, 10 and 14 mM). Sol-gel matrices with one enzyme, two or three enzymes were used. The mixture was covered with parafilm™, and left undisturbed for 48 hours, allowing NADH to diffuse into the sol-gel. After this period, $CO_2$ (99.98%, Air Liquide) was bubbled in the mixture, during 24h using a nozzle with an approximate outlet diameter of 0.9 mm. Samples/Aliquots were taken before adding the matrix and the $CO_2$, after 30 minutes of bubbling the $CO_2$ and at 1h to 8h (1 h interval between measurements), and 24 h. The reaction was followed by UV/Vis spectroscopy using a DU® 800 Spectrophotometer from Beckman Coulter, Brea, USA. The experimental set-up is summarized in Figure 2.1.

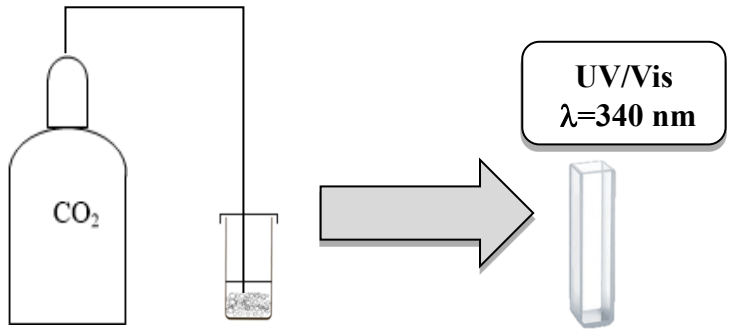


**Figure 2.1 –** Experimental set-up for the reactions in aqueous medium.

It is clear, from the reaction stoichiometry (Figure 1.10), that for each mole of methanol produced, 3 moles of NADH are consumed, so the methanol concentration in solution will be at the maximum 3 times less the NADH in solution. An indirect method for the methanol detection is used, in which NADH conversion is followed by measuring the absorbance at 340 nm. This is possible because NADH absorbs at 340 nm and the oxidized form ($NAD^+$) does not (Figure 2.2), so NADH conversion can be followed.

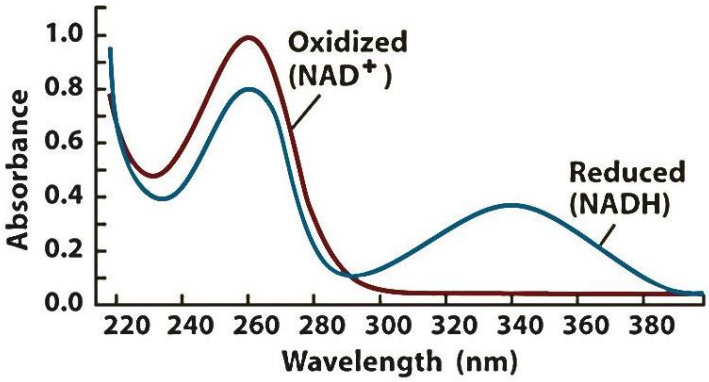


**Figure 2.2 –** UV/Visible absorption spectra of $NAD^+$ and NADH [107].

## 2.4. QUANTIFYING $CO_2$ REDUCTION TO METHANOL -IONIC LIQUID MEDIUM

When the reduction of $CO_2$ to methanol was carried out in ionic liquid, the quantification by UV/Vis spectroscopy was no longer possible since ILs contain an imidazolium ring that has a non-negligible absorption at 300 nm and at longer wavelengths [108]. Also ILs are not colourless, they are normally yellow or even brown, depending of the contamination by coloured impurities, and this can interfere with the UV/Vis detection method. So, a different method for methanol quantification in IL, was used headspace gas chromatography (HS-GC).

Methanol was quantified by HS-GC analysis performed with a Trace GC Ultra equipped with flame ionization detector (FID) and a split/splitless (SSL) inlet and automated by a TriPlus Autosampler headspace injector (Figure 2.3) from Thermo Scientific, Milan, Italy.

**Figure 2.3 –** Chromatograph Trace GC Ultra, with a TriPlus Autosampler headspace injector.

The Capillary Column used was a non-polar 100% Dimethyl Polysiloxane from Thermo (Thermo Fischer Scientific, TRACE TR-BIODIESEL (M), Milan, Italy), with a 30m×0.32mm I.D. column coated with a 3.0 µm thickness film. The system was controlled via Chrom-Chard, with the parameters in Table 2.1 adapted from EN 14110 (in 6.3 EN 14110).

**Table 2.1** – Method parameters for the TRACE GC Ultra and TriPlus HS Injector, adapted from EN 14110 (in 6.3 EN 14110)

| **Gas chromatograph** | |
|---|---|
| Carrier Gas | Helium, 1.5 mL/min, constant flow mode |
| Oven Program | 50 °C (1 min) to 130 °C (2min) at 10°C/min |
| SSL injector | 160ºC, Split flow 100 mL/min |
| FID detector Temperature | 250ºC |
| **HS Injector** | |
| Injected Amount | 500 µL |
| Syringe Size | 2.5 mL-80 mm needle |
| Syringe Temperature | 85ºC |
| Equilibration temperature | 80ºC |
| Agitation time | Turned on for 3s and of for 3s, during 40 minutes |

The calibration solutions were made with methanol (HPLC grade, ≥ 99.9% from Carlo Erba reagents), with concentrations of 10; 25; 50; 80 and 100mM, in 2 mL of ionic liquid with 7.5 % (v/v) of TBS, and transferred into 20 mL headspace vials, which were crimped in order to prevent leaking. To simulate experimental conditions when the enzymes are immobilized, sol-gel matrixes were prepared as described in 2 -
Sol-Gel immobilization, but without enzymes.

Five ionic liquids were tested as solvents: Tricaprylylmethylammonium chloride (Aliquat® 336, Sigma), 1-butyl-3-methylimidazolium acetate ([BMIM][Ac]) (≥ 95%) from Aldrich, 1-butyl-3-methylimidazolium tetrafluoroborate ([BMIM][$BF_4$]) (> 99%), 1-butyl-3-methylimidazolium dicyanamide ([BMIM][DCA]) (> 98%) and 1-ethyl-3-methylimidazolium ethyl sulphate ([EMIM][$EtSO_4$]) (99%) from IoLiTec.

The ionic liquid selected for the current experiments was [BMIM][$BF_4$], mixed with just enough TBS volume (3.5 µL TBS / mg NADH and 8; 11; 23 µL TBS / mg $NAD^+$) sufficient to dissolve the cofactor (NADH or $NAD^+$ ≥ 99 and 97% from Sigma).

The enzymes immobilized in TMOS sol-gel matrix were mixed into the IL with NAD(H) solution in a 4 mL vial. The final volume (4.250 mL) was sufficient to the inexistence of a dead

volume during the 24 hours of reaction, and after that, was transfered it to a 20 mL headspace vial which was then crimped.

In order to simplify the reactions, and to gain more knowledge about the system, separated reactions were performed.

To follow methanol consumption catalysed by ADH, both free and immobilized in sol-gel, methanol concentrations of 28, 80 and 100 mM were used as well as $NAD^+$ concentrations of 5, 10 and 28mM.

To the complex of the three immobilized enzymes, a concentration of 30 mM of NADH was used for the methanol formation, and to follow the methanol conversion using $NAD^+$ concentration of 30 mM was also used.

### 2.4.1. HIGH-PRESSURE BATCH EXPERIMENTS

For the high-pressure experiments only the first reaction was under study. Using pressurized $CO_2$ will allow the system to have a higher amount of the reactant available, for the production of formate.

To follow the formation of formate catalysed by FateDH, (the first step of the reaction depicted in Figure 1.14) a high pressure apparatus was used (Figure 2.4), and after slow depressurization the samples were analysed by $^{13}$C-NMR and $^{1}$H-NMR.

High pressure batch experiments with free and immobilized FateDH were carried out, with NADH (30mM) dissolved in 175 µL of TBS and 925 µL of [BMIM][$BF_4$], at 40 ºC and 10.0 MPa for 48 hours. Briefly, the sample is loaded into a high-pressure vessel (Figure 2.4) and heated in a thermostatic water bath to the desired temperature (± 2 ºC). Carbon dioxide (99.98%, Air Liquide) is liquefied in a refrigerator containing a water/ethylene glycol solution, before being pumped with an HPLC pump (flow of 15 mL/min; KNAUER preparative Pump 1800, Berlin, Germany), until the desired pressure is attained. The pressure is measured with a pressure transducer within ± 0.25MPa. A schematic representation of the experimental apparatus is presented in Figure 2.5.

**Figure 2.4 –** High-pressure vessel.

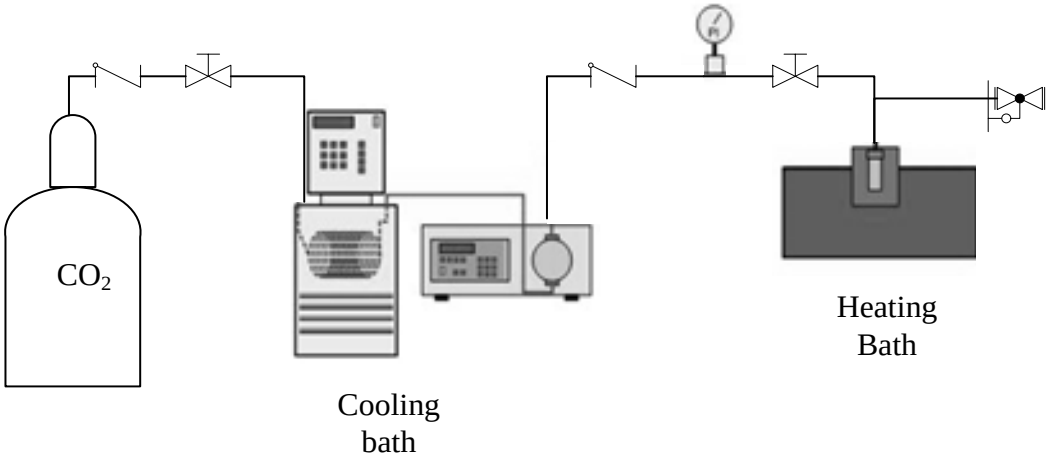


**Figure 2.5 –** Schematic representation of the experimental apparatus used for the batch experiments.

At the end of the experiment, the vessel is slowly depressurized until it reaches atmospheric pressure, and the sample is transferred to an NMR tube, with a minimum of 10% of Deuterium oxide ($D_2O$, 99.9%, Cambridge Isotope Laboratories). When sol-gel is present, the sample was filtered with a microcentrifuge filter with 0.2 µm pore size. The NMR experiments were carried out in a Bruker ARX 400 at 400.13 MHz for protons and 100.61MHz for carbon equipped with a 5 mm QNP $^{1}H/13C$ probe at ambient temperature. Spectra were processed using Bruker Topspin 3.0 and MestReNova 6.0.

## 2.5. HP-NMR

To follow the formation of formate, formaldehyde and methanol (Figure 1.14) the technique of HP-NMR that allows *in situ* analysis was used.

In a High-Pressure NMR experience (HP-NMR). Carbon dioxide was supplied by Air Liquide with purity above 99.998%. Labelled carbon dioxide $^{13}CO_2$ was supplied by ISOTEC ($^{13}CO_2$, 99%).

The HP-NMR experiments were conducted in a 5 mm Heavy Wall Pyrex NMR tube, with a PTFE valve from Wilmad LabGlass, using a Bruker Avance III 400 spectrometer equipped with a temperature control unit and a pulsed field gradient unit capable of producing magnetic pulsed field gradients in the z-direction of 56.0 G/cm, operating at 400.15 MHz for hydrogen, 100.61 MHz for carbon. Chemical shifts were referenced to internal TMS. Spectra were processed using Bruker Topspin 2.1. and MestReNova 6.0.

The enzyme concentration was about 10 mg/mL of each enzyme; NADH concentration was 28mM when only FateDH was used and 50 mM of NADH for FateDH, FaldH and ADH.

In a typical HP-NMR experiment, the three enzymes, as well as the cofactor NADH, were dissolved in 500 μL Tris-DCl (100mM) buffer made from Tris $d_{11}$ (98%, 1M in D2O, CortecNet) and loaded into the HP-NMR tube. After the mixture was placed under vacuum the HP-NMR tube was pressurized up to of 1.05 MPa with $CO_2$. The tube was then transferred to the NMR apparatus using a protective polycarbonate structure.

# 3. RESULTS AND DISCUSSION

# 3. RESULTS AND DISCUSSION

## 3.1. AQUEOUS MEDIUM

In the biocatalytic system under study, the amount of methanol produced will be limited by the cofactor concentration. Indeed, because of the stoichiometry of the reaction (Figure 1.14), the maximum methanol molar quantity will be three times less than the NADH added, if we assume that all the NADH added was oxidized.

The low molecular weight of methanol and its correspondent high volatility enables the detection by gas chromatography. However, in aqueous samples, injection of samples dissolved in aqueous media presents some drawbacks; when water is vaporized, there is a volume expansion which can damage the GC column, and the sample can expand above the maximum injectable volume. Prior solvent extraction may be a solution for this problem, but only if the concentration of analyte is appreciable.

Alcohols such as methanol, ethanol, and propanol have a structural similarity to water, but they have poor molar absorptivities. In aqueous samples, there is no method for their quantitative analysis at micro- and sub- micromolar levels, so they cannot be quantified by traditional absorption methods, such as UV/Vis spectroscopy. Derivatization can be an alternative, but with methanol this is hard and, but will increase the detection limit, making its quantification even harder. Some strategies for methanol quantification are oxidizing it in its corresponding aldehyde, which is easier to derivatize in aqueous media, or by using probes or sensors.

Because of the various detection limitations described above, for experiments carried out in aqueous medium, the conversion of $CO_2$ to methanol was followed indirectly, by UV/Vis spectroscopy, through the NADH conversion to $NAD^+$, measuring the absorbance at 340 nm.

### 3.1.1. INITIAL EXPERIMENTS - PROOF OF CONCEPT

Sol-gel matrixes containing the following enzymes were studied: FateDH; FateDH + FaldDH; FaldDH + ADH and FateDH + FaldDH+ADH in sodium phosphate buffer 0.1 M at pH 7. The NADH conversion expressed in concentration (Figure 3.1) and in percentage it is represented over time (Table 3.1.).

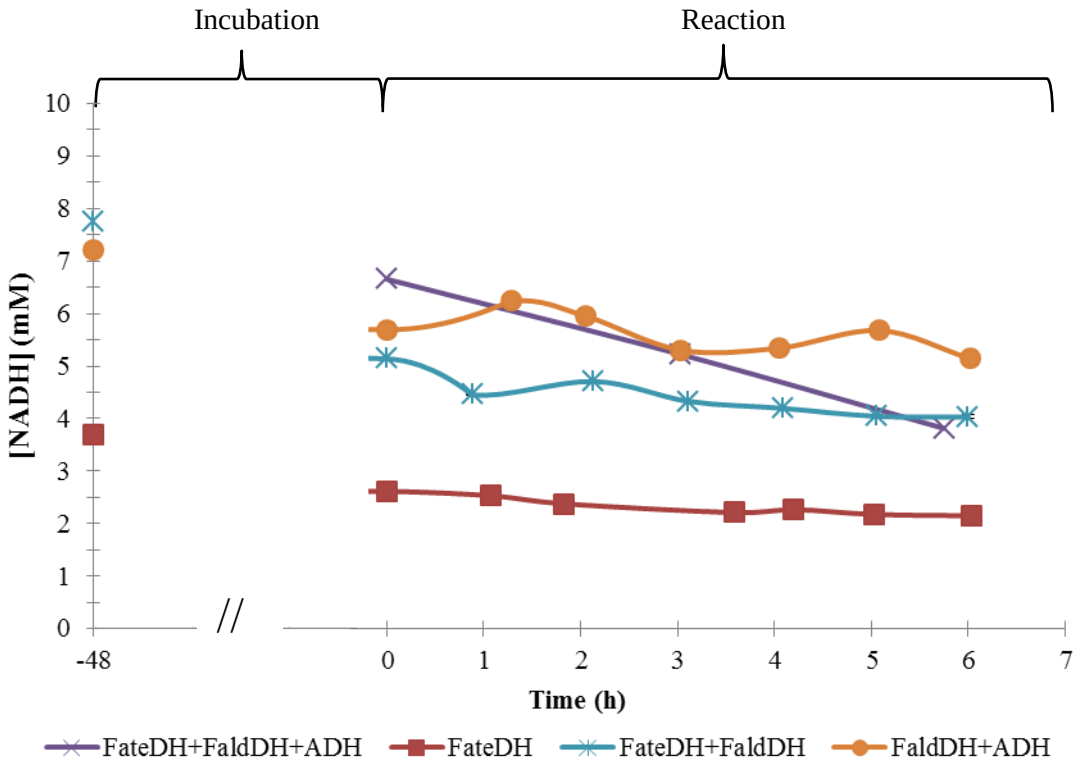


**Figure 3.1** – NADH conversion over time by enzymes immobilized in sol-gel, from before the incubation (-48 h) to 6 h after starting bubbling the $CO_2$, in sodium phosphate buffer 0.1M at pH 7. In FateDH + ADH the raw material as formic acid.

**Table 3.1** – Reactions with incubation (48 hours at 4ºC) in sodium phosphate buffer 0.1 M at pH 7. The NADH was indirectly quantified by UV/Vis absorption at 340 nm by UV/Vis spectroscopy.

| **Enzymes in the sol-gel matrix** | **NADH (conversion) %** | | | | | **Reutilization** | | | | |
|---|---|---|---|---|---|---|---|---|---|---|
| | **Incubation (48h at 4ºC)** | **2h** | **3h** | **4h** | **6h** | **Incubation (48h at 4ºC)** | **2h** | **4h** | **6h** | **24h** |
| Without enzymes and sol--gel matrix | 7 | 13 | 0 | 8 | 25 | --------- | --- | --- | --- | ---- |
| FateDH | 30 | 36 | 40 | 39 | 42 | 3 | 26 | 30 | 41 | ---- |
| FateDH + FaldDH | 34 | 40 | 44 | 45 | 49 | --------- | --- | --- | --- | ---- |
| FaldDH + ADH | 21 | 18 | 27 | 26 | 29 | --------- | --- | --- | --- | ---- |
| FateDH + FaldDH + ADH | no data | --- | 22 | --- | 43 | 15 | 31 | 32 | 41 | 51 |

To perform a proof of concept, the initial experiments were carried out in a similar protocol as the one described by Obert and Dave [30]; the NADH solution was added to the sol-gel and left to

incubate for 48 h, allowing the NADH to diffuse into the sol-gel matrix. After that, with the addition of $CO_2$ (bubbling $CO_2$ into the system), and taking aliquots of the system, UV/Vis spectra were recorded.

In this study, the NADH concentrations present in the reaction varied from 5 mM, 9 mM and 14 mM to the reaction with one, two or three enzymes respectively. In all the experiments reported a diminishing in NADH concentration is observed in sodium phosphate buffer 0.1M at pH 7.

Comparing the conversion values (Table 3.1) in the presence of one, two or three enzymes, it is seen that the conversion is smaller when only FateDH is present, although the reactions with FateDH + FaldDH and FateDH + FaldDH + ADH, result in very similar conversion values. It is also possible to see that the reaction is limited by the leading enzyme – FateDH.

Comparing de conversion rate of FateDH with the different enzyme combinations in Table 3.1, is possible to observe an enhancement of the conversion rate, when more enzymes were added, which means a faster conversion of NADH, reinforcing the proposed continuation of the enzyme cascade.

In the reaction with FaldDH and ADH, the substrate was formic acid, in an amount corresponding to a formate (product) concentration of 31.2 mM at pH=7 close to the value of $CO_2$ that can be dissolved in water, at atmospheric temperature and pressure, (33mM). The conversion by FaldDH and ADH after 6 hours of the addition of formic acid was of 29 % of NADH added. This means that proceed with the cascade reaction, and were mainly limited by the formate production by FateDH.

It is also demonstrated that the reutilization of the biocatalyst is possible, without high loss of enzyme activity, although there was some matrix mass loss in the process of washing the gel. The difference in activity in the three enzymes experiments can be explained by the fact that the sol-gel matrix is under the second reutilization.

The *in situ* quantification of NADH is an ideal procedure (previously performed by Addo *et. al.* [109]). However, in this case, without dilution this procedure would only enable NADH detection up to a concentration of approximately 0.2 mM, which is low cofactor concentration. Also, the gel particles in suspension present in the reaction vial can interfere with the light beam passing through the sample.

Some experimental errors are associated with sampling, since measurements are not direct, but made by taking aliquots and the homogeneity of the sample.

One of the major problems, that can affect these reactions are diffusional limitations. They can occur once the different intermediates of the pathway are used for the next reaction, and they are diluted in the solvent and need to get through the sol-gel matrix. Also some degradation of NADH can occur.

Indeed some deterioration was observed in the incubation process (21 to 34% of NADH conversion without reaction), so further analysis of the different possible interferences was discussed below, namely the buffer influence.

### 3.1.2. BUFFER SELECTION

To evaluate the buffer influence in the quantification of NADH, experiments were performed without $CO_2$ and with $CO_2$ addition (Figure 3.2 and Figure 3.3, respectively), using different buffers.

These results are a way to determine NADH stability during the reaction time. The media under analysis were: water, sodium phosphate buffer, Tris-HCl buffer and TBS buffer. Results of NADH conversion are depicted in Table 3.2.

**Table 3.2** – Stability test of NADH in buffer without sol-gel matrix. NADH as quantified by the absorption at 340 nm by UV/Vis spectroscopy.

| **Reaction** | **Solvent composition (Buffer/Medium)** | **NADH (conversion) %** | | | | |
|---|---|---|---|---|---|---|
| | | **Incubation (48h at 4ºC)** | **2h** | **3h** | **4h** | **6h** |
| Without $CO_2$ | Sodium Phosphate 0.1 M pH 7 | ----- | 3 | ≈0 | 4 | 8 |
| With $CO_2$ | Sodium Phosphate 0.1 M pH 7 | ------ | 1 | 4 | 10 | 18 |
| Without $CO_2$ | Sodium Phosphate 0.1M pH 7 | 8 | ≈0 | 12 | 12 | 17 |
| With $CO_2$ | Sodium Phosphate 0.1 M pH 7 | 7 | 13 | 0 | 8 | 25 |
| Without $CO_2$ | Tris-HCl 0.1 M pH 7 | 0 | ≈0 | ≈0 | 0 | ≈0 |
| With $CO_2$ | Tris-HCl 0.1 M pH 7 | 0 | 8 | 8 | 8 | 15 |
| Without $CO_2$ | TBS (0.05 M Tris-HCl 0.15 M NaCl pH 7.6) | 2 | 2 | ≈0 | ≈0 | ≈0 |
| With $CO_2$ | TBS (0.05 M Tris-HCl 0.15 M NaCl pH 7.6) | ≈0 | 1 | ≈0 | 6 | 9 |
| Without $CO_2$ | $H_2O$ | 5 | ≈0 | ≈0 | ≈0 | ≈0 |
| With $CO_2$ | $H_2O$ | 1 | 36 | 50 | 59 | 70 |

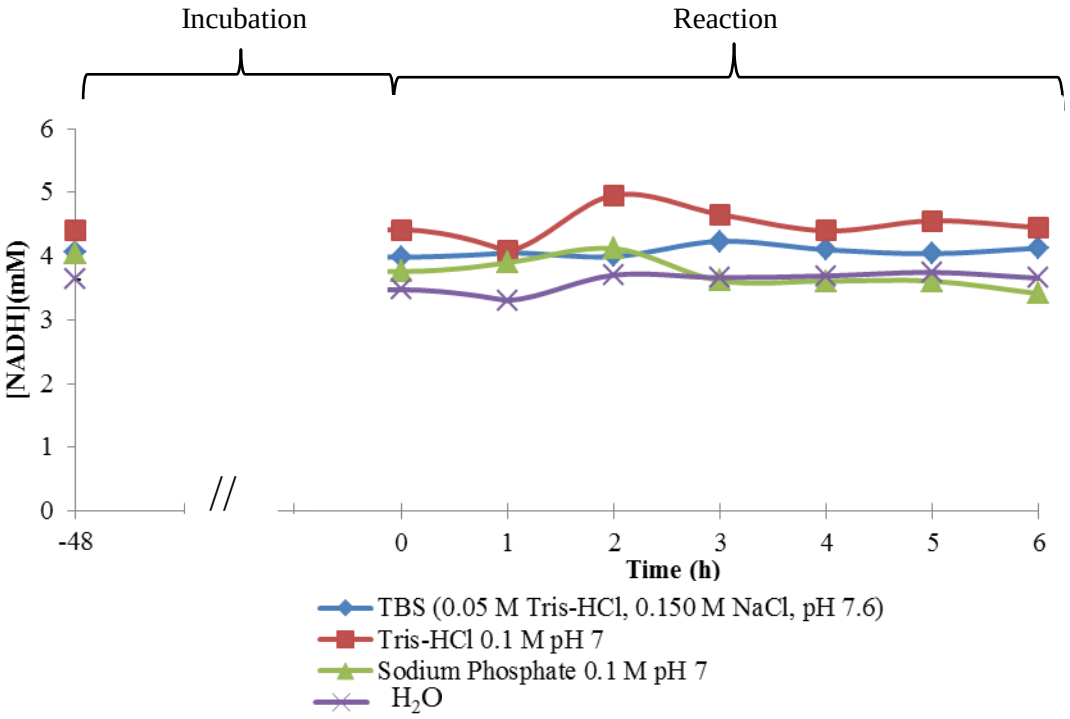


**Figure 3.2 –** NADH conversion in different aqueous media, from before the incubation (-48 h) to 6 h without $CO_2$ bubbling.

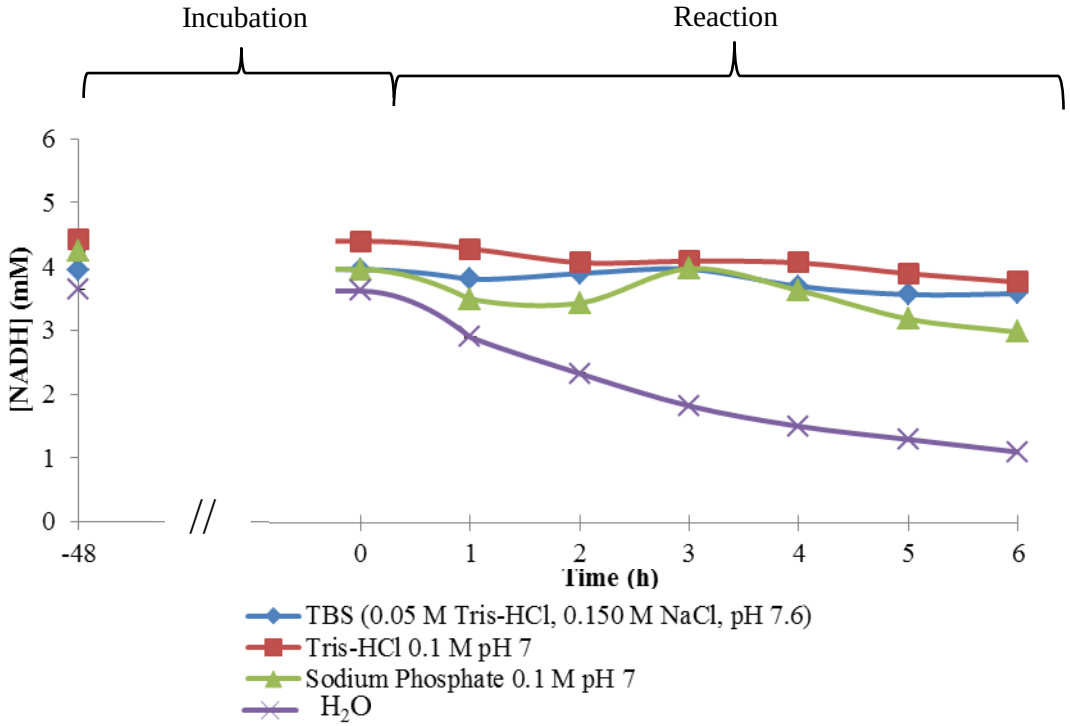


**Figure 3.3 –** NADH conversion in different aqueous media over time, from before the incubation (-48 h) to 6 h after bubbling with $CO_2$ started.

In literature is reported that, when NADH is dissolved in a phosphate based buffer, an adduct can be formed between the phosphate anion and the pyridine ring of the NADH/$NAD^+$ (Figure 3.4), leading to cofactor decomposition. This is also enhanced by the diminishing of pH and an increasing of temperature in the pH range between 6.8 and 7.8 [110]. Previous studies also confirmed this theory showing NADH [58] and NADPH decomposition, having the last one a faster degradation rate [57,59].

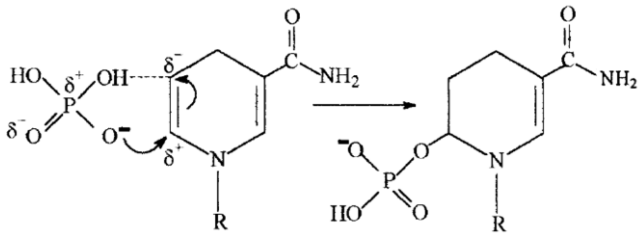

**Figure 3.4 –** Mechanism proposed to the NADH decomposition in phosphate-based buffer. R represent the remaining groups of the NADH molecule [110].

The experiments performed to evaluate the NADH stability without adding the $CO_2$, show low degradation in water, probably because of its slightly acidic pH (≤ 7). This degradation is more expressive in sodium phosphate buffer (confirming the proposed degradation mechanism in Figure 3.4.). In the buffers tested that do not contain phosphate anion, such as Tris-HCl and TBS, the degradation is almost inexistent (≈0%), when $CO_2$ is not in the medium.

When $CO_2$ is bubbled into the reaction mixture, NADH degradation is higher in all the media tested. This is more noticeable in water, because without the pH control of a buffer, the reversible conversion of $CO_2$ to carbonic acid occurs, acidifying the media and degrading NADH (up to 70% after 6 h).

Comparing the three buffers tested after the addition of $CO_2$, the one in which NADH shows a higher degradation rate is the sodium phosphate buffer (25% after 6 h); in some extension because of the side reaction explained above (Figure 3.4).

The pH is an important factor to consider in a biological system, but another important factor is the ionic strength [28]. Indeed, the cofactor degradation rate at neutral pH decreases with the increase of the ionic strength [59].

Comparing the ionic strength of Tris-HCl buffer at 100 mM, pH 7) with the TBS buffer at 50 mM Tris-HCl, 150mM NaCl pH 7.6, the latter has a higher ionic strength, 93 mM for Tris-HCl against 188mM for TBS at 25ºC, and pH 7. This explains the higher stability of NADH in TBS buffer, and also a higher pH can also contribute to the stabilization.

Alternative buffers that do not react with NADH are also suggested in the literature namely PIPES (1,4-Piperazinediethanesulfonic acid) buffer [110], and Tris-HCl [57,58]. However, because

TrisHCl was previously used in this enzymatic system by Xu, *et. al.* [33], Qianyun, *et. al.* [32] and Dibenedetto, *et. al.* [34], was evaluated its response to NADH degradation as well as the similar buffer - TBS,. TBS was adopted because it shows a better NADH stability.

After evaluating the influence of the buffer in the detection method (UV/Vis spectroscopy), it was verified that this is not the only factor to consider. In addition, the sol-gel matrix seems to have some influence in the detection method, Table 3.3.

**Table 3.3 -** Sol-gel matrix effect in NADH quantification in TBS buffer. The NADH was indirectly quantified by UV/Vis absorption at 340 nm by UV/Vis spectroscopy.

| **Sol-gel matrix** | **$[NADH]_{initial}$ (mM)** | **Incubation (48h at 4ºC)** | **NADH (conversion) %** | | | | | | |
|---|---|---|---|---|---|---|---|---|---|
| | | | **1h** | **2h** | **3h** | **4h** | **6h** | **8h** | **24h** |
| Empty (Control) | 5 | 17 | 23 | 25 | 29 | 27 | 31 | 34 | 51 |
| FateDH + FaldDH + ADH | 14 | 19 | 23 | 24 | 35 | 32 | 36 | --- | ---- |
| Empty (Control) | 5 | ---------- | 29 | 30 | 32 | 35 | --- | --- | ---- |
| Empty (Control) | 14 | ---------- | 26 | 26 | 28 | 28 | 32 | 38 | 54 |

The sol-gel matrix used is considered chemically inert and hydrophobic [49,104,111], being a way to entrap the biomolecules. It is composed by pores with a high surface area, so it may be possible that some of the cofactor molecules can be adsorbed in the sol-gel matrix surface, through the interaction between phosphate groups from the cofactor and the silanol (Si-OH) groups [112] at the matrix surface.

As it is possible to see in Table 3.3, namely in the incubation process (48h at 4ºC), 17% of the NADH added was not quantifiable by the UV/VIS spectroscopy. One possible explanation is that the interactions described above, but it is more likely to be due to the limitation of the method itself, because the only NADH that is quantified is the one dissolved in the medium, and any NADH that is entrapped or adsorbed in the matrix is not quantified.

The following strategy was to eliminate the incubation step, diminishing the possible NADH adsorption to the matrix at the time of the $CO_2$ addition. Having thus, a bigger concentration of NADH in solution to be consumed by the enzymes.

Comparing the reaction with and without the incubation step, without enzymes and with the same NADH concentration (5mM), the conversion after $CO_2$ bubbling is slightly superior over time (35% without the incubation against 27% after 4h of $CO_2$ bubbling). In this specific case (reaction in

sol-gel without enzymes and with incubation), it must be noted that the first point (-48h) is not referent to an accurate "zero", since the sol-gel was added prior to the sampling step, and this can have some influence in the results (as it is explained above).

The reaction with different NADH concentrations (5 and 14 mM), without incubation and with empty sol-gel shows conversion values with differences of ca. 6-7 %. This indicates a dependence between the NADH that is available in the medium and its absorption, being more expressive when less NADH is present (5mM). This may also help to explain the same effect observed in the NADH concentration, when the three enzymes were dissolved in the medium versus the empty sol-gel, because the last one has a smaller initial NADH concentration. Although faster conversion are expected when the enzymes were added, the results are the ones present in Figure 3.5.

To exclude side-reaction of the enzymes with the $CO_2$ inherently dissolved in the reaction medium during the incubation process, the samples were degased.

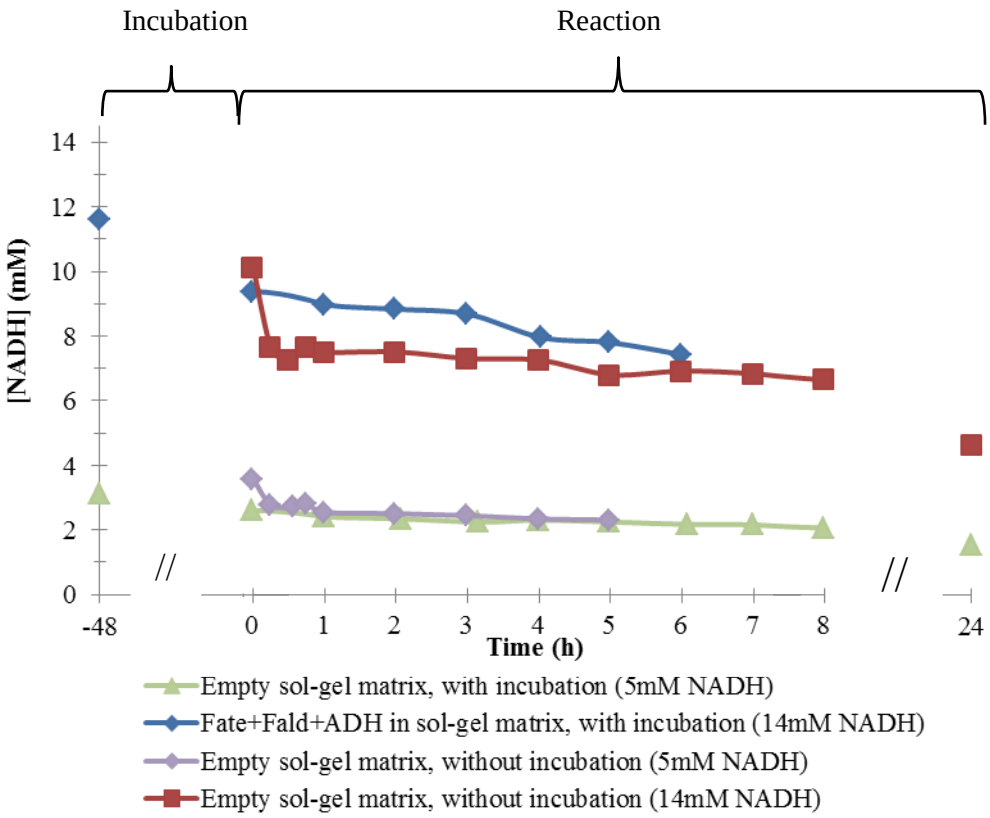


**Figure 3.5 –** NADH conversion in TBS buffer over time to evaluate the matrix effect, from before the incubation (-48 h) to 6 h after starting bubbling the $CO_2$.

### 3.1.3. STUDY OF ENZYME ACTIVITY- TBS BUFFER

After studying the buffer effect and evaluating the effect of the matrix, experiments with the immobilized enzymes were performed in TBS buffer and without the incubation process, (Table 3.4, Figure 3.6 and Figure 3.7).

**Table 3.4 –** NADH conversion in TBS buffer. The NADH was indirectly quantified by UV/Vis absorption at 340 nm by UV/Vis spectroscopy.

| Sol-gel matrix | $[NADH]_{initial}$ (mM) | NADH (conversion) % | | | | | | |
|---|---|---|---|---|---|---|---|---|
| | | 1h | 2h | 3h | 4h | 6h | 8h | 24h |
| Empty (Control) | 5 | 29 | 30 | 32 | 35 | --- | --- | ---- |
| | 14 | 26 | 26 | 28 | 28 | 32 | 38 | 54 |
| FateDH + FaldDH +ADH | 14 | 36 | 32 | 30 | 34 | 33 | 37 | 50 |
| | 14 | 35 | 38 | 37 | 39 | 42 | 43 | 50 |
| FateDH + FaldDH | 5 | 33 | 23 | 26 | 32 | 35 | --- | 49 |
| | 9 | 34 | 34 | 34 | 34 | 36 | 41 | 47 |
| FateDH | 5 | 29 | 26 | 30 | 30 | 33 | 35 | 42 |
| | 9 | 25 | 27 | 31 | 30 | 35 | --- | 59* |
| FateDH +FaldDH + (2X ADH) | 14 | 30 | 29 | 31 | 34 | 35 | 35 | 50 |
| (2X FateDH) + FaldDH + ADH | 14 | 25 | 28 | 29 | 30 | 34 | 39 | 57 |

* The 59% value for conversion of methanol by FateDH can be consider an outlier.

Comparing the results in Table 3.4 with the different enzymes in TBS, it is seen that the conversion of NADH is more accentuated when more enzymes are present (as seen previously). The FateDH catalysed reaction is the limiting step of the sequential conversion of $CO_2$ to methanol (conversion of 42% for FateDH versus a conversion of 50% by FateDH + FaldDH + ADH after 24h of

bubbling $CO_2$). In the FateDH experiment where the value of 59% was determinate after 24 h of bubbling $CO_2$ is consider an outlier and can be due NADH degradation or a sampling error. Also this added a high error bar in Figure 3.6.

In addition, a pronounced decrease is observed in the first hour of reaction, more specifically in the first 15 minutes, due to initial absorption of NADH in the matrix.

The replicas with FateDH + FaldDH and FateDH were performed at higher temperature (around 28ºC versus the 18/19ºC) and with more NADH (reaction catalysed by FateDH + FaldDH) and less NADH (reaction catalysed by FateDH), which also justifies the difference in the conversion values.

Comparing the results when the amount of the first enzyme is doubled ((2X FateDH) + FaldDH + ADH) and with the double amount of the last enzyme (FateDH + FaldDH + (2X ADH)), an increase in the NADH conversion rate was not observed. This can be explained by the fact that the enzymes in nature catalyse specifically the reverse reaction (methanol to $CO_2$), being energetically more favoured. By adding more enzyme units on FateDH or ADH to the enzyme support the equilibrium may be shifted towards the conversion of methanol to $CO_2$. However, this is less prominent when more ADH is added to the medium.

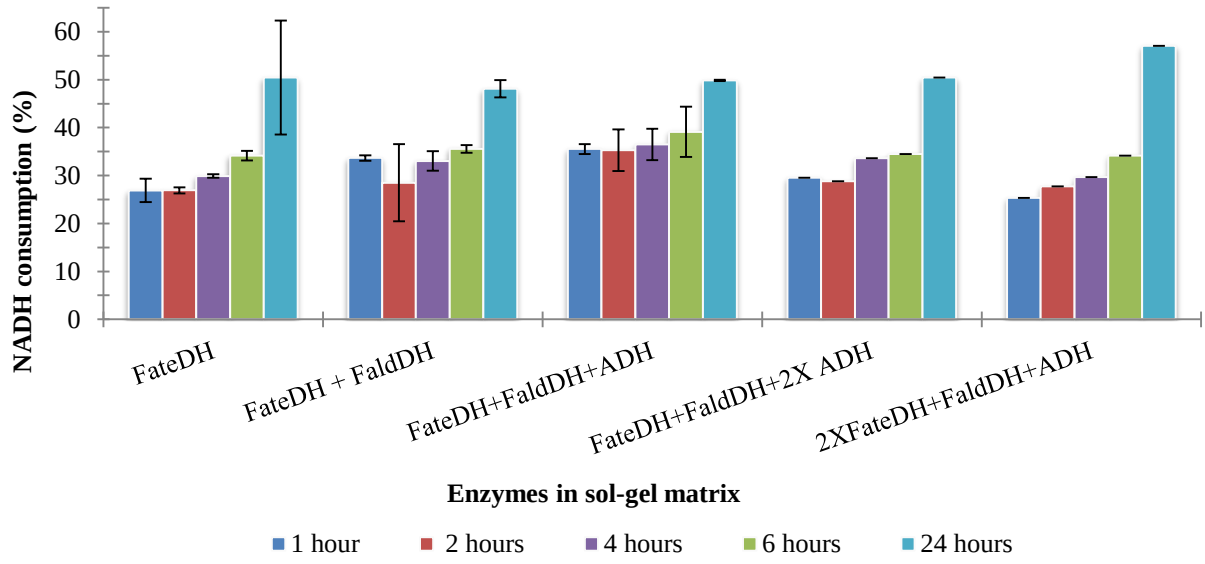


**Figure 3.6 –** NADH conversion by enzymes immobilized in sol-gel matrix and in TBS buffer over time with the respective replicas represented by the error bars.

Comparing the data of the from the reutilizations FateDH+FaldDH+ADH_3 and 4 in Figure 3.7, they are similar to fresh prepared matrix, FateDH+FaldDH+ADH_1 and 2, which indicates that

enzyme activity is maintained. However, the conversion in FateDH+FaldDH+ADH_4 is slightly superior; this fact can be explained by some prior NADH absorption from previous experiments.

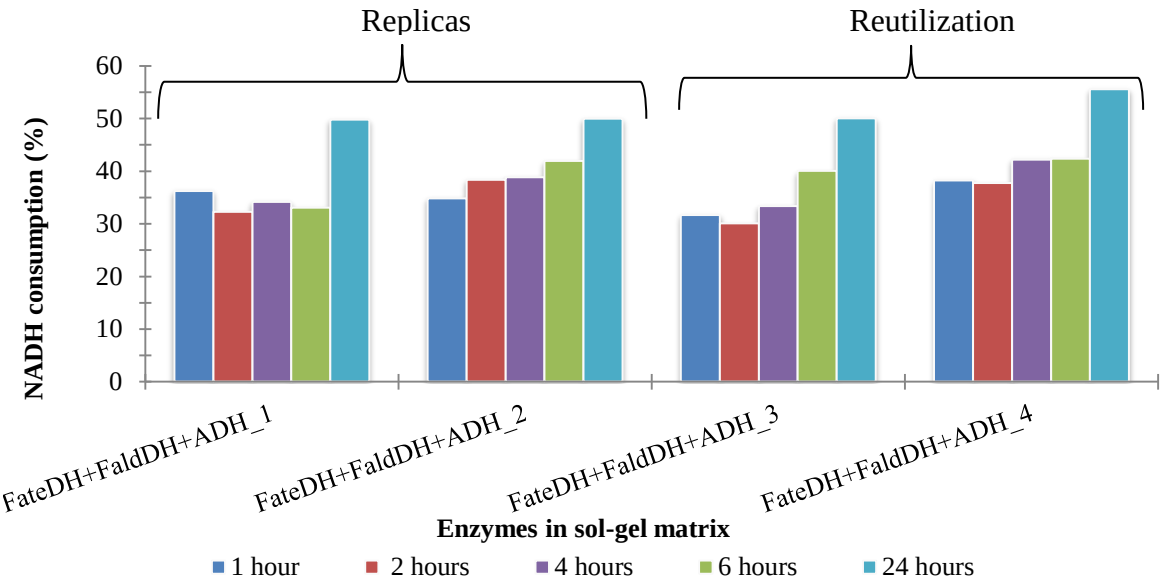


**Figure 3.7 –** NADH conversion by FateDH+FaldDH+ADH immobilized in sol-gel matrix and in TBS buffer. Samples 1 and 2 were replicas and 3 and 4 reutilizations.

### 3.1.4. NON-IMMOBILIZED ENZYMES

To evaluate the impact of the sol-gel matrix in the NADH oxidation reaction, experiments were performed without sol-gel and using the first enzyme – FateDH. Different amounts of enzyme and different NADH concentrations were used, as is possible to observe in Figure 3.8.

With an increase in enzyme concentration, a significant increase in the NADH conversion rate occurs (Figure 3.8), which may be explained by the increase in catalytic centres. When more NADH was added, the increase in NADH conversion does not have a very expressive value (due to method limitations) and it is not totally internally consumed.

The conversion values are not as high as expected comparing the reactions conducted using sol-gel immobilized enzymes, which may be related with a series of factors. Indeed some authors such as Obert and Dave [30], state a substantially enhancement in the methanol production by sol-gel immobilization, however they used higher NADH and enzyme concentration.

Mass transfer problems can occur when the enzymes are immobilized. It cannot only decrease the reaction rate, but also inhibit the reaction or even induce undesirable pH gradients [49]. It was observed that for higher NADH concentrations some precipitation occurs, namely when the concentration NADH is 14mM. This occurs even in a larger extent when a concentration of 10 mg/mL

of FateDH is used, possibly due to a salting out effect, or some protein agglomeration with the $CO_2$ addition to the medium. This was not previously observed since NADH precipitation when sol-gel is present is not observable.

The hypothesis of the sol-gel itself producing methanol as a by-product (in the sol-gel process, precursor (TMOS) hydrolysis releases methanol) is discarded, because extensive dialysis was applied. Enzyme leaching is also not considered since, by the Lowry method, an immobilization percentage of 95.9 up to 99.1% was obtained

Also, the methanol forming during the $CO_2$ reduction can accumulate in the matrix, because of diffusional limitations, and cannot evaporate from the gel within a short time. This accumulation of alcohol can contribute to the enzyme inactivation [33,49] by damaging its three-dimensional structure. Factors such as pore size and non-open-pore structure can cause low NADH conversion [113].

It is also important to consider that $CO_2$ is not the limiting reagent, because when dissolved in the medium it has a concentration of 33 mM, 2.35 to 6.6 times higher than NADH concentration.

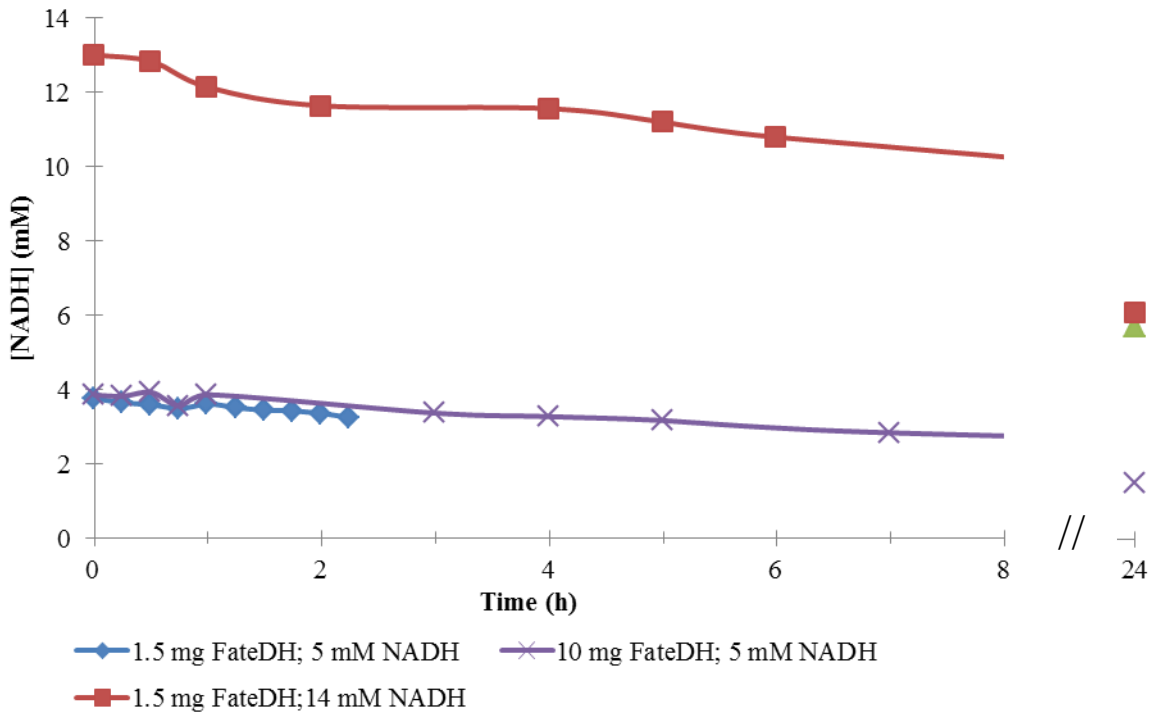


**Figure 3.8 –** NADH conversion over time for different amounts of non-immobilized FateDH starting from different NADH concentrations

### 3.1.5. EFFECT OF TEMPERATURE

The influence of the temperature in the reaction was also a parameter under study. Reactions at higher temperature (37ºC) were conducted in TBS buffer and with sol-gel immobilized enzymes (conditions are described in Table 3.5).

Jiang, *et al.* and also other authors [32,33,114,115], studied the immobilization of this enzymatic system in sol-gel (using TEOS as a precursor), in a alginate-silica hybrid-gel and in biotitania nanoparticles. They concluded that the optimum temperature for both free and immobilized enzymes from the multi-enzymatic system was 37 ºC, more specifically, 37 ºC for FateDH, 37 ºC for FaldDH and 25ºC to ADH.

The immobilized enzymes were submitted to 37ºC (data on Table 3.5), comparing the conversion of NADH at 37ºC with the data at room temperature, in Table 3.4.,the conversion is higher at 37ºC, because the temperature is closer to the overall enzymes optimum temperature catalysing the conversion of $CO_2$ to methanol more efficiently, up to 92% of NADH conversion.

It must be noted that the differences in the NADH conversion values may not be due to the presence of more enzymes, it can also be due to some degradation of the NADH may occur over time and that may explain the larger NADH conversion after 24 h.

**Table 3.5 –** NADH conversion in TBS buffer by immobilized enzymes at 37ºC. The NADH was indirectly quantified by UV/Vis absorption at 340 nm by UV/Vis spectroscopy.

| **Sol-gel matrix** | **$[NADH]_{initial}$ (mM)** | **NADH (conversion) %** | | | | | | | |
|---|---|---|---|---|---|---|---|---|---|
| | | **1h** | **2h** | **3h** | **4h** | **5h** | **6h** | **7 h** | **24h** |
| FateDH + FaldDH + ADH | 14 | 41 | 39 | 49 | 52 | 58 | 58 | --- | 90 |
| FateDH + FaldDH | 9 | 32 | 33 | 36 | 43 | 51 | 57 | 57 | 92 |
| FateDH | 5 | 32 | 37 | 42 | 51 | 49 | 63 | 60 | 91 |

From Figure 3.9, it is clear that the first steps of NADH oxidation occur at a higher rate, since the conversion in the first hour is much more significant than in the remaining reaction time (24 hours total). This has an influence in the total conversion percentage of NADH, that is higher at 37ºC.

Smaller differences occur between the conversion rate between FateDH + FaldDH to FateDH + FalDH + ADH, which can be explained by the fact that ADH it is not at its optimum temperature.

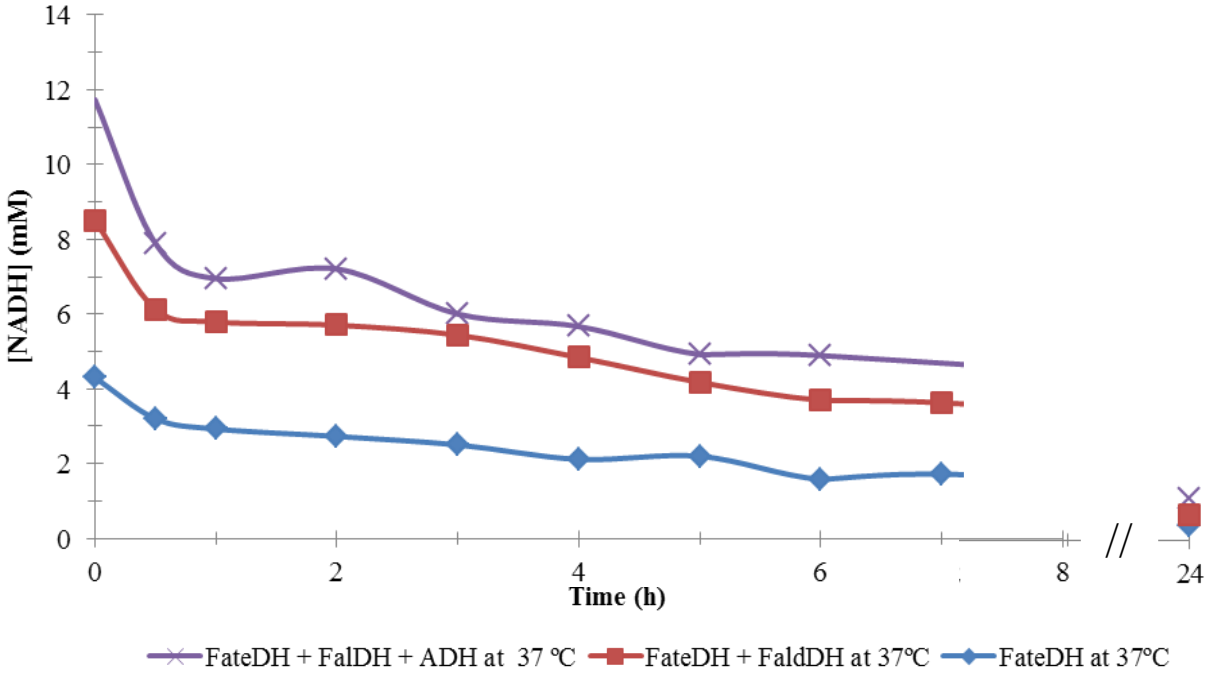


**Figure 3.9 –** NADH conversion by enzymes immobilized in sol-gel matrix at 37ºC in TBS.

## 3.2. IONIC LIQUID MEDIUM

In the reactions carried out in ionic liquid (IL), the quantification method previously used - UV/Vis spectroscopy – is no longer appropriate. Due to the imidazolium ring, which has an interference with the NADH detection by spectrophotometry because absorbs light at λ= 300 nm [108].

Considering that the IL properties such as low vapour pressure and low volatility, it is a suitable solvent to be used in headspace gas chromatography (HS-GC), where the sample is heated and only the vapour phase of the sample is injected. In this specific case, since IL is not volatile, only the analytes dissolved in the IL will be part of the vapour phase and injected in the GC. IL is also used to enhance the response of volatile compounds in HS-GC [116].

Since the cofactor NADH/$NAD^+$ is not soluble in organic solvents, it is necessary provide some water to the system to solubilize the cofactor, so a small amount of water is present in the sample.

When an enzyme is exposed to an organic solvent which is non-polar, it will not mix with water; these hydrophobic solvents do not strip the crucial water from the enzyme surface not affecting its activity. However when hydrophilic organic solvents are used, they can remove this crucial water

leading to protein unfolding [10]. Because of the addition of the water in this specific enzymatic system, lower activities can be expected.

Immobilization may have a stabilization effect, contributing to a higher stability, by optimization of enzyme dispersion, improvement of the accessibility for the substrates, as well as to avoid the aggregation of the hydrophilic protein particle [49]. Also enables enzyme reutilization

ILs, compared to current solvents, have a good $CO_2$ solubility dissolving higher amounts than in water. In addition, by having more $CO_2$ dissolved in the medium theoretically, a greater methanol rate can be achieved.

A commitment between water miscibility, $CO_2$ solubility and the respective effects of the ionic liquid in enzyme activity was established.

### 3.2.1. HS-GC - SCREENING OF DIFFERENT IONIC LIQUIDS

Ionic liquids cannot be considered completely inert [10]. Indeed the anion and the cation can dissociate by the interaction with the water in the system and reduce enzyme activity.

The ILs tested were the ones that showed some water miscibility, appreciated $CO_2$ solubility, and not have a very negative effect in the enzymes.

Initially five ionic liquids were tested as solvents: Aliquat® 336, [BMIM][Ac], [BMIM][$BF_4$], [BMIM][DCA] and [EMIM][$EtSO_4$].

The ionic liquid tested Aliquat® 336 is the most water immiscible and the one that presents a better $CO_2$ solubility. [EMIM][$EtSO_4$] it is composed by an 1-ethyl-3-methylimidazolium cation that, because of the small alkyl chain, can have an inhibitory effect in the enzymes because of its structural similarity with imidazole ring of the NADH.

1-Butyl-3-methylimidazolium cation was tested, using [BMIM][Ac], [BMIM][$BF_4$], and [BMIM][DCA], which have the least chance to interact with the enzymes by the longer alkyl chain (butyl).

Ionic liquids with anion such as [$PF_6^-$] – hexafluorophosphate - are not suitable to enzymatic catalysis, not necessarily by the IL impurity's but mainly due to the release of phosphate into the media, which can contribute to enzyme deactivation, that fact was also reported for ADH [95].

To determinate the IL that can give a better methanol response in HS-GC, a reaction with ADH and a blank experiment was performed with the same methanol concentration and a water percentage of 7.5% (v/v).

Comparing the chromatogram of the different ILs with methanol, (Figure 3.10), the peak correspondent to methanol has a retention time from 2.58 to 2.65 min. The corresponding peek areas

are represented in Table 3.6. The IL that presents a higher methanol peak area is Aliquat® 336, however this one it is the most water immiscible.

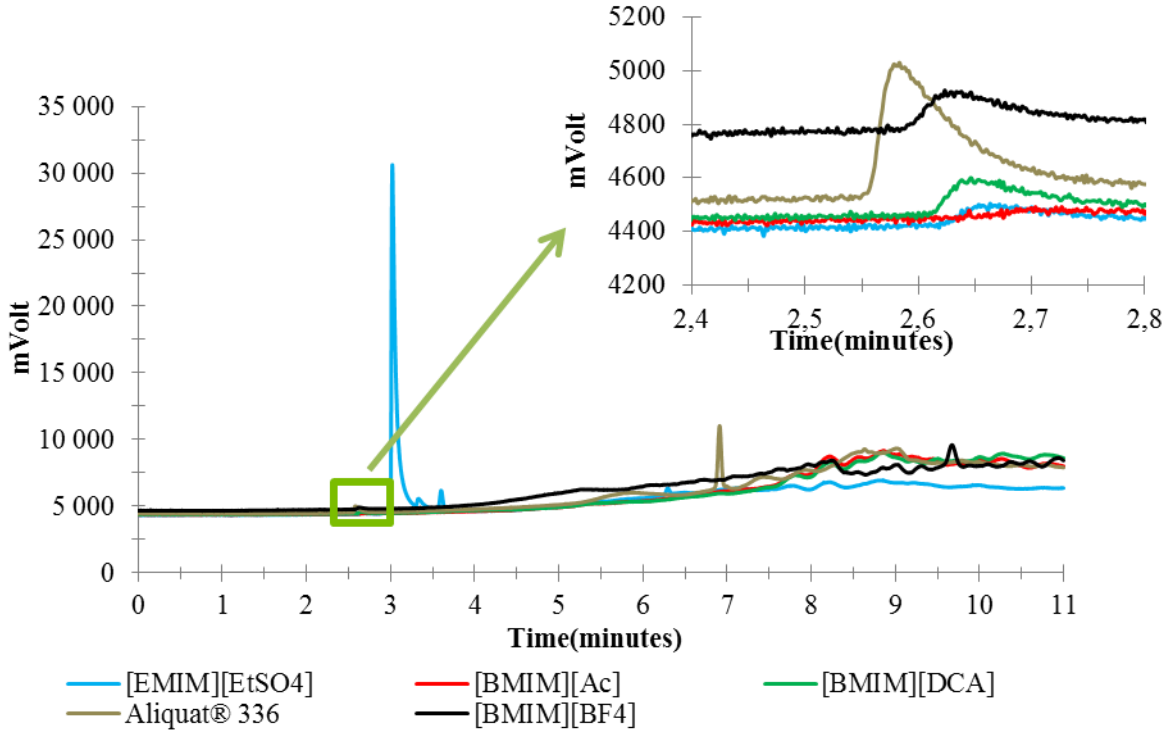


**Figure 3.10 –** Chromatogram from HG-GC analysis of methanol in different ionic liquids, with an expansion at the methanol retention time.

**Table 3.6-** Methanol response in HS-GC with different ionic liquid.

| Ionic Liquid | Peak Area MeOH |
|---|---|
| Aliquat® 336 | 25953 |
| [BMIM][$BF_4$] | 15304 |
| [BMIM][DCA] | 8703 |
| [EMIM][$EtSO_4$] | 3634 |
| [BMIM][Ac] | ~ 0 |

The enzymatic methanol conversion by ADH in solution, with the cofactor $NAD^+$ dissolved in ionic liquids, was also tested and results are presented in the Table 3.7. The respective peak areas,

reveal in all the cases an diminishing of the methanol concentration possibly due to enzymatic conversion/catalysis. Aliquat® 336, is the most water immiscible and difficult to work it, So the ionic liquid that has chosen as solvent to the following reactions was [BMIM][$BF_4$], that has the second best results and response to the method,

**Table 3.7 –** Methanol peak areas in different ionic liquid after enzymatic conversion by ADH.

| **Ionic Liquid** | **Peak Area MeOH ADH in solution** |
|---|---|
| Aliquat® 336 | 17605 |
| [BMIM][$BF_4$] | 9186 |
| [BMIM][DCA] | 2895 |

### 3.2.2. CALIBRATION METHOD

The calibration of the method can be made using an internal standard, however this would possibly interfere with methanol detection. Also, the standard recommended in the literature is an alcohol such as propanol, being this inconvenient since it is one of ADH substrates.

The calibration was made with a calibration curve, based in the instructions of EN 14110 (in 6.3. EN 14410)

However this method has some drawbacks. Indeed, when the ionic liquid in the vial is heated an equilibrium was established between the liquid and the gaseous phases, this can be influenced not only by the polarity of the solvent, but by the preparation of the sample. ILs are quite viscous and each sampling has an associated error and cannot be reinjected because the vial is no longer sealed, and some of the volatile substances, are already on the gas phase. The reproducibility of the calibration curve is not very good, since it is greatly affected by many external factors (temperature, operator, etc.), and this is more noticeable for higher methanol concentrations (80 to 100 mM) (Figure 3.11).

The experimental data were data plotted in Figure 3.11, and the best possible calibration curve was in one experiment (the data were from the same day) were determinate and the correspondent curve was Peak area = 121,29 x [Methanol](mM) + 1967,6, and use to quantify methanol in [BMIM][$BF_4$].

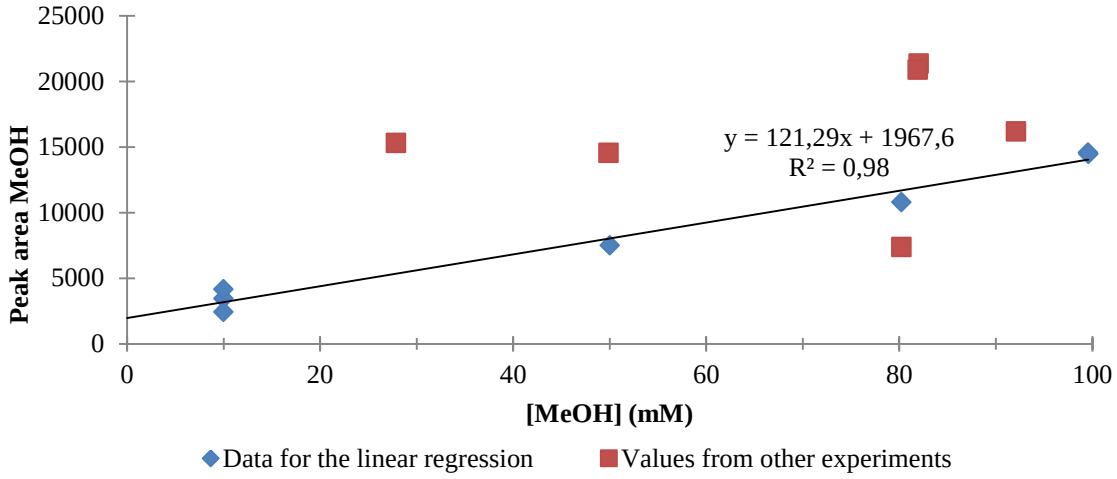


**Figure 3.11** – Calibration curve for methanol in [BMIM][$BF_4$] with 7.5% (v/v) of TBS buffer, ranging from a methanol concentration of 10 to 100 mM .

The influence of the sol-gel matrix as also evaluated, to assess its impact in reactions with immobilized enzyme (transformation of methanol to formaldehyde).

In literature its effect is not reported, but the experimental data reveal that when sol-gel was directly and freshly added to the mixture, an increase in response was observed, however the results are not linear.

### 3.2.3. METHANOL CONVERSION TO FORMALDEHYDE

As determined by the calibration curve, Figure 3.11, the minimum methanol concentration detected was 10 mM. The enzymatic methanol production from $CO_2$ requires about 3 times more NADH, assuming that we have a complete reaction.

Also, to perform the enzymatic conversion of $CO_2$ without a high pressure apparatus, by bubbling $CO_2$, an exit is needed. The $CO_2$ can transport some of the methanol formed, which is then not being detected, even if the solution was saturated in carbon dioxide, the concentration of $CO_2$ may not be sufficient.

To ensure more accurate measurements, different experiments were performed without adding NADH but adding $NAD^+$, and not measuring methanol production but its conversion/consumption. Therefore, the conversion of methanol into formaldehyde catalysed by ADH (Figure 3.12) became the viable option.

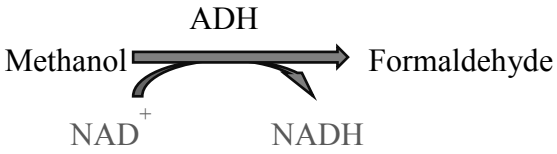


**Figure 3.12 –** Methanol oxidation to formaldehyde catalysed by ADH, with the reduction of $NAD^+$.

In these experiments to ensure a minimum error induced from the partition between the gas and the liquid, no "dead" volume existed prior to the analysis. However, if the reaction vial were not properly seal the results obtained are not dependable of the catalysis, but mainly by methanol diffusion. A control experiment was performed, and submitted to the same conditions as the reaction vessels.

In Table 3.8 are the data from methanol conversion by non–immobilized ADH in [BMIM][$BF_4$], with different percentages of the buffer. Comparing the results of the methanol peak, the higher conversion seems to be with ADH_1, the sample with less water content, although this may be explained by the difference in polarity between the reaction media. The conversions are also higher than expected because, the enzymes are not protected from the reaction medium, and in ionic liquid, they can be denatured. Also the cofactor has a low solubility [117] and was used in poor concentration (5mM), much smaller than methanol concentration, so an error can be associated.

The data from methanol conversion by non–immobilized ADH in [BMIM][$BF_4$], with 7.5%(v/v) of buffer are plotted in Figure 3.13, with the correspondent expansion in the methanol peak region.

**Table 3.8 –** Methanol conversion (24h) by non-immobilized ADH in [BMIM][$BF_4$] in all the cases the $[MeOH]_{initial}$ was of 100 mM. The final Methanol concentration was determined by calibration curve Peak area = 121,29 x [Methanol](mM) + 1967,6.

| Sample | $[NAD^+]$ (mM) | TBS $\frac{[BMIM][BF_4]}{}$ in % (v/v) | Peak Area MeOH | [Methanol] (mM) | Methanol Conversion (%) |
|---|---|---|---|---|---|
| Control | 0 | 7.5 | 25905 | 197 | ---- |
| [ADH]=1.5 mg/mL _1 | 5 | 7.5 | 21592 | 162 | 18 |
| [ADH]=1.5 mg/mL _2 | 5 | 20 | 22440 | 169 | 14 |

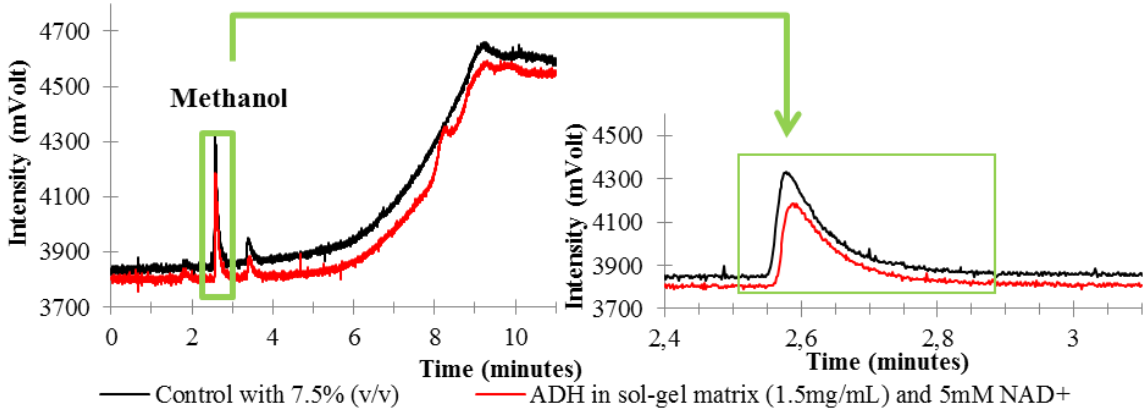


**Figure 3.13 –** Chromatogram from HG-GC analysis of the methanol conversion (24 h) by non-immobilized ADH in [BMIM][BF4] with 7.5% (v/v) of TBS buffer, a [MeOH]initial of 100 mM and [$NAD^+$]=5mM. An expansion at the methanol retention time is also represented.

When sol-gel is added to the medium, Figure 3.14 and Figure 3.15, the methanol response decreases, making the controls and the samples areas quite similar. This can be explained by some methanol absorption in the matrix over time, as is possible to see by the methanol areas; when sol-gel is present those are approximately 7 times smaller.

In the reaction with FateDH+FaldDH+ADH, Table 3.9, a proportional NADH concentration was used. In an attempt for methanol production, a 3 times superior NADH concentration was used, to the minimum methanol detectable in the calibration curve in Figure 3.11. (30 mM). However no methanol production was detected.

**Table 3.9 –** Methanol conversion/production (24h) by immobilized ADH and FateDH+FaldDH+ADH in [BMIM][$BF_4$] medium.In the control and when only ADH were used the $[MeOH]_{initial}$ was of 100 mM. The final Methanol concentration was determined by calibration curve Peak area = 121,29 x [Methanol](mM) + 1967,6.

| Sample | [NADH] (mM) | [$NAD^+$] (mM) | TBS / [BMIM][$BF_4$] in % (v/v) | Peak Area MeOH | [Methanol] (mM) | Methanol Conversion (%) |
|---|---|---|---|---|---|---|
| Control (with empty sol-gel matrix) | 0 | 0 | 7.5 | 3767 | 9.6 | ---- |
| [ADH]=1.5 mg/mL_3 | 0 | 10 | 7.5 | 3642 | 9.1 | 5 |
| [FateDH+FaldDH+ADH] = 3; 1.5; 1.5 mg/mL | 30 | 0 | 7.5 | 0 | 0 | ------ |

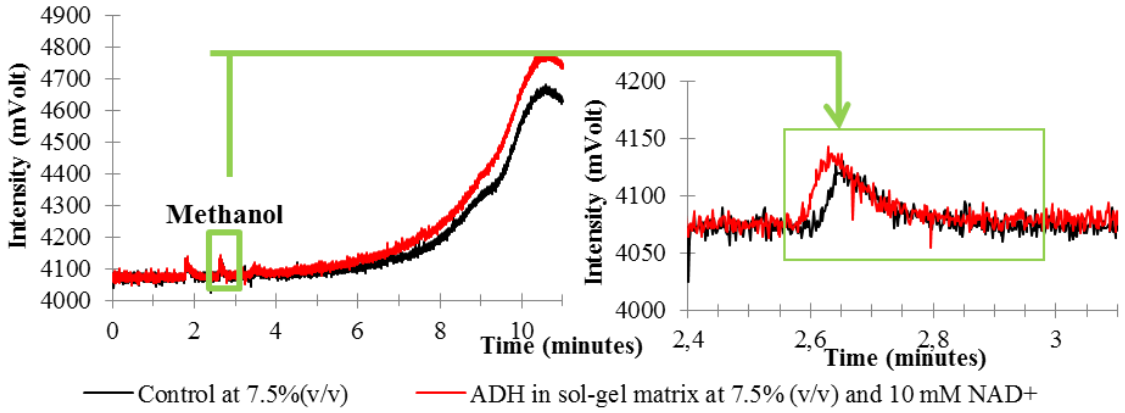


**Figure 3.14** – Chromatogram from HG-GC analysis of the methanol conversion (24 h) by immobilized ADH in [BMIM][$BF_4$] with 7.5% (v/v) of TBS buffer and a $[MeOH]_{initial}$ of 100 mM and $[NAD^+]$=10mM. An expansion at the methanol retention time is also represented.

Comparing the ADH conversion of methanol from Table 3.9 and the FateDH+FaldDH+ADH conversion of methanol in Table 3.10, it is possible to observe a higher methanol conversion percentage when the 3 enzymes are used (26 to 5 %) versus when only ADH is present. This can be a positive indicator to our system, by showing an interaction between the different intermediates and the enzymes.

**Table 3.10 -** Methanol conversion (24h) by immobilized FateDH+FaldDH+ADH in [BMIM][$BF_4$] medium. In all the cases the $[MeOH]_{initial}$ was of 100 mM. The final Methanol concentration was determined by calibration curve Peak area = 121,29 x [Methanol](mM) + 1967,6.

| **Sample** | **$[NAD^+]$ (mM)** | **TBS [BMIM][$BF_4$] in % (v/v)** | **Peak Area MeOH** | **[Methanol] (mM)** | **Methanol Conversion (%)** |
|---|---|---|---|---|---|
| Control | 0 | 17 | 3903 | 10.1 | ------- |
| [FateDH+FaldDH+ADH] = 1.5; 1.5; 3 mg/mL | 30 | 17 | 3255 | 7.5 | 26 |

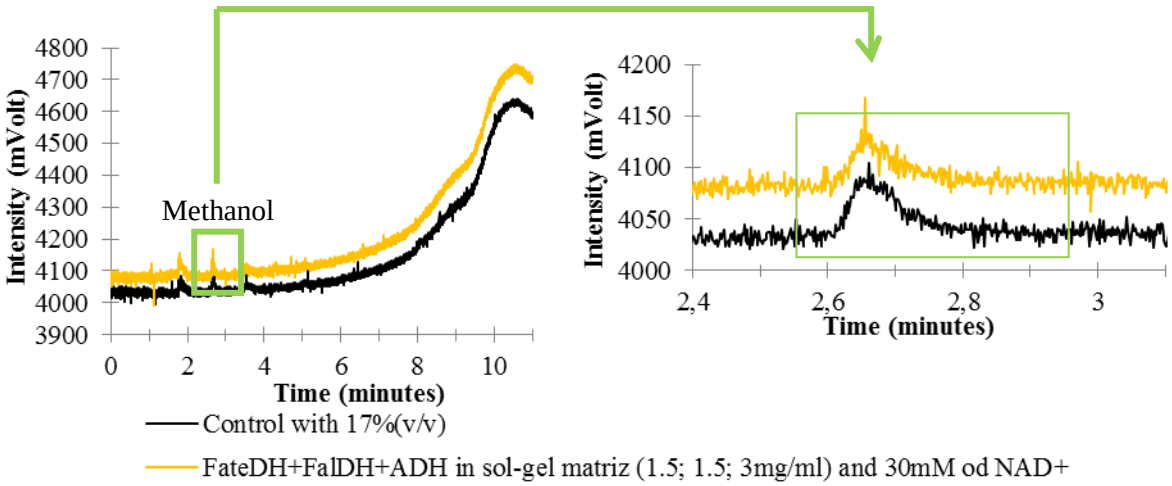


**Figure 3.15** – Chromatogram from HG-GC analysis of the methanol conversion (24 h) by immobilized ADH in [BMIM][$BF_4$] with 17% (v/v) of TBS buffer and a $[MeOH]_{initial}$ of 100 mM and [$NAD^+$]=30mM. An expansion at the methanol retention time is also represented.

## 3.3. NMR

As described previously a high pressure apparatus was used in an attempt to detect the reduction of $CO_2$ to formate catalysed by FateDH immobilized and non-immobilized, (the first step of the reaction depicted in Figure 1.14) in ionic liquid - [BMIM][$BF_4$]- medium.

The enzyme as the NADH did not dissolve in the ionic liquid, so it was added to the reaction medium an aqueous solvent, which may contribute to a less efficient catalysis. The resulting $^{13}C$ (Figure 3.16) and $^{1}H$-NMR (Figure 3.17) spectra only revealed the presence of the ionic liquid.

However, the final step in which a slow depressurization is conducted, can contribute to some sample deterioration and led to escape of the remaining $CO_2$. So, a different approach in which the *in situ* quantification by NMR was conducted, and the respective results were analysed in the next section.

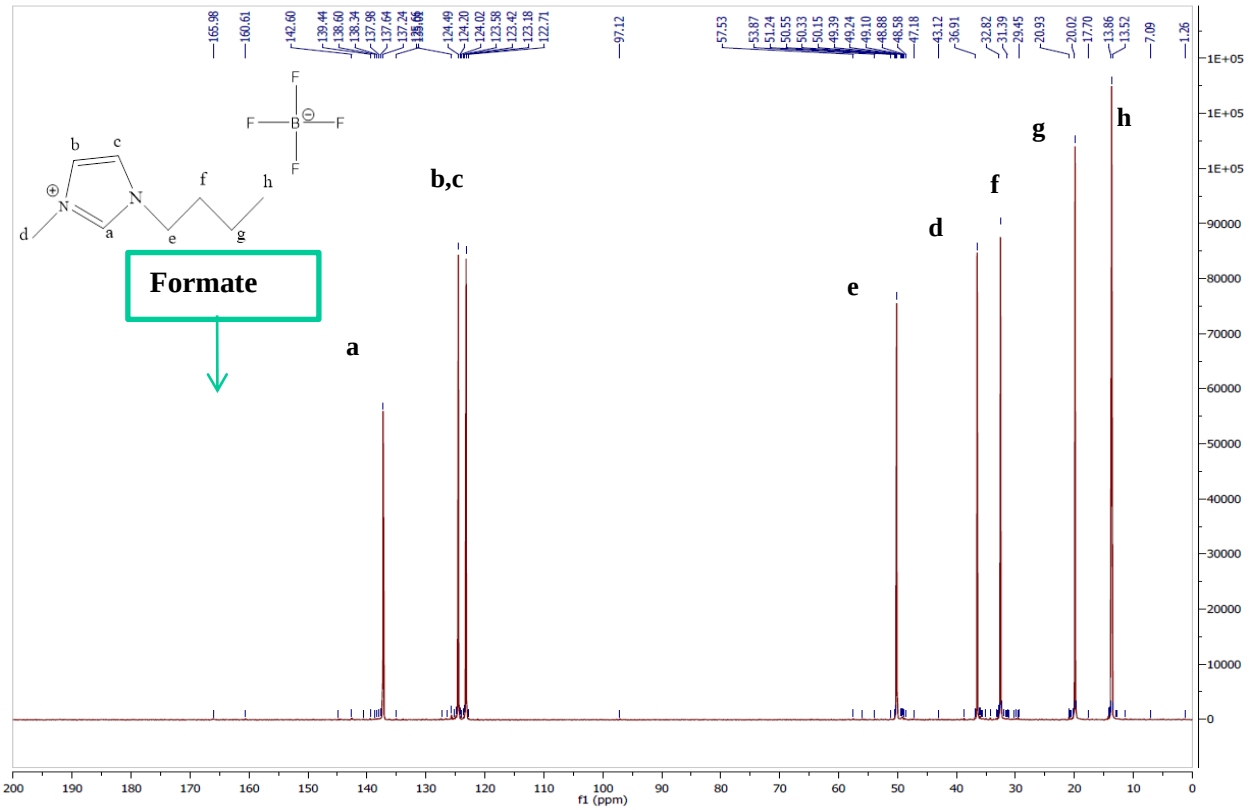


**Figure 3.16 –** $^{13}C$ NMR (100 MHz) spectrum in [BMIM][$BF_4$] with TBS of FateDH with NADH. Sample was acquired after slow depressurization and added 10% (v/v) of $D_2O$.

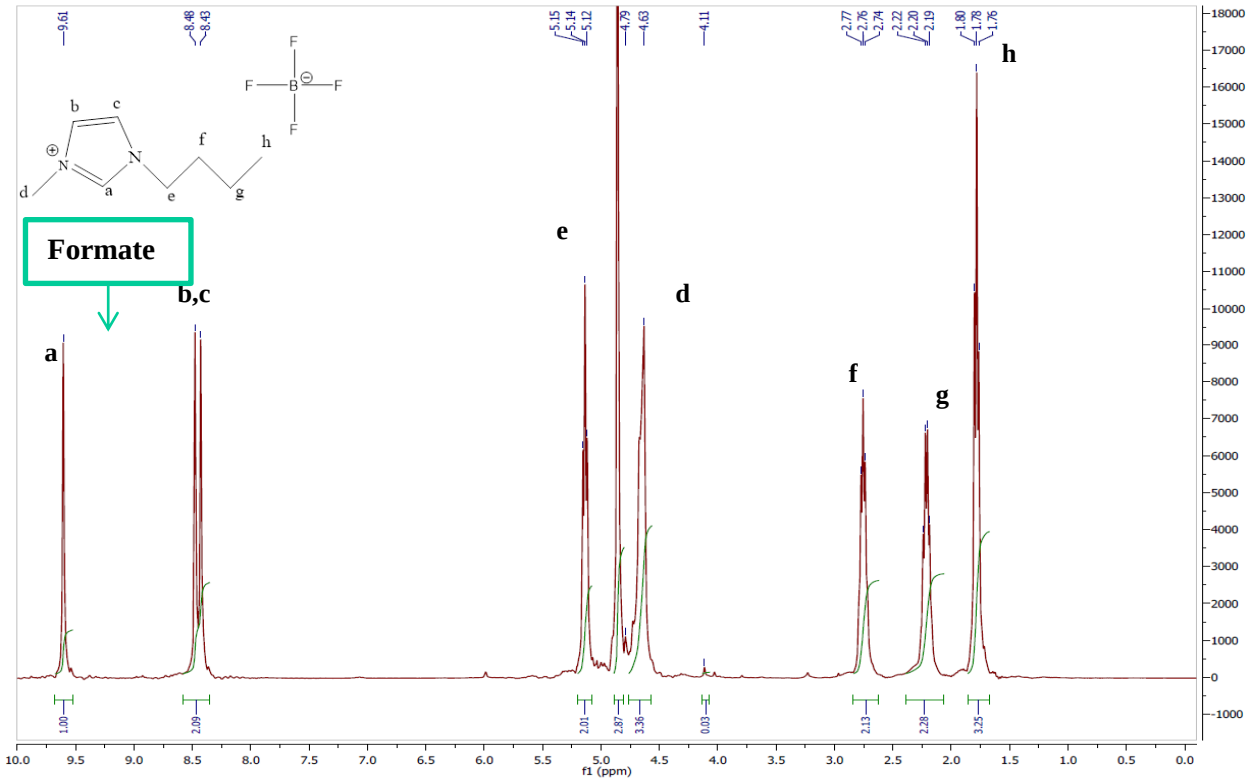


**Figure 3.17 –** $^{1}H$ NMR (400 MHz) spectrum in [BMIM][$BF_4$] with TBS of FateDH with NADH. Sample was acquired after slow depressurization and added 10% (v/v) of $D_2O$.

### 3.3.1. HP-NMR

HP-NMR experiments were performed to evaluate the enzymatic conversion of $CO_2$ to formate by FateDH, and the sequential conversion of $CO_2$ to methanol by FateDH + FaldH + ADH. All the experiments in HP-NMR were performed in Tris-$d_{11}$Cl buffer 100 mM pH 7. Both proton ($^1$H) and carbon ($^{13}$C) NMR spectra were collected at different times during the whole reaction period.

The $^{13}$C spectrum enables a better perception of the different $CO_2$ derivated metabolites and the $^1$H spectra enables the visualization of the formate anion being formed and the different protons present in the NADH molecule.

Blank experiments were performed to determinate the chemical shift of the different compounds.

When we used labelled $CO_2$, in the HP-NMR experiments we detected three different signals in the $^{13}$C spectrum (Figure 3.18). The most abundant, at 125 ppm corresponds to the dissolved $CO_2$ in the mixture. The two other signals are different species resulting from $CO_2$. At 160 ppm a second peak emerges, and after $CO_2$ this is the most abundant species, the other at 171 ppm is a much less abundant.

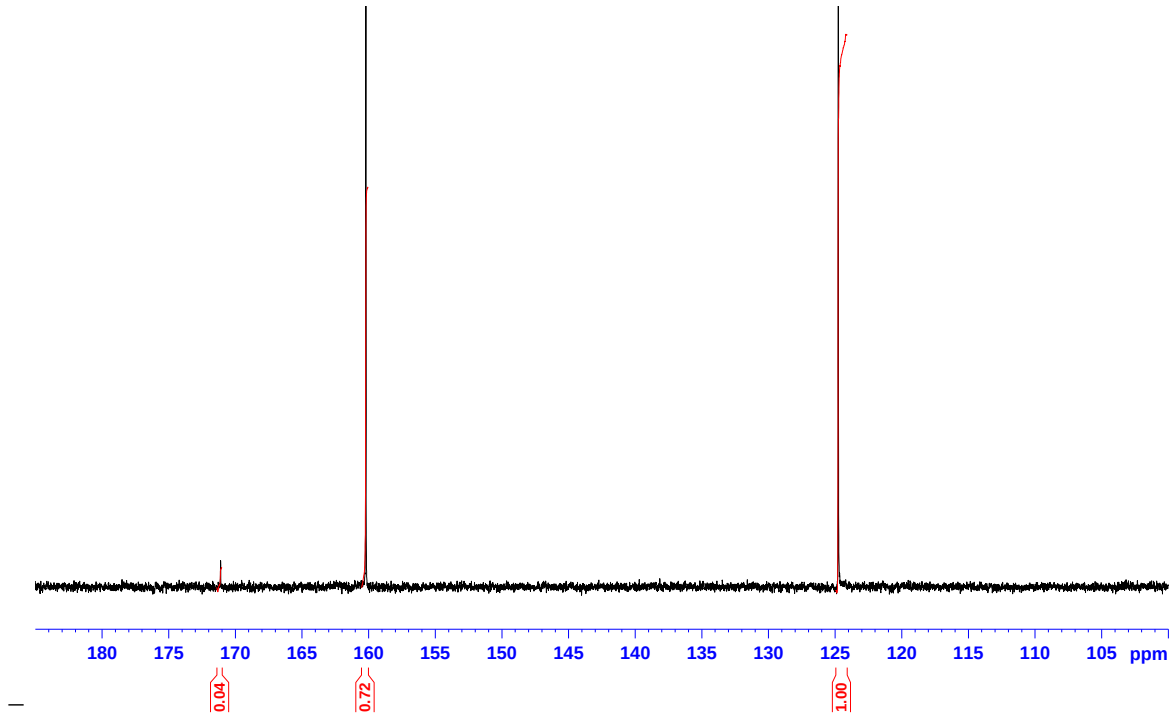


**Figure 3.18 –** $^{13}$C NMR (100 MHz) spectrum in Tris-$d_{11}$ of FateDH+FaldDH+ADH with NADH and after 77 h from the pressurized with $^{13}CO_2$ at 37ºC.

The 160 ppm signal is consistent with an amide formation. This is probably due to a side reaction between the amine of the tris buffer with the carbon dioxide, (Eq. 5). To further clarify this

idea we performed a blank experiment by pressurizing $CO_2$ into a HP-NMR tube (1.05 MPa) containing only Tris-DCl buffer 100 mM pH 7 – Figure 3.19 (b).

$$RNH_2 + CO_2 \rightarrow RNHCOOH \qquad [118] \qquad (5)$$

The resulting spectrum (Figure 3.19 (b)) supports the carbamate formation. A direct consequence of this buffer side reaction can be a decrease on the pH of the media and consequently the absence of the optimum pH for the enzyme reaction. Also, if side reactions are present, less $CO_2$ will be available in the medium for the enzymatic reaction.

The 171 ppm signal remained to be identified. This small peak can possibly be related to the enzymatic production of formate from $CO_2$. However none of the other intermediated species involved in the enzymatic cascade (formaldehyde and methanol) were detected. The enzymatic reaction taking place leads to the formate production, so we needed to determine the chemical shift of formate in the same experimental conditions as $CO_2$ in TBS (Figure 3.19 (b))A spectrum of formic acid (formic acid concentration 4.4 M, was acquired (Figure 3.19 (a)). The formic acid spectra exhibits a carbonile chemical shift at 165 ppm in $^{13}C$ spectrum which is different from the 171 ppm signal present in our reaction (Figure 3.19 (c)).

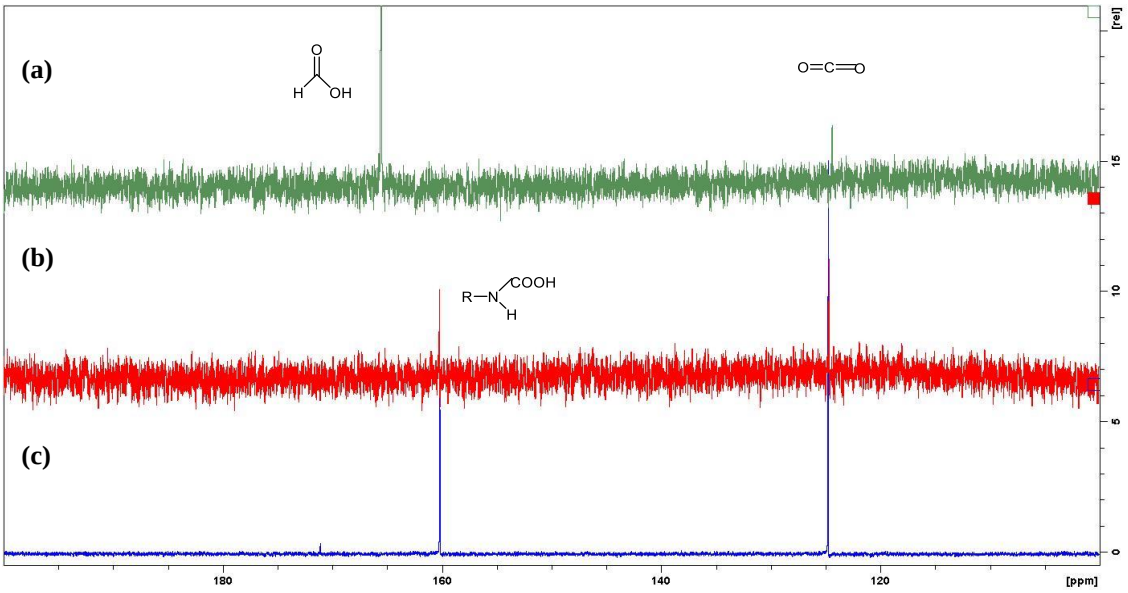


**Figure 3.19 –** $^{13}C$ NMR (100 MHz) spectra in Tris-$d_{11}$ of **(a)** formic acid (after $CO_2$ depressurization) at 25ºC; **(b)** pressurized tube with $CO_2$ at 25ºC and **(c)** FateDH+FaldDH+ADH with NADH and after 65 h from the pressurized with $^{13}CO_2$ at 37ºC

When comparing in Figure 3.20, the integral from the $CO_2$ peak, and the integral from carbamate peak, the molar proportion of carbamate to $CO_2$ is 0.7604, indicating that if all the tris (100 mM) added to the tube had reacted, the $CO_2$ initially added to the medium would be ca. 232 mM. At 1 MPa and 37ºC the Henry constant ($k_{CO_2,\ 25ºC}$) was about 200 MPa, indicating that the maximum $CO_2$ dissolved in the medium would correspond to 279 mM. So, considering the different equilibrium between the liquid and the gaseous phase it is possible that most of the tris from the buffer reacted with the $CO_2$. This can cause a decrease of the pH, and destabilize the enzymes and its activity.

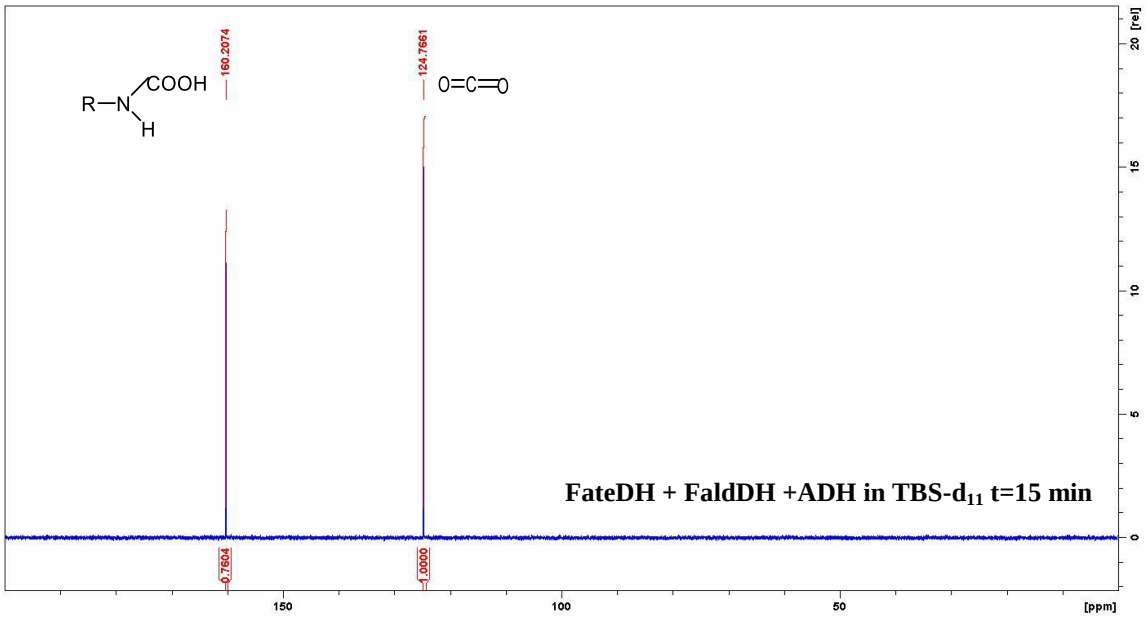


**Figure 3.20 –** $^{13}C$ NMR (100 MHz) spectrum in Tris-$d_{11}$ FateDH+FaldDH+ADH with NADH and after 15minutes from the pressurized with $^{13}CO_2$ at 37ºC.

A blank of NADH in Tris-HCl buffer 100 mM pH 7 with NADH was collected. $^1$H-NMR spectra shows several peaks, correspondent to NADH (Figure 3.22). The highlight is in H-r and H-q from NADH (Figure 3.21) since in the catalysed reaction a hydride transfer occurs between NADH and the oxido-reductases and the hydrogen (H-q) is involved in NADH oxidation.

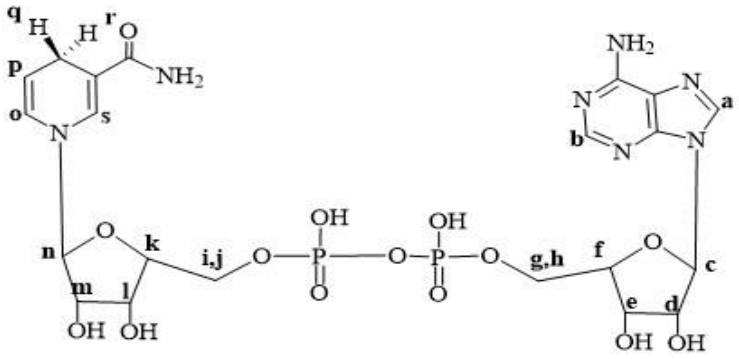


**Figure 3.21 –** Proton attribution in NADH molecule.

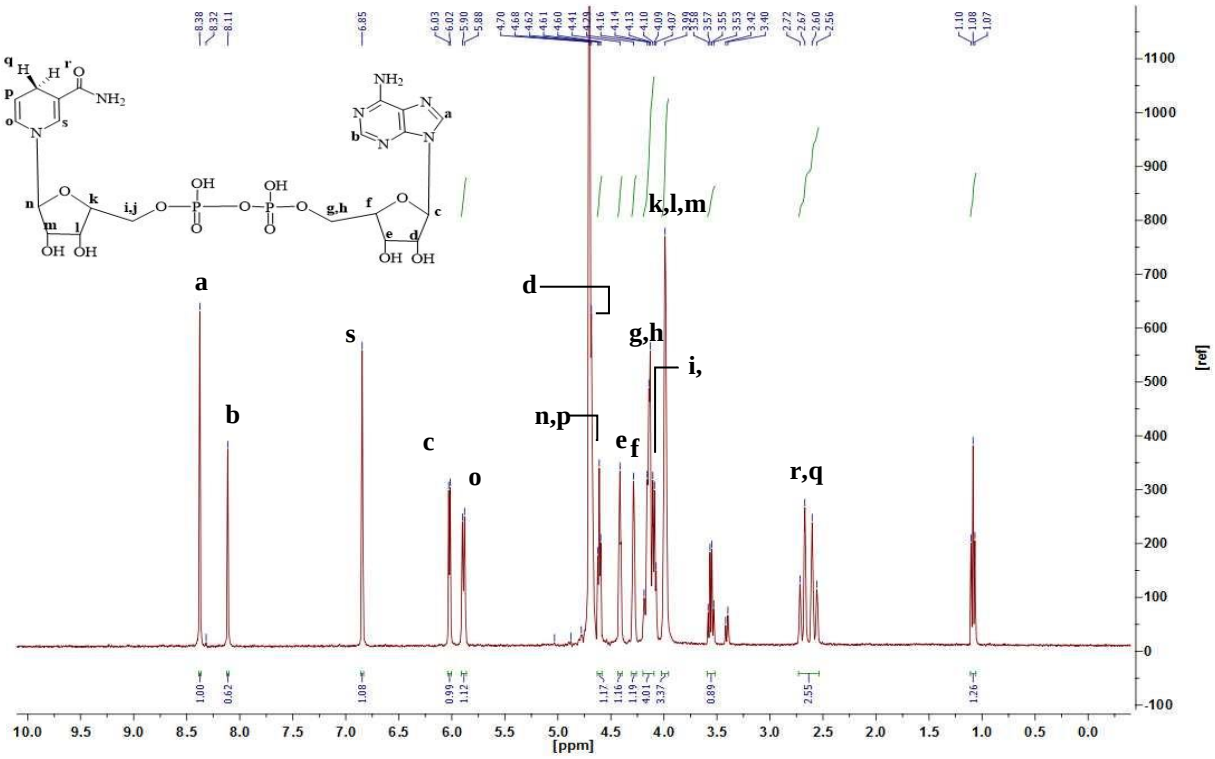


**Figure 3.22 –** $^{1}$H NMR (400 MHz) spectrum of NADH in Tris-$d_{11}$ at 25ºC.

$^{1}$H spectra collected over time from both the reaction catalysed by FateDH - $CO_2$ in formate and FateDH + FaldH + ADH - sequential conversion of $CO_2$ to methanol, are represented in the Figure 3.23 and Figure 3.24, respectively.

This $^{1}$H-NMR spectra confirmed a transformation of NADH to $NAD^+$ evidence, in the form of the diminishing of the signal attributed to H-r and H-q peak at 2.9 ppm at 37 ºC and 2.6 ppm at 25ºC. and subsequent formation of the $NAD^+$ resulting signals at approximately 8.9 ppm.

In addition, it was seen previously, there is strong evidence that the pH of the medium decreases with $CO_2$ presence. However in the literature when this multy-enzymatic system, in combination with tris-based buffer was used, this is not also notice.

With time, at ca. 8.5 ppm, a very small peak appears. This can be related with the formation of formate, although this needs further confirmation.

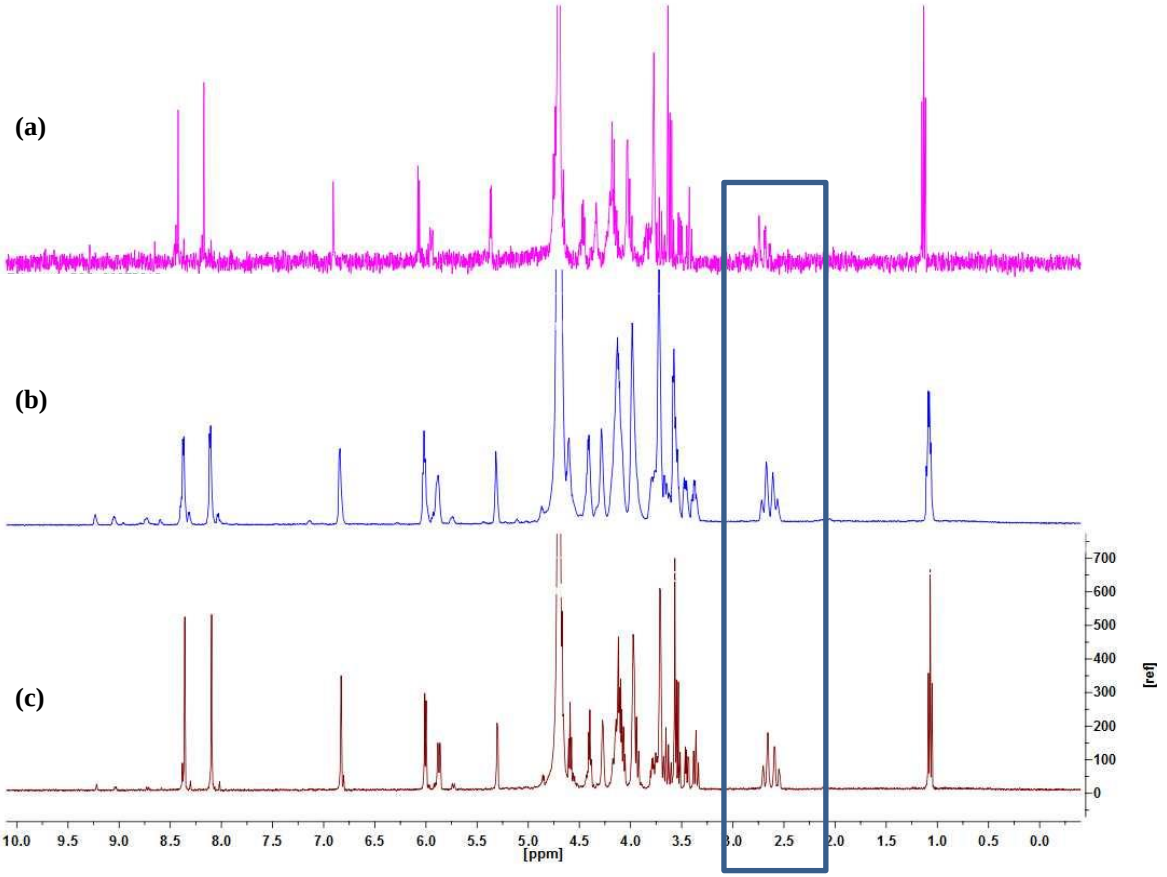


**Figure 3.23 –** $^{1}H$ NMR (400 MHz) spectrum in Tris-$d_{11}$ of FateDH with NADH and after 50 hours **(a)**; 23hours **(b) and** 5.5 hours **(c)** from the pressurized with $^{13}CO_2$ at 25ºC.

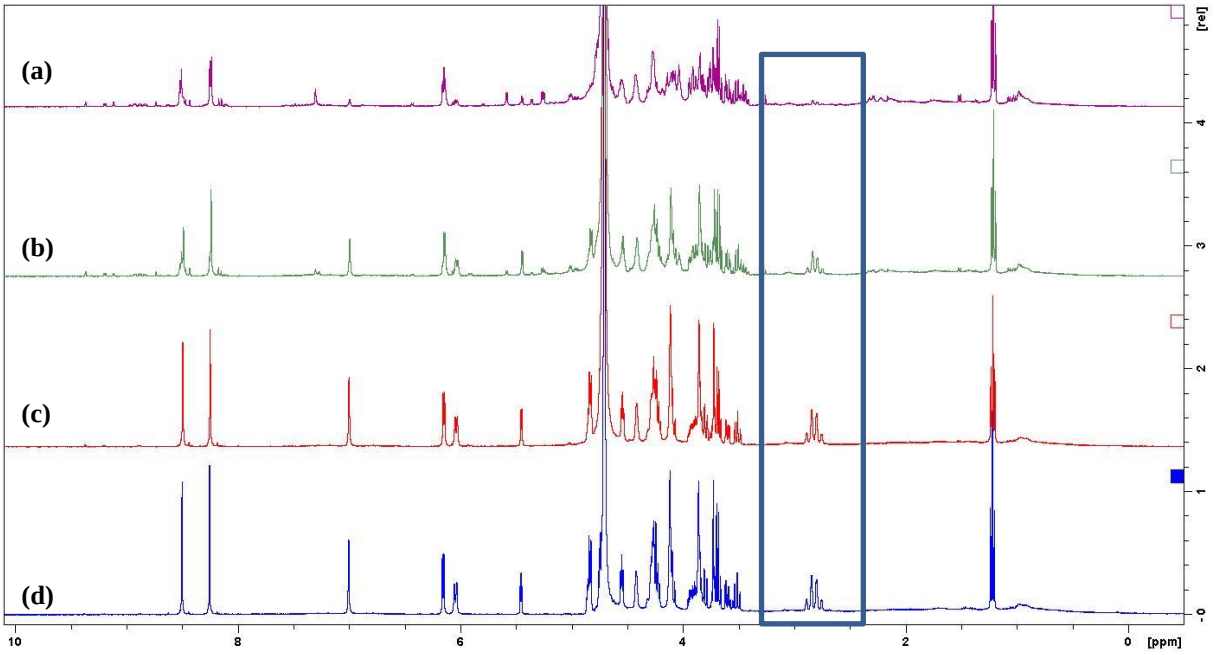


**Figure 3.24 –** $^{1}H$ NMR (400 MHz) spectrum in Tris-$d_{11}$ of FateDH+FaldDH+ADH with NADH and after 65 hours **(a)**; 49hours **(b)**; 12 hours **(c)** and 15minutes **(d)** from the pressurized with $^{13}CO_2$ at 37ºC.

# 4. CONCLUSIONS AND FUTURE WORK

# 4. CONCLUSIONS AND FUTURE WORK

The results achieved during this work showed that the enzymatic cascade to produce methanol from $CO_2$ has many limitations. In this system the different substrates/products need to go from one enzyme to another so that all reactions can take place. The experiments revealed some interaction between the different reaction components, namely phosphate-based buffers with NADH, as evidenced by UV/Vis spectroscopy), and Tris with $CO_2$, as evidenced by HP-NMR.

The results in aqueous medium lead to the conclusion that the most important enzyme for the conversion of $CO_2$ to methanol is FateDH. The HP-NMR experiments reveal NADH conversion when $CO_2$ is in the presence of FateDH, but without significant formate production.

Through the analysis of these results some conclusions can be made. The pH of the aqueous solution at atmospheric pressure versus 1 MPa (used in HP-NMR experiments) does not seem to change the reaction rate drastically. This is clear from the experiment where after 6 h of bubbling $CO_2$, only 9% of the NADH added was consumed. The concentration of $CO_2$ in the media is, at most1.5 times smaller than the tris concentration in TBS buffer. This leads to a high $CO_2$ conversion via carbamate formation through reaction with amine groups of the buffer, leaving less $CO_2$ available to be consumed by the enzymes.

In experiments with ionic liquid, which were analysed by HS-GC, it was only possible to observe methanol conversion by the enzymes and not the formation of methanol. This is probably because of the methanol detection limit being too high for the quantity of the methanol produced in the reaction of interest. However to increase the cofactor concentration and the resulting methanol concentration, a higher amount of water in the ionic liquid is needed. This can damage the GC column.

Considering all the different aspects described above, it is clear that the enzymatic production of methanol using this strategy is difficult, and so is the quantification of methanol. The direct observation of methanol production was not possible, but a better knowledge of this system and its previously unknown limitations was acquired. To improve methanol production, recombinant enzymes can be used, or even microorganisms.

In the future, to assess the occurrence of acidification of a medium containing Tris with high-pressure $CO_2$, an experiment can be performed, adding a pH indicator to the buffer prior to its pressurization.

Also in HS-GC, experiments with higher enzyme amount and a higher NADH concentration should be performed, to better assess the methanol conversion/production in ionic liquid medium.

Another important factor is the need to use a different buffer, because of the side reaction occurring between phosphate and Tris-based buffers. An alternative may be PIPES buffer (1,4-piperazinediethanesulfonic acid) [110] or MOPS buffer (3-(n-morpholino) propanesulfonic acid), which work in an adequate pH range (6.1-7.5 and 6.5-7.9, respectively).

After assuring minimum buffer interference, another HP-NMR experiment can be performed, using immobilized enzymes in ionic liquid medium.

To improve catalysis, one of the main aspects is the lack of NADH regeneration, making this cofacfor a limitation reagent. By taking advantage of the high ionic conductivity of the ionic liquid [41], electrochemical NADH regeneration is a possibility. Another alternative is enzymatic regeneration, through the use of a fourth enzyme such as glutamate dehydrogenase (GDH) [31].

The operation of the system in continuous mode, as in Figure 4.1, will also be interesting in the future, enabling $CO_2$ recycling and an enrichment in methanol production.

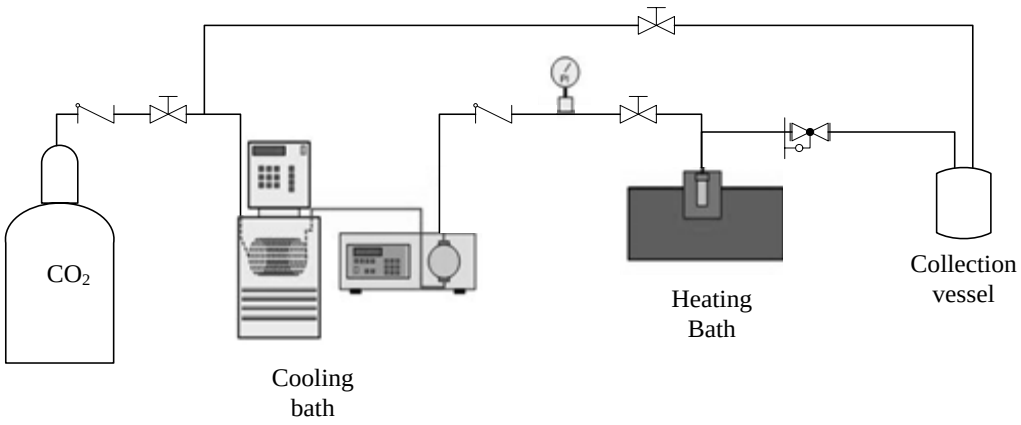


**Figure 4.1** – Schematic representation of the experimental apparatus used for the batch experiments.

As alternative detection/quantification of methanol in aqueous samples in the future could be HPLC (High Pressure Liquid Chromatography).

To enhance the stability of the system different approaches can be taken, namely enzyme engineering and modification of enzymes [113,119], and changing the sol-gel matrix with m-PEG (methoxy-poly(ethylene) glycol) [113]. This method was already applied to the stabilization of FateDH [119] and ADH [113]. Another strategy may be the thermal stabilization of the enzymes and NADH encapsulation in liposomes [120].

# 5. REFERENCES

# 5. REFERENCES


[1] G.A. Olah, A. Goeppert, G.K.S. Prakash, Chemical recycling of carbon dioxide to methanol and dimethyl ether: from greenhouse gas to renewable, environmentally carbon neutral fuels and synthetic hydrocarbons, J. Org. Chem. 74 (2009) 487–498.

[2] G.A. Olah, A. Goeppert, G.K.S. Prakash, Beyond oil and gas : the methanol economy, 1st ed., Wiley-VCH Verlag GmbH & Co. KGaA, Los Angeles, 2006.

[3] T.A. Boden, G. Marland, R.J. Andres, Global, Regional, and National Fossil-Fuel CO2 Emissions, Carbon Dioxide Information Analysis Center Oak Ridge National Laboratory U.S. Dep. Energy. (2010). Available at :http://cdiac.ornl.gov/ftp/ndp030/global.1751_2008.ems.

[4] E.J. Beckman, Supercritical and near-critical CO2 in green chemical synthesis and processing, J. Supercrit. Fluids. 28 (2004) 121–191.

[5] M.O. Adebajo, R.L. Frost, Recent Advances in Catalytic/Biocatalytic Conversion of Greenhouse Methane and Carbon Dioxide to Methanol and Other Oxygenates, in: G. Liu (Ed.), Greenh. Gases - Capturing, Util. Reduct., InTech, 2012: pp. 31–56.

[6] A. Boddien, F. Gärtner, C. Federsel, I. Piras, H. Junge, R. Jackstell, et al., Catalytic Utilization of Carbon Dioxide: Actual Status and Perspectives, in: K. Ding, L.-X. Dai (Eds.), Organic Chemistry -Breakthroughs and Perspective, 1st ed., Wiley-VCH Verlag GmbH & Co. KGaA, Weinheim, Germany, 2012: pp. 685–724.

[7] R. Skouta, Selective chemical reactions in supercritical carbon dioxide, water, and ionic liquids, Green Chem. Lett. Rev. 2 (2009) 121–156.

[8] W. Leitner, Designed to dissolve, Nature. 405 (2000) 129–130.

[9] S. Keskin, D. Kayrak-Talay, U. Akman, Ö. Hortaçsu, A review of ionic liquids towards supercritical fluid applications, J. Supercrit. Fluids. 43 (2007) 150–180.

[10] S. Cantone, U. Hanefeld, A. Basso, Biocatalysis in non-conventional media—ionic liquids, supercritical fluids and the gas phase, Green Chem. 9 (2007) 954–971.

[11] G.K.S. Prakash, G.A. Olah, Reversing Global Warming: Chemical Recycling and Utilization of CO2, Los Angeles, 2008.

[12] A.P. Keiboom, J. Moulijn, R.A. Sheldon, P.W.N.M. van Leeuwen, Catalytic processes in industry, in: R.A. van Santen, P.W.N.M. van Leeuwen, J.A. Moulijn, B.A. Averill (Eds.), Studies in Surface Science and Catalysis,123 - Catalysis: An Integrated Approach, 2nd ed., Elsevier, 2000: pp. 29–80.

[13] P.G. Cifre, O. Badr, Renewable hydrogen utilisation for the production of methanol, Energy Convers. Manag. 48 (2007) 519–527.

[14] X.-M. Liu, G.Q. Lu, Z.-F. Yan, J. Beltramini, Recent Advances in Catalysts for Methanol Synthesis via Hydrogenation of CO and CO2, Ind. Eng. Chem. Res. 42 (2003) 6518–6530.

[15] C.-J. Yang, R.B. Jackson, China's growing methanol economy and its implications for energy and the environment, Energy Policy. 41 (2012) 878–884.

[16] A.P. Keiboom, J. Moulijn, P.W.N.M. van Leeuwen, R.A. van Santen, History of catalysis, in: R.A. van Santen, P.W.N.M. van Leeuwen, J.A. Moulijn, B.A. Averill (Eds.), Studies in Surface Science and Catalysis,123 - Catalysis: An Integrated Approach, 2nd ed., Elsevier, 2000: pp. 3–28.

[17] Methanex Corporation, Methanex - Methanol Price, Methanex Corp. (2013). Available at : http://www.methanex.com/products/methanolprice.html

[18] Methanol Market Services Asia, MMSA Methanol Supply and Demand Balance, Methanol Inst. (2012). Available at: http://www.methanol.org/getattachment/827c8c64-fb2a-4520-aa5a-210612b903cd/MMSA-Supply---Demand-Tables-2008---2013.pdf.aspx.

[19] Methanex Corporation, Methanex Investor Presentation - August 2013, (2013) 1–31. Available at: http://www.methanex.com/investor/documents/MXPresentation-Aug2013_000.pdf.

[20] G.A. Saade, Methanol - Chemical Economics Handbook, 2011.

[21] Merchant Research & Consulting ltd, Methanol: 2013 World Market Outlook and Forecast up to 2017, 2013. Avaiable at: http://mcgroup.co.uk/researches/methanol

[22] M. Laughlin, Methanol, IHC Chem. (2013). Available at: http://www.ptq.pemex.com/productosyservicios/eventosdescargas/Documents/Foro PEMEX Petroqu%C3%ADmica/2013/Marc Laughlin 2013 PEMEX.pdf.

[23] J. Brent, K. McMartin, S. Phillips, C. Aaron, K. Kulig, Fomepizole for the treatment of methanol poisoning, New Engl. Jounal Med. 344 (2001) 424–429.

[24] E. Skrzydlewska, Toxicological and Metabolic Consequences of Methanol Poisonig, Toxicol. Mech. Methods. 11 (2003) 277–293.

[25] I. Chorkendorff, J.W. Niemantsverdriet, Introduction to Catalysis, in: Concepts of Modern Catalysis and Kinetics, 2nd ed., WILEY-VCH Verlag, 2007: pp. 1–21.

[26] A.K. Williams, J.T. Hupp, Sol-Gel-Encapsulated Alcohol Dehydrogenase as a Versatile, Environmentally Stabilized Sensor for Alcohols and Aldehydes, J. Am. Chem. Soc. 120 (1998) 4366–4371.

[27] M. Ben Ali, M. Gonchar, G. Gayda, S. Paryzhak, M.A. Maaref, N. Jaffrezic-Renault, et al., Formaldehyde-sensitive sensor based on recombinant formaldehyde dehydrogenase using capacitance versus voltage measurements, Biosens. Bioelectron. 22 (2007) 2790–5.

[28] F.S. Baskaya, X. Zhao, M.C. Flickinger, P. Wang, Thermodynamic feasibility of enzymatic reduction of carbon dioxide to methanol, Appl. Biochem. Biotechnol. 162 (2010) 391–398.

[29] S. Kuwabata, R. Tsuda, H. Yoneyama, Electrochemical Conversion of Carbon Dioxide to Methanol with the Assistance of Formate Dehydrogenase and Methanol Dehydrogenase as Biocatalysts, J. Am. Chem. Soc. 116 (1994) 5437–5443.

[30] R. Obert, B.C. Dave, Enzymatic Conversion of Carbon Dioxide to Methanol: Enhanced Methanol Production in Silica Sol−Gel Matrices, J. Am. Chem. Soc. 121 (1999) 12192–12193.

[31] B. El-zahab, D. Donnelly, P. Wang, Particle-Tethered NADH for Production of Methanol From CO2 catalyzed by Coimmobilized Enzymes, Biotechnol. Bioeng. 99 (2008) 508–514.

[32] Q. Sun, Y. Jiang, Z. Jiang, L. Zhang, X. Sun, J. Li, Green and Efficient Conversion of CO2 to Methanol by Biomimetic Coimmobilization of Three Dehydrogenases in Protamine-Templated Titania, Ind. Eng. Chem. Res. 48 (2009) 4210–4215.

[33] S. Xu, Y. Lu, J. Li, Z. Jiang, H. Wu, Efficient Conversion of CO2 to Methanol Catalyzed by Three Dehydrogenases Co-encapsulated in an Alginate−Silica (ALG−SiO2) Hybrid Gel, Ind. Eng. Chem. Res. 45 (2006) 4567–4573.

[34] A. Dibenedetto, P. Stufano, W. Macyk, T. Baran, C. Fragale, M. Costa, et al., Hybrid Technologies for an Enhanced Carbon Recycling Based on the Enzymatic Reduction of CO2 to Methanol in Water: Chemical and Photochemical NADH Regeneration, ChemSusChem. 5 (2012) 373–378.

[35] Y. Amao, T. Watanabe, Photochemical and enzymatic synthesis of methanol from formaldehyde with alcohol dehydrogenase from Saccharomyces cerevisiae and water-soluble zinc porphyrin, J. Mol. Catal. B Enzym. 44 (2007) 27–31.

[36] Y. Amao, T. Watanabe, Photochemical and enzymatic methanol synthesis from HCO3− by dehydrogenases using water-soluble zinc porphyrin in aqueous media, Appl. Catal. B Environ. 86 (2009) 109–113.

[37] J.-Y. Xin, J.-R. Cui, J. Niu, S. Hua, C.-G. Xia, S.-B. Li, et al., Biosynthesis of Methanol from CO2 and CH4 by Methanotrophic Bacteria, Biotechnology. 3 (2004) 67–71.

[38] J.-Y. Xin, Y.-X. Zhang, S. Zhang, C.-G. Xia, S.-B. Li, Methanol production from CO2 by resting cells of the methanotrophic bacterium Methylosinus trichosporium IMV 3011, J. Basic Microbiol. 47 (2007) 426–435.

[39] T. Matsuda, R. Yamanaka, K. Nakamura, Recent progress in biocatalysis for asymmetric oxidation and reduction, Tetrahedron: Asymmetry. 20 (2009) 513–557.

[40] C. Roosen, P. Müller, L. Greiner, Ionic liquids in biotechnology: applications and perspectives for biotransformations, Appl. Microbiol. Biotechnol. 81 (2008) 607–614.

[41] V. V. Singh, A.K. Nigam, A. Batra, M. Boopathi, B. Singh, R. Vijayaraghavan, Applications of Ionic Liquids in Electrochemical Sensors and Biosensors, Int. J. Electrochem. 2012 (2012) 1–19.

[42] N. Kaftzik, P. Wasserscheid, U. Kragl, Use of Ionic Liquids to Increase the Yield and Enzyme Stability in the β-Galactosidase Catalysed Synthesis of N-Acetyllactosamine, Org. Process Res. Dev. 6 (2002) 553–557.

[43] S. Park, R.J. Kazlauskas, Biocatalysis in ionic liquids - advantages beyond green technology, Curr. Opin. Biotechnol. 14 (2003) 432–437.

[44] A. Vioux, L. Viau, S. Volland, J. Le Bideau, Use of ionic liquids in sol-gel; ionogels and applications, Comptes Rendus Chim. 13 (2010) 242–255.

[45] L.A. Blanchard, Z. Gu, J.F. Brennecke, High-Pressure Phase Behavior of Ionic Liquid/CO2 Systems, J. Phys. Chem. B. 105 (2001) 2437–2444.

[46] S.N.V.K. Aki, B.R. Mellein, E.M. Saurer, J.F. Brennecke, High-Pressure Phase Behavior of Carbon Dioxide with Imidazolium-Based Ionic Liquids, J. Phys. Chem. B. 108 (2004) 20355–20365.

[47] B.-H. Lim, W.-H. Choe, J.-J. Shim, C.S. Ra, D. Tuma, H. Lee, et al., High-pressure solubility of carbon dioxide in imidazolium-based ionic liquids with anions [PF6] and [BF4], Korean J. Chem. Eng. 26 (2009) 1130–1136.

[48] W. Wang, M.-H. Zong, W.-Y. Lou, Use of an ionic liquid to improve asymmetric reduction of 4′-methoxyacetophenone catalyzed by immobilized Rhodotorula sp. AS2.2241 cells, J. Mol. Catal. B Enzym. 56 (2009) 70–76.

[49] U. Hanefeld, L. Gardossi, E. Magner, Understanding enzyme immobilisation, Chem. Soc. Rev. 38 (2009) 453–468.

[50] B.A. Averill, I.M.C.. Reitjens, P.W.N.M. van Leeuwen, Bonding and elementary steps in catalysis, in: R.A. van Santen, P.W.N.M. van Leeuwen, J.A. Moulijn, B.A. Averill (Eds.), S Studies in Surface Science and Catalysis,123 - Catalysis: An Integrated Approach, 2nd ed., Elsevier, 2000: pp. 109–206.

[51] L. Cao, I Introduction: Immobilized Enzymes: Past, Present and Prospects, in: Carrier-bound Immobilized Enzymes: Principles, Application and Design, 1st ed., Wiley-VCH Verlag GmbH & Co. KGaA, Weinheim, 2005: pp. 1–52.

[52] K. Schirwitz, A. Schmidt, V.S. Lamzin, High-resolution structures of formate dehydrogenase from Candida boidinii, Protein Sci. 16 (2007) 1146–1156.

[53] V.S. Lamzin, A.E. Aleshin, B. V Strokopytov, M.G. Yukhnevich, V. Popov, E.H. Harutyunyan, et al., Crystal structure of NAD-dependent formate dehydrogenase, Eur. J. Biochem. 206 (1992) 441–452.

[54] M.G. Rossmann, D. Moras, K.W. Olsen, Chemical and biological evolution of nucleotide-binding protein, Nature. 250 (1974) 194–199.

[55] T. Schmidt, C. Michalik, M. Zavrel, A. Spiess, W. Marquardt, M.B. Ansorge-Schumacher, Mechanistic model for prediction of formate dehydrogenase kinetics under industrially relevant conditions., Biotechnol. Prog. 26 (2010) 73–8.

[56] S.H. Lee, J. Ryu, D.H. Nam, C.B. Park, Photoenzymatic synthesis through sustainable NADH regeneration by SiO2-supported quantum dots., Chem. Commun. 47 (2011) 4643–4645.

[57] A.D. Winer, G.W. Schwert, Lactic dehydrogenase. IV. The influence of pH on the kinetics of the reaction, J. Biol. Chem. 231 (1958) 1065–1083.

[58] R.B. McComb, L.W. Bond, R.W. Burnett, R.C. Keech, G.N. Bowers Jr., Determination of the molar absorptivity of NADH, Clin. Chem. 22 (1976) 141–150.

[59] J.T. Wu, L.H. Wu, J.A. Knight, Stability of NADPH: Effect of various factors on the kinetics of degradation, Clin. Chem. 32 (1986) 314–319.

[60] M.T. Reetz, Biocatalysis in Organic Chemistry and Biotechnology: Past, Present and Future, J. Am. Chem. Soc. 135 (2013) 12480–12496.

[61] P.S. Wagenknecht, J.M. Penney, R.T. Hembre, Transition-Metal-Catalyzed Regeneration of Nicotinamide Coenzymes with Hydrogen1, Organometallics. 22 (2003) 1180–1182.

[62] A. Šalić, M. Ivanković, E. Ferk, B. Zelić, ADH based NAD+ regeneration in a microreactor, J. Chem. Technol. Biotechnol. 88 (2013) 1721–1729.

[63] A.V. Presečki, Đ. Vasić-Rački, Mathematical modelling of the dehydrogenase catalyzed hexanol oxidation with coenzyme regeneration by NADH oxidase, Process Biochem. 44 (2009) 54–61.

[64] I. Ali, B. Soomro, S. Omanovic, Electrochemical regeneration of NADH on a glassy carbon electrode surface: The influence of electrolysis potential, Electrochem. Commun. 13 (2011) 562–565.

[65] X. Tong, B. El-zahab, X. Zhao, Y. Liu, P. Wang, Enzymatic Synthesis of L -Lactic Acid From Carbon Dioxide and Ethanol With an Inherent Cofactor Regeneration Cycle, Biotechnol. Bioeng. 108 (2011) 465–469.

[66] V.I. Tishkov, V.O. Popov, Catalytic Mechanism and Application of Formate Dehydrogenase, Biochem. 69 (2004) 1252–1267.

[67] D. Zhu, Y. Yang, L. Hua, Stereoselective Enzymatic Synthesis of Chiral Alcohols with the Use of a Carbonyl Reductase from Candida magnoliae with Anti-Prelog Enantioselectivity, J. Org. Chem. 71 (2006) 4202–4205.

[68] C. Rodríguez, G. de Gonzalo, D.E.T. Pazmiño, M.W. Fraaije, V. Gotor, Selective Baeyer–Villiger oxidation of racemic ketones in aqueous–organic media catalyzed by phenylacetone monooxygenase, Tetrahedron: Asymmetry. 19 (2008) 197–203.

[69] J. Liu, M. Antonietti, Bioinspired NADH regeneration by carbon nitride photocatalysis using diatom templates, Energy Environ. Sci. 6 (2013) 1486–1493.

[70] E. Siu, K. Won, C.B. Park, Electrochemical Regeneration of NADH Using Conductive Vanadia-Silica Xerogels, Biotechnol. Prog. 23 (2007) 293–296.

[71] T. Matsuda, Y. Yamagishi, S. Koguchi, An effective method to use ionic liquids as reaction media for asymmetric reduction by Geotrichum candidum, Tetrahedron Lett. 47 (2006) 4619–4622.

[72] A. Damian, S. Omanovic, Interactive Adsorption Behavior of NAD+ at a Gold Electrode Surface, Langmuir. 23 (2007) 3162–3171.

[73] V. Höllrigl, K. Otto, A. Schmid, Electroenzymatic Asymmetric Reduction of rac-3-Methylcyclo-hexanone to (1S,3S) -3-Methylcyclohexanol in Organic/Aqueous Media Catalyzed by a Thermophilic Alcohol Dehydrogenase, Adv. Synth. Catal. 349 (2007) 1337–1340.

[74] I. Ali, M. Mcarthur, N. Hordy, S. Coulombe, S. Omanovic, Electrochemical Regeneration of the Cofactor NADH Employing a Carbon Nanofibers Cathode, Int. J. Electrochem. Sci. 7 (2012) 7675–7683.

[75] R. Castillo, M. Oliva, S. Martı, V. Moliner, A Theoretical Study of the Catalytic Mechanism of Formate Dehydrogenase, Jounal Phys. Chem. 112 (2008) 10012–10022.

[76] V.O. Popov, V.S. Lamzin, NAD+-dependent formate dehydrogenase, Biochem. J. 301 (1994) 625–643.

[77] E.G. Romanova, A.A. Alekseeva, E. V Pometun, V.I. Tishkov, Determination of the Concentration of Active Sites and the Catalytic Rate Constant of Recombinant Formate Dehydrogenase from Glycine max, Moscow Univ. Chem. Bull. 65 (2010) 156–159.

[78] N.E. Labrou, D.J. Rigden, Active-site characterization of Candida boidinii formate dehydrogenase, Biochem. J. 463 (2001) 455–463.

[79] H. Schutte, J. Flossdorf, H. Sahm, M. Kula, Purification and Properties of Formaldehyde Dehydrogenase and Formate Dehydrogenase from Candida boidinii, Eur. J. Biochem. 62 (1976) 151–160.

[80] J.C. Boyington, V. Gladyshev, S. V Khangulov, T.C. Stadtman, P.D. Sun, Crystal Structure of Formate Dehydrogenase H: Catalysis Involving Mo, Molybdopterin, Selenocysteine, and an Fe4S4 Cluster Crystal, Science (80-. ). 275 (1997) 1305–1308.

[81] N. Tanaka, Y. Kusakabe, K. Ito, T. Yoshimoto, K.T. Nakamura, Crystal structure of glutathione-independent formaldehyde dehydrogenase, Chem. Biol. Interact. 143-144 (2003) 211–218.

[82] K. Tulpule, M.C. Hohnholt, R. Dringen, Formaldehyde metabolism and formaldehyde-induced stimulation of lactate production and glutathione export in cultured neurons, J. Neurochem. 125 (2013) 260–272.

[83] N. Tanaka, Y. Kusakabe, K. Ito, T. Yoshimoto, K.T. Nakamura, Crystal Structure of Formaldehyde Dehydrogenase from Pseudomonas putida: the Structural Origin of the Tightly Bound Cofactor in Nicotinoprotein Dehydrogenases, J. Mol. Biol. 324 (2002) 519–533.

[84] B. Persson, J.S.J. Zigler, H. Jörnvall, A super-family of medium-chain dehydrogenases/reductases (MDR). Sub-lines including zeta-crystallin, alcohol and polyol dehydrogenases, quinone oxidoreductase enoyl reductases, VAT-1 and other proteins, Eur. J. Biochem. 226 (1994) 15–22.

[85] K. Ito, M. Takahashi, T. Yoshimoto, D. Tsuru, Cloning and High-Level Expression of the Glutathione-Independent Formaldehyde Dehydrogenase Gene From Pseudomonas putida, J. Bacteriol. 176 (1994) 2483–2491.

[86] T. Pourmotabbed, D.J. Creighton, Substrate Specificity of Bovine Liver Formaldehyde Dehydrogenase*, J. Biol. Chem. 261 (1986) 14240–14244.

[87] S. Ogushi, M. Ando, D. Tsuru, Formaldehyde Dehydrogenase from Pseudomonas putida: A zinc metalloenzyme, J. Biochem. 96 (1984) 1587–1591.

[88] M. Ando, T. Yoshimoto, S. Ogushi, K. Rikitake, S. Shibata, D. Tsuru, Formaldehyde dehydrogenase from Pseudomonas putida. Purification and some properties, J. Biochem. 85 (1979) 1165–1172.

[89] B.F.M. Dickinson, G.P. Monger, A Study of the Kinetics and Mechanism of Yeast Alcohol Dehydrogenase with a Variety of Substrates, Biochem. J. 131 (1973) 261–270.

[90] N. Wen, W. Liu, Y. Hou, Z. Zhao, The Kinetics Behavior of the Reduction of Formaldehyde Catalyzed by Alcohol Dehydrogenase (ADH) and Partial Uncompetitive Substrate Inhibition by NADH, Appl. Biochem. Biotechnol. 170 (2013) 370–380.

[91] V. Leskovac, The three zinc-containing alcohol dehydrogenases from baker's yeast, Saccharomyces cerevisiae, FEMS Yeast Res. 2 (2002) 481–494.

[92] H. Jörnvall, The Primary Structure of Yeast Alcohol Dehydrogenase, Eur. J. Biochem. 72 (1977) 425–442.

[93] B. V. Plapp, B.R. Savarimuthu, S. Ramaswamy, Asymmetry in a structure of yeast alcohol dehydrogenase, Protein Data Bank. (2006).

[94] Q. Zhao, Y. Hou, G.-H. Gong, M.-A. Yu, L. Jiang, F. Liao, Characterization of alcohol dehydrogenase from permeabilized brewer's yeast cells immobilized on the derived attapulgite nanofibers, Appl. Biochem. Biotechnol. 160 (2010) 2287–2299.

[95] Y. Zhang, X. Huang, Y. Li, Negative effect of [bmim][PF6] on the catalytic activity of alcohol dehydrogenase : mechanism and prevention, J. Chem. Technol. Biotechnol. 83 (2008) 1230–1235.

[96] B. Dabirmanesh, K. Khajeh, B. Ranjbar, F. Ghazi, A. Heydari, Inhibition mediated stabilization effect of imidazolium based ionic liquids on alcohol dehydrogenase, J. Mol. Liq. 170 (2012) 66–71.

[97] X.-A. Shi, M.-H. Zong, W.-Y. Lou, Effect of Ionic Liquids on Catalytic Characteristics of Horse Liver Alcohol Dehydrogenase, Chinese J. Chem. 24 (2006) 1643–1647.

[98] M. Eckstein, M. Villela Filho, A. Liese, U. Kragl, Use of an ionic liquid in a two-phase system to improve an alcohol dehydrogenase catalysed reduction, Chem. Commun. (Camb). 7 (2004) 1084–1085.

[99] M. Andre, J. Loidl, G. Laus, H. Schottenberger, G. Bentivoglio, K. Wurst, et al., Ionic liquids as advantageous solvents for headspace gas chromatography of compounds with low vapor pressure, Anal. Chem. 77 (2005) 702–705.

[100] P. Atkins, J. De Paula, Molecular spectroscopy 3: magnetic resonance, in: Atkins' Phys. Chem., 8th ed., W. H. Freeman and Company, New York, 2006: pp. 513–559.

[101] R.M. Silverstein, F.X. Webster, D.J. Kiemle, Proton Magnetic Resonance Spectrometry, in: Spectrom. Identif. Org. Compd., 7th ed., John Wiley & Sons, 2005: pp. 127–203.

[102] M. Temtem, T. Casimiro, A.G. Santos, A.L. Macedo, E.J. Cabrita, A. Aguiar-Ricardo, Molecular interactions and CO2-philicity in supercritical CO2. A high-pressure NMR and molecular modeling study of a perfluorinated polymer in scCO2, J. Phys. Chem. B. 111 (2007) 1318–1326.

[103] C. Harrison, C. Yang, A. Jindal, R.J. DeBerardinis, M. a Hooshyar, M. Merritt, et al., Comparison of kinetic models for analysis of pyruvate-to-lactate exchange by hyperpolarized 13C NMR, NMR Biomed. 25 (2012) 1286–1294.

[104] P. Vidinha, V. Augusto, J. Nunes, J.C. Lima, J.M.S. Cabral, S. Barreiros, Probing the microenvironment of sol-gel entrapped cutinase: the role of added zeolite NaY, J. Biotechnol. 135 (2008) 181–189.

[105] O.H. Lowry, N.J. Rosebrough, A.L. Farr, R.J. Randall, Protein Measurement with the Folin Phenol Reagent, J. Biol. Chem. 193 (1951) 265–275.

[106] R.I. Krohn, The Colorimetric Detection and Quantitation of Total Protein, in: Curr. Protoc. Cell Biol., John Wiley & Sons, Inc., 2011: p. A.3H.1–A.3H.28.

[107] D.L. Nelson, M.M. Cox, Principles of Bioenergetics, in: Lehninger Princ. Biochem., 4th ed., W H Freeman & Co, New York, 2004: pp. 489–520.

[108] A. Paul, A. Samanta, Optical absorption and fluorescence studies on imidazolium ionic liquids comprising the bis(trifluoromethanesulphonyl)imide anion, J. Chem. Sci. 118 (2006) 335–340.

[109] P.K. Addo, R.L. Arechederra, A. Waheed, J.D. Shoemaker, W.S. Sly, S.D. Minteer, Methanol Production via Bioelectrocatalytic Reduction of Carbon Dioxide: Role of Carbonic Anhydrase in Improving Electrode Performance, Electrochem. Solid-State Lett. 14 (2011) E9–E13.

[110] L.J. Rover, J.C. Fernandes, G.O. Neto, L.T. Kubota, E. Katekawa, S.H.P. Serrano, Study of NADH stability using ultraviolet-visible spectrophotometric analysis and factorial design, Anal. Biochem. 260 (1998) 50–55.

[111] M.T. Reetz, A. Zonta, J. Simpelkamp, Efficient Immobilization of Lipases by Entrapment in Hydrophobic Sol-Gel Materials, Biotechnol. Bioeng. 49 (1996) 527–534.

[112] T. Soga, T. Ishikawa, S. Igarashi, K. Sugawara, Y. Kakazu, M. Tomita, Analysis of nucleotides by pressure-assisted capillary electrophoresis-mass spectrometry using silanol mask technique, J. Chromatogr. A. 1159 (2007) 125–133.

[113] H. Wu, S. Huang, Z. Jiang, Effects of modification of silica gel and ADH on enzyme activity for enzymatic conversion of CO2 to methanol, Catal. Today. 98 (2004) 545–552.

[114] H. Wu, Z.Y. Jiang, S.W. Xu, S.F. Huang, A New Biochemical Way for Conversion of CO2 to Methanol via Dehydrogenases Encapsulated in SiO2 Matrix, Chinese Chem. Lett. 14 (2003) 423–425.

[115] Z. Jiang, H. Wu, S. Xu, S. Huang, Enzymatic Conversion of Carbon Dioxide to Methanol by Dehydrogenases Encapsulated in Sol-gel Matrix, Fuel Chem. Div. Prepr. 47 (2002) 306.

[116] E. Hollender, E.W. Hammersley, Ionic Liquids: Sensitivity Enhancement in Headspace Gas Chromatography, Chromatogr. Today. 4 (2011) 30–33.

[117] M. Bekhouche, L.J. Blum, B. Doumèche, Ionic Liquid-Inspired Cations Covalently Bound to Formate Dehydrogenase Improve its Stability and Activity in Ionic Liquids, ChemCatChem. 3 (2011) 875–882.

[118] M. Grønvald, M.B. Jensen, V.S. Andersen, Reactions between Carbon Dioxide and Amino Alcohols. IV. Tris(hydroxymethyl)aminomethane, Acta Chem. Scand. 17 (1963) 2461–2465.

[119] J. Ratzka, L. Lauterbach, O. Lenz, M.B. Ansorge-Schumacher, Stabilisation of the NAD+-reducing soluble [NiFe]-hydrogenase from Ralstonia eutropha H16 through modification with methoxy-poly(ethylene) glycol, J. Mol. Catal. B Enzym. 74 (2012) 219–223.

[120] M. Yoshimoto, T. Yamashita, S. Kinoshita, Thermal stabilization of formaldehyde dehydrogenase by encapsulation in liposomes with nicotinamide adenine dinucleotide, Enzyme Microb. Technol. 49 (2011) 209–214.

# 6. APPENDIX

# 6. APPENDIX

## 6.1. BUFFER PREPARATION

**Sodium phosphate buffer (0.2 M at pH 7)**

To 1L of buffer: dissolve:

- Dissolve 32.7 g of sodium phosphate dibasic heptahydrate ($Na_2HPO_4.7H_2O$) with 9.4 mg of sodium phosphate monobasic monohydrate ($NaH_2PO_4.H_2O$),
- Adjust pH with 1 M HCl;
- Adjust volume to 1 liter with $H_2O$;
- Store at 4°C.

**Tris- HCl buffer (0.2 M at pH 7)**

To 1L of buffer:

- Dissolve 24.3 g of Trizma, in 800 µL of water;
- Adjust pH with 1 M HCl;
- Adjust volume to 1 liter with $H_2O$;
- Store at 4°C.

**TBS buffer 1X ( 0.05M Tris-HCL 0.15 M NaCl at pH 7.6)**

To 1L of buffer :

- Dissolve 6.05 g of Trizma and 8.86 g NaCl, in 800 µL of water;
- Adjust pH with 1 M HCl;
- Adjust volume to 1 liter with $H_2O$;
- Store at 4°C.

## 6.2. IONIC LIQUID STRUCTURES

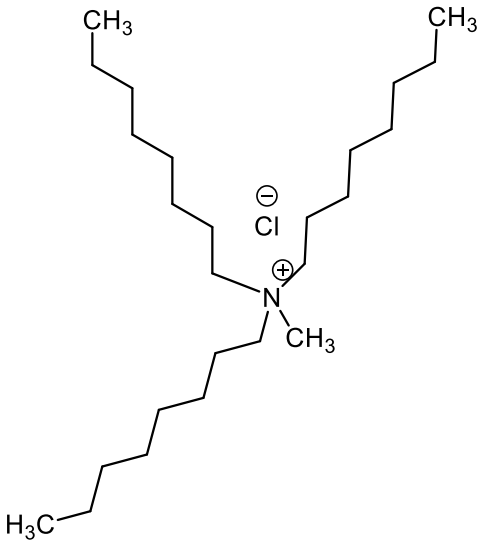


**Figure 6.1 –** Aliquat ® 336.

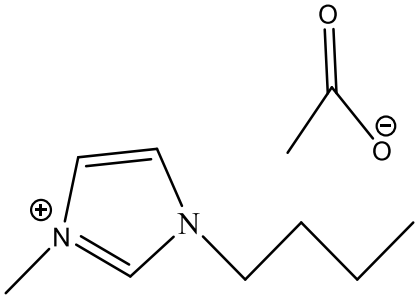


**Figure 6.2 –** [BMIM][Ac].

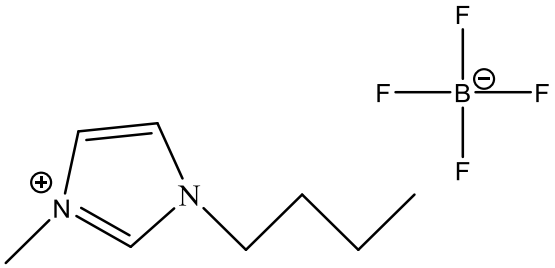


**Figure 6.3** – [BMIM][$BF_4$].

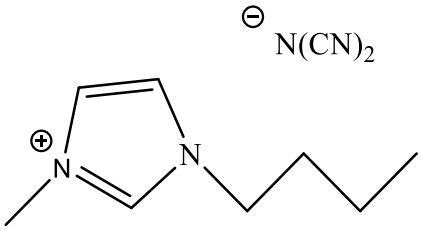


**Figure 6.4 –[**BMIM][DCA].

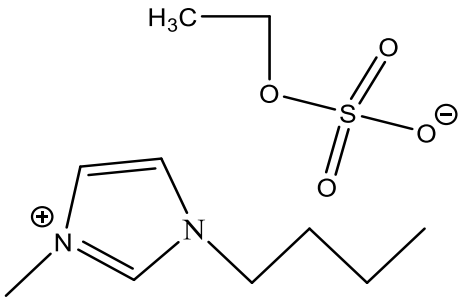


**Figure 6.5 –** [EMIM][$EtSO_4$].

## 6.3. EN 14110

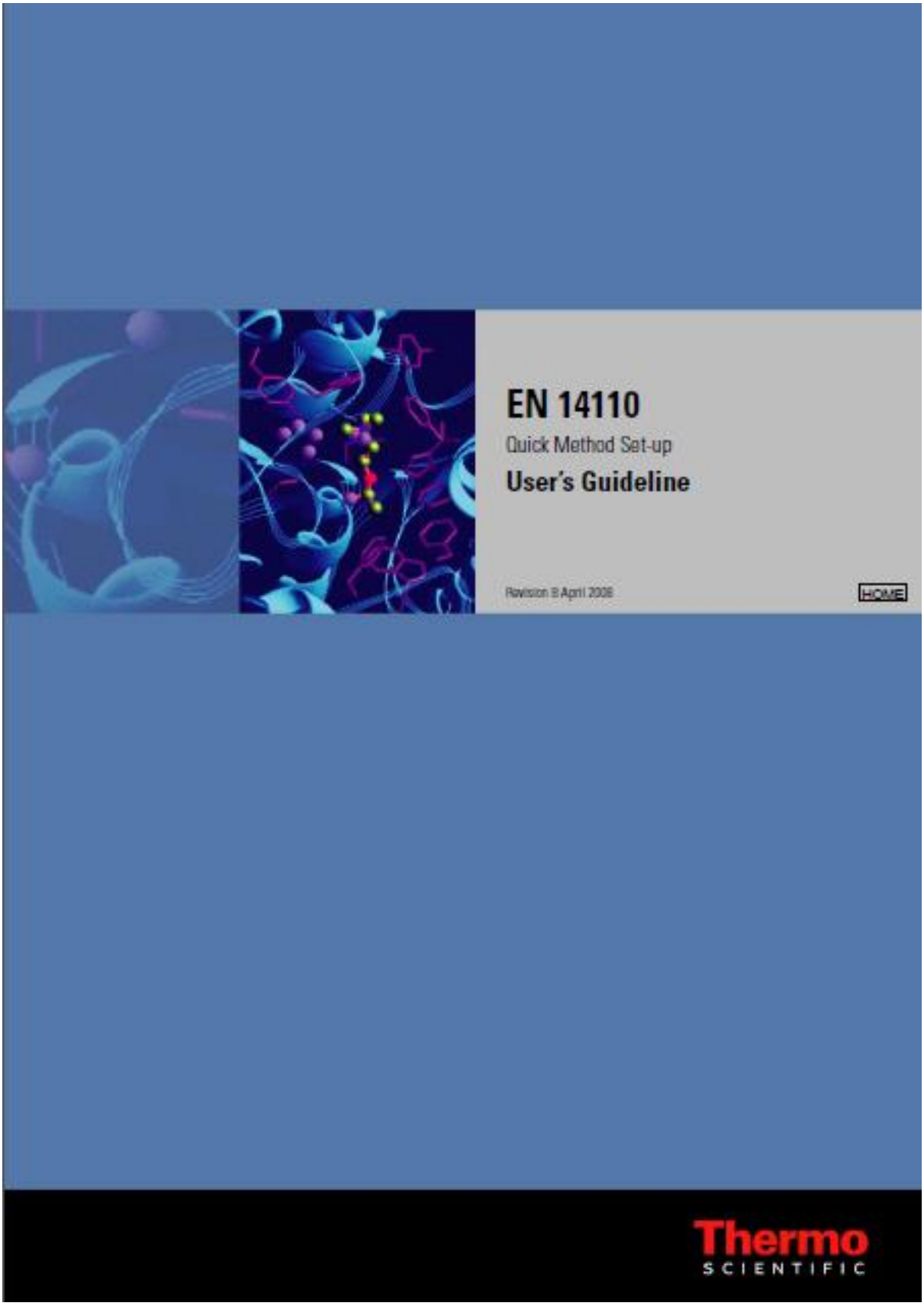
EN 14110
Quick Method Set-up
User's Guideline
Revision B April 2008
HOME
Thermo
SCIENTIFIC

# Quick Method Set-up EN 14110

Contents



Either external or internal standard calibration methods can be applied for this analysis. The external calibration is preferred when an automatic headspace sampling system is available.

## Sample Preparation

A reference sample of FAME can be prepared by extraction of residual methanol with water to ensure low methanol content, taking 30 mL of biodiesel and extracting four times with 10 mL of water. Then, the extracted biodiesel layer must be dried with $MgSO_4$ for 15 minutes, and analyzed using the parameters reported below. This prepared sample has to provide methanol content less than 0.001% m/m, for use as a standard.

Such a reference FAME can also be obtained from various commercial sources. The use of raw sunflower oil, featuring a very low methanol content, is suggested, and does not require any sample prep at all.
Using the reference FAME, three calibration solutions (A, B and C) have to be prepared by adding pure methanol to obtain concentrations of 0.5, 0.1 and 0.01% m/m respectively.

- **Solution A**
  Fill a flask with 25 mL of FAME and add 112 mg ± 0.1 mg (about 142 µL), of pure methanol. Ensure thorough mixing by vigorous shaking.
- **Solution B**
  Transfer 5mL of solution A into a 25 mL flask, and fill to the mark with FAME.
- **Solution C**
  Transfer 1mL of solution B into a 10 mL flask, and fill to the mark with FAME.

2 mL from each calibration solution and unknown biodiesel sample are transferred into 20 mL headspace vials, which are tightly crimped in order to prevent leaking.

For the analysis, 0.5 mL of the headspace is automatically injected into the gas chromatograph, following the instrumental conditions reported below.

# Method Parameters

**Table 1.** Method Parameters

| Parameter | Description |
|---|---|
| Capillary Column | TR-BIODIESEL (M), 30 m, 0.32 mm ID, 3.0 µm f.t. |
| TRACE GC Ultra | |
| Carrier Gas | Helium, 1.5 mL/min, constant flow mode |
| Oven Program | 50 °C (1 min) to 130 °C (0.5 min) @ 10 °C/min |
| S/SL Injector | 160 °C, Split flow 100 mL/min |
| FID Detector Temperature | 250 °C |
| TriPlus HS | |
| Syringe Size | 2.5 mL - 80 mm needle |
| Incubation mode | Costant |
| Sample Draw | 0.5 mL |
| Sampling Vial Depth | 24 mm |
| Incubation Parameters | |
| Agitator Temperature | 80 °C |
| Agitator On Time | 3 s |
| Agitator Off Time | 3 s |
| Incubation Time | 40.0 min |
| Syringe Parameters | |
| Syringe Temperature | 85 °C |
| Filling Volume | 1.0 mL |
| Filling Counts | 1 # |
| Filling Delay | 4 s |
| Pre-injection Syringe Flush | Yes |
| Speed Parameters | |
| Filling Speed | 8 mL/min |
| Injection Speed | 50 mL/min |
| Injection Parameters | |
| Injection Depth | 25 mm |
| Pre-injection Delay | 1 s |
| Post-injection Delay | 1 s |

The pre-set method files EN14110.gcm and EN14110.asm can be loaded and automatically used.

# ChromCard Set-up

**Note** The following procedure indicates the method set-up from the beginning. However, it is possible to use the pre-set method file "EN14110.mth", and modify the retention time window after analyzing a calibration solution.

1. Enter **Edit Method > Calculation Parameters 4**. Set **External STD** as the Calculation method.
2. Analyze a std solution following the parameters reported in Table 1.

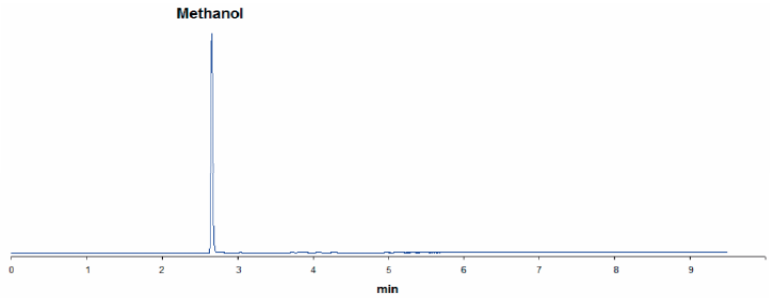


3. Adjust the integration parameters, if necessary. Then, in the Component Table, identify the Methanol peak.

| | Time | Component name | Window | Type | Group | Index | Low limit | High limit |
|---|---|---|---|---|---|---|---|---|
| 1 | 2.673 | Methanol | 0.5 | | | | 0.2 | 0.2 |
| 2 | | | | | | | | |
| 3 | | | | | | | | |
| 4 | | | | | | | | |

4. Enter the **Sample Table**, and fill it to run the calibration standard solutions and unknown biodiesel samples. Indicate for each calibration solution the content of Methanol in % m/m, setting the numbers reported above (0.01 – 0.1 – 0.5%).

| | ID | Sample name | Filename | Type | S.A. | I.S. | X.F. |
|---|---|---|---|---|---|---|---|
| 1 | Act. | Calibration solution A | Calibration solution A | Std | | | |
| 2 | | Calibration solution B | Calibration solution B | Std | | | |
| 3 | | Calibration solution C | Calibration solution C | Std | | | |
| 4 | | Unknown Biodiesel 1 | Unknown Biodiesel 1 | Unk | | | |
| 5 | | | | | | | |

| | Component name | Concentration |
|---|---|---|
| 1 | Methanol | 0.01 |

5. Run the calibration analyses.
6. Enter **View >View Calibration Curve**. Check linearity of the Methanol curve.

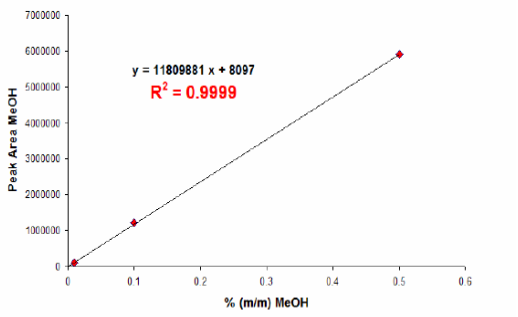


7. Enter **Edit Method** > **Report Parameters 5**. Set the **Report type** as **Custom**. Click the button on the right and set the **component name**, the original **concentration** in %, the **flag limit**, the **retention time** and the **peak area** in the reporting page.

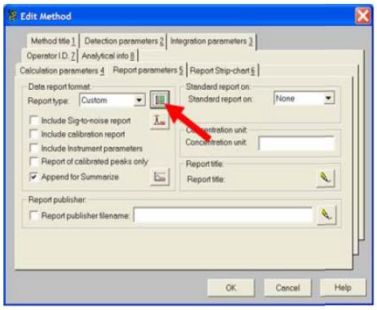


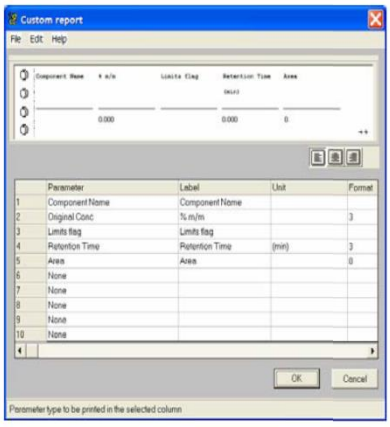

# Example of Automatic Sample Report

Chrom-Card Report

```
Method Name    : Biodiesel_HS
Method File    : C:\...\Appl.notes\BioDiesel\AN\Data\EN14110\Biod_HeadSpace_EN14110 Ext Std.mth
Chromatogram   : 5ml_Biod_Mar2
GC Method      : HS_MetOH_Split100mlmin Sampler Method: Biodiesel_H  Vial # 36
Operator ID    :                        Company  Name :
Analysed       : 14/06/2007  21:51      Printed       : 31/03/2008  23:16
Sample ID      : 5ml_Biod_Mar2
                                        Channel       : (Channel 1)
Analysis Type : UnkNown (Area)          Calc.  Method : External STD

Calib. method : using Least Squares to Linear fit

  S.A.     X.F.
-------- --------
  1.0000   1.0000

Component Name  % m/m           Limits flag     Retention Time  Area
                                                (min)
--------------- --------------- --------------- --------------- ---------------
Methanol        0.122           Below limit     2.653           1440445
                ------                                          -------
                0.122                                           1440445
```